Simulations of Neocortical Columnar Oscillations

Thesis

Richard Jon Arthur Colenso BSc MSc

Simulations of Neocortical Columnar Oscillations

Submitted for PhD Psychology 18 December 2003

Submission date: 19 December 2003
Award date: 1 September 2004

Abstract

The intention of this thesis is to examine the role of the neocortical local circuit in supporting synchronisation and fast (gamma) oscillation. The aim is to include stereotypical features of the local neocortex in model simulations of cortical activity. Modelling is limited by scale in number and detail. Model features include three neuron types (RS, FS and IB) and synapses with three time courses taken from reported tri-phasic PSPs (fEPSP, fIPSP and sIPSP). Cell types and synapses are distributed in a two layer model.

The contribution of the layers to column activity is investigated. The upper layer has a tendancy towards precise synchronisation and can dominate the activity producing synchronisation and oscillation in the whole column. This is attributed to the stronger inhibitory circuit in the upper layer. The lower layer achieves a less precise synchronisation, this is attributed to a lower level of inhibition and the intraburst duration of IB neurons.

The significance of this difference in the temporal properties of the two layers is discussed in relation to existing theories and models of local cortical function. Following a further consideration of local cortical physiology a new model of cortical functioning is proposed. The key features of this model include: the generation of local oscillations in a vertical interlaminar reciprocal circuit; the apical dendrite providing a sharp coincidence detection function between the layers; slow axonal lateral propagation providing a time delay network; apical dendrites of bursting cells (CH and IB) providing coincidence detection between inputs from distant areas (layer 1 inputs) and local activity; bursting cell innervation of interneurons, linking the local oscillation cycle to coincidence detection. This model is termed an 'intrinsically oscillating time coding network' (IOTCN). Specific predictions are made concerning the functioning of the local circuit in neocortex, and the connectivity of CH neurons.

Contents

Glossary

		comment
FS	Fast Spiking	inhibitory interneuron
RS	Regular Spiking	pyramid or small stellate cell
IB	Intrinsically Bursting	large pyramid (usu. layer 5a)
CH	Chattering	pyramid (usu layer 3b)
PSP	Post Synaptic Porential	
PSC	Post Synaptic Current	
AP	Action Potential	synonyms: impulse or spike
EPSP	Excitatory PSP	
EPSC	Excitatory PSC	
IPSP	Inhibitory PSP	
IPSC	Inhibitory PSC	
fEPSP	fast PSP	PSP, PSC prefix
sIPSP	slow PSP	PSP, PSC prefix
LTP	Long Term Potentiation	strengthening synaptic action
LTD	Long Term Depression	weakening synaptic action
adapting	reduction in neuron spike rate or PSP amplitude in a train of activations	
LFP	Local Field Potential: voltage potential due to collective local activity	
MUA	Multi Unit Activity: Impulse time series of many local neurons	
SUA	Single Unit Activity Impulse time series of one local neuron	
spike	synonym for AP	
impulse	synonym for AP	
apical dendrite	thick dendrite ascending vertically from a pyramidal cell	
apical tuft	arbourisation at the top of the apical dendrite	
isocortex	same cortical area	
allocortex	diferent cortical area	
ipsilateral	same cortical hemisphere	
conralateral	opposite cortical hemisphere	
thalamocortical	from thalamus to cortex	
cortico-cortical	from allocortex to local cortex	

laminae	layers of the cortex
superficial layer	upper cortical layer (nearer the skull) eg layers 1 to 3
deep layer	lower cortical layer (away from the skull) eg layers 5 to 6
granular layer	layer of small neurons - layer 4
supra granular	upper layers above layer 4
infra granular	lower layer below layer 4
RBF	Radial Basis Function: a pattern classification algorithm for the non-linear segmentation of multidimensional space
LDCM	Layer Difference Column Model. neocortical column model
IOTCN	Intrinsically Oscillating Time Coding Network: a proposal for a local cortical functional circuit that implements RBF patern matching.

List of Tables and Figures

Tables

Figures

1 Introduction

Observations of high frequency synchronised oscillatory cortical responses, correlated across distances, (for example Gray et al 1989) have led to various proposals regarding their significance. The basic proposal of 'temporal binding' argues that the various responses corresponding to a single perceptual object are synchronised in a single oscillatory neural assembly. This idea is proposed in a modified form by Engel et al (2001), where the local synchronised neural assembly participates in a hierarchy of assemblies.

A variation on the basic hypothesis of temporal binding by synchronised oscillations is proposed by Eckhorn et al. Eckhorn notes that the lateral extent of high frequency oscillations is limited, and proposes that more distant interactions occur by amplitude modulation of the high frequency oscillation envelope (Eckhorn et al 2001).

The antithesis to theories of oscillatory temporal binding is given by Lamme et al (1998). Receptive field responses are observed in the absence of fast oscillations. Eckhorn (2001) replies that measurement difficulties may obscure the observations of synchronised oscillations (this is discussed further in chapter 7).

Few modelling studies implement details of local neocortical physiology that may contribute to the generation of synchronised oscillations. Bush and Sejnowski (1996) implement a simplified model of the local neocortical column that supports collective synchronised oscillations. Traub et al propose a model where oscillations provide a time frame and the neural response is a phase time code (Traub et al 1997b). In this model the oscillations are generated by a mutually inhibitory population. Both the Bush and Traub models include model neurons that represent typical pyramidal and interneuron cell types.

The empirical results of Stewart indicate that the intact column vertical circuit is important for the lateral propagation of local activity and the intact column supports fast oscillations (Stewart 1999). This in vitro result indicates the importance of modelling the interlaminar vertical circuit.

This thesis attempts to model local neocortex including 'typical' physiology in an attempt to discover how local functioning supports (or fails to support) collective synchronised and oscillating activity. A simplified two layer column model is developed. Features of local cortical physiology include the distribution of different cell types. An emphasis has been placed on portraying layer differences and representing the different impulse firing characteristics of the main neuron types.

1.1 Thesis structure

Chapter 2 includes a review of neurophysiology and proposes the development of neuron and synapse models. Particular emphasis is placed on layer differences. The distribution of different neuron types and the asymmetry of interlaminar connections are considered. The relative strengths of inhibitory and excitatory connections is estimated from empirical results involving the actions of populations of synapses in compound PSPs

Chapter 3 examines models of the excitable membrane and a simplified synapse. The excitable membrane model is based on a simplified physiological model that preserves the basic impulse firing properties of the different neuron types. The frequency response of the neuron and synapse models are examined using correlograms and power spectra. Pyramidal neuron types act as band pass filters, the interneuron passes all frequencies (in the range of interest) and the model synapse acts as a low pass filter.

Chapter 4 examines illustrative simple circuits implemented with small numbers of neuron models. The consistency of timing of pyramidal regular spiking neurons (RS)

to RS impulse recruitment is noted. This is consistent with a time delay model (but does not rule out many other models).

Chapter 5 implements a model network including 100 neurons of RS and Fast Spiking (FS) model neurons. The network model represents the upper layers of a neocortical column. The behaviour of the network is examined under different conditions. The model exhibits a tendency for RS impulse synchronisation and oscillation, but the collective oscillation is not robust.

The model is adjusted to include parameters similar to the Bush and Sejnowski column model (Bush and Sejnowski 1996). Oscillation and synchronisation is strengthened, broadly reproducing their single column results.

Chapter 6 implements a simplified neocortical column model comprising two layers. Features include a difference in the layer distribution of neuron types: FS and RS occur in both layers, Intrinsically Bursting (IB) cells are restricted to the lower layer. Layers differ in their connectivity, the upper layer has stronger inhibitory connections and the lower layer does not send direct inhibitory connections to the upper layer. No other published models incorporate these features.

Strong synchronisation and oscillation of the whole column is demonstrated. The upper layer is more tightly synchronised than lower layer. It is proposed that the collective action of the upper layer supports a finer temporal resolution than the lower layer.

Chapter 7 discusses the results from the simplified column model in relation to different theories of neural integration. Further features of local neocortex neurophysiology are considered. A new model of cortical function is proposed and features of the model include: the generation of local oscillations in a vertical interlaminar reciprocal circuit; the apical dendrite providing a sharp coincidence detection function between the layers; slow axonal lateral propagation providing a time delay network; apical dendrites of bursting cells (IB) providing coincidence

detection between inputs from distant areas (layer 1 inputs) and local activity; bursting cell innervation of interneurons, linking the local oscillation cycle to coincidence detection. This model has been termed an intrinsically oscillating time coding network (IOTCN). Specific predictions are made concerning the functioning of the local circuit in neocortex, and the connectivity of chattering (CH) neurons.

Further modelling work is suggested to test the proposal of the IOTCN. Initial studies should concentrate on defining the coincidence function that pyramidal neurons support, and how this varies with different pyramidal types. It is suggested that interneuron types might be classified according to their effect on the coincidence function achieved by a pyramidal cell.

Chapter 8 provides a summary of the thesis and some concluding comments.

1.2 Thesis contributions

Chapter 3 implements a modification of the Hindmarsh and Rose excitable membrane model. A parameter is introduced to modify the phase plane and allow the control of the 'triggered firing' property of the Hindmarsh and Rose system. This allows the implementation of simple excitable neuron models with contrasting properties using different parameter sets. FS, RS and IB impulse firing patterns can be achieved.

Chapter 5 implements a single layer model of spiking, adapting neurons and interneurons. The model is based on different empirical sources and the model is developed using a different method to the Bush and Sejnowski (1996) column model. Similar results are obtained when the fast inhibitory postsynaptic current rise time (fIPSC rise time) is set to a similar value to that used by Bush and Sejnowski. The fIPSC rise time used by Bush and Sejnowski is based on single inhibitory postsynaptic potential (IPSP) studies. The fIPSC rise time value used throughout this thesis (except in model 5f) is based on population fIPSP studies that record the time course of

collective IPSPs (evoked by local electrical stimulation). This highlights the importance of the fIPSC time course in determining the quality of synchronisation and oscillation in a local neuron network.

Chapter 6 makes a strong contribution to the understanding of local cortical activity. The upper layer exhibits a more tightly synchronised and oscillatory pattern of population activity than is evident in the lower layer. This contrast appears to be robust. The relatively sharp synchronisation of the upper layer is attributed to the stronger inhibition implemented in the upper layer and the feedback from the lower layer (note that the isolated 'upper' layer model 5a includes the same level of inhibition but does not achieve the same level of synchronisation).

I am not aware of any published model that includes layer differences of connectivity and the distribution of different neuron types (including spiking, adapting pyramid type behaviour). By itself this is a modest result. (The immediate result is not astonishing; layer differences are implemented and a difference in layer behaviour is found.) However the consequences for the understanding of local cortical activity may be far reaching. This is discussed in chapter 7.

Chapter 7 makes a contribution to the understanding of local cortical function by proposing a model that integrates local and distant inputs. The model arises from a synthesis of:

i. theoretical proposals for a neural time code (Hopfield 1995; Sejnowski 1995);

ii. the distribution of interlaminar connections (Thomson and Bannister 2003);

iii. response timing properties of active apical dendrites (Larkum et al 1999);

iv. and the chapter 6 results showing a differential in the synchronisation of the layers of an oscillating column model.

The model is briefly described in section 1.1 above (paragraph describing chapter 7).

The novel feature of the model is the relationship between the local oscillatory circuit and the neurons that mediate the integration of inputs from distant cortical areas and local activity. Because of this the local oscillatory 'clock' is coupled to the coincidence function that the bursting neurons achieve. This may have subtle effects on the timing of subsequent local activity. This feature also opens up the possibility of distant interactions coupling to local activity at a lower frequency (consistent with proposals of Eckhorn et al 2001; von Stein and Sarnthein 2000).

2 Neurophysiology of the local neocortex

This chapter selectively surveys the local physiology of the neocortex with the intention of developing a generalised model of local neocortex. This sketch is limited to a consideration of 'fast local' action where duration is in milliseconds and distances are within a few cortical columns. The aim is to include the functional qualitative properties which appear to be typical of local cortical neurons.

Studies of local neocortical form and function are considered:

distribution of cell types through the layers;
synaptic function and connection frequency;
columnar organisation of neuron responses;
comparative electrophysiology of different neurons.

The individual functional studies provide a fragmentary picture of local neuronal action and connectivity. However, by generalising from these results a stereotyped scheme of connectivity is obtained and a prototype of a 'typical' area of local neocortex is suggested. A simplified set of models, representing different types of neurons and synapses, is proposed. This prototype of local neocortical organisation provides the basis for the modelling of neuron activity in subsequent chapters. Simplified models of neuron impulse production and synaptic transmission are examined in chapter 3. Subsequent chapters examine networks based on these models, culminating in a model that implements neocortical layer differences in chapter 6.

2.1 Uniformity of neocortical areas

Different brain areas exhibit similarities in the organisation of neocortical tissue. The absolute number of neurons though the thickness of a cortical area (beneath a unit area, through the layers of the cortex) is nearly a constant in the brains of different mammals (Rockel et al 1980) and is the same in functionally different cortical areas.

The striate cortex (primary visual cortex) is an exception to the neuron population 'rule' of uniformity between areas. It is thicker than other cortical areas and has twice the number of neurons per unit area. Its most distinctive feature is the greater differentiation of the middle layers compared to the other areas, besides this the organisation and variety of cell types and synapses appears similar to extrastriate areas. Allowing for these differences, studies based on the striate cortex are considered, below, alongside results from other areas.

2.1.1 Neocortical laminae

Historically six layers have been identified in the neocortex. In a discussion of the general organisation and functioning of the neocortex, Crick simplifies this division into four main layers (Crick and Asanuma 1986):

a superficial layer, consisting mainly of axons and apical dendrites;
an upper layer containing small pyramidal neurons;
a middle layer with many small stellate neurons;
a deep layer containing large pyramidal neurons.

The distribution of neurons through the layers has been quantified. O'Kusky and Colonnier counted cells and synapses in Macaque visual cortex (O'Kusky and Colonnier 1982). The overall volume density is about 120×10^3 mm^3 neurons and 276×10^6 mm^3 synapses. The numbers beneath a surface area of one mm^2 of cortex and the variation in densities between the cortical layers is shown in table 2.1 below.

The highest density of neurons occurs in the middle layers and the highest synaptic density appears in the upper layers. This suggests some contrast in the functional roles of the layers regarding the integration of neural activity. The upper layers possess a high synapse to neuron ratio and so may integrate activity across a larger number of neuron sources compared to the other layers.

Proportions of neurons and synapses in laminae of striate cortex			
layer	neuron %	synapse %	synapse/neuron
1-3	28	40	3380
4	45	35	1840
5,6	27	25	2200
total mm^{-2}	$202x10^3$	$478x10^6$	2370

Table 2.1 Neuron and synapse frequency after O'Kusky and Colonnier (1982)

This interpretation of the synapse/neuron ratio must be treated with care as the layers are not isolated. The apical dendrites and axon collaterals from lower layer (5,6) neurons ascend into the upper layers (1-3), so although a synapse may physically occur in a more superficial layer, it may be between an axon and an apical dendrite originating from neuron bodies in lower layers.

2.1.2 Neuron and synapse types

Many neuron types have been distinguished, however, this account is limited to a sketch of some of the distinguishing features of the commonest neurons (pp224-226, Gilbert and Wiesel 1983).

Two broad groups of cortical neurons may be distinguished by the presence of spines on the surface of their dendrites (in the mature neocortex). The presynaptic membrane of the typical spiny neuron's synaptic bouton, overlying the synaptic cleft, appears thicker than the underlying postsynaptic membrane (an asymmetric synapse). In contrast, the aspiny neuron forms a synapse which appears symmetrical. The thickening of the presynaptic membane of the aspiny cell is comparable to the thickness of the postsynaptic membrane underlying the synaptic bouton. Spiny cell axons possess asymmetric synapses and smooth cell axons make symmetric synapses. It may be assumed that this binary division of morphology corresponds to the neurons' synaptic function. It appears that spiny neurons make excitatory synapses on their targets and aspiny neurons form inhibitory connections with the postsynaptic targets.

2.1.2a Spiny neurons

The great majority of neurons are spiny and pyramidal. Crick (1986 p361) estimates that 80% of cortical neurons are spiny. Spiny cells in the upper and lower layers are predominately pyramidal. Layer 4 (the middle layer) contains large numbers of small stellate cells which are spiny, but layer 4 has comparatively few pyramidal cells.

The excitatory neurochemistry of the middle layer differs from the upper and lower layers. Glutamic acid and aspartic acid have a strong excitatory effect on neocortical neurons. Glutamergic neurons can be identified by immunocytochemistry. It is suggested that glutamic acid is associated with descending and inter-area pathways. Layer IV, the middle layer which receives the bulk of thalamic afferents (ie 'ascending' connections), has 19% of its neurons glutamic acid positive. In the upper and lower layers 40 to 50% of neurons are glutamic acid positive (in macaque, Conti et al 1987).

Gilbert (1983) describes the local projections of spiny neurons and proposes a local circuit (simplified in figure 2.1). The small stellate cells of the middle layers have dendrites which arbourise locally and their axons ascend to the upper layers. The pyramidal neurons of the upper layers support locally projecting axons which innervate the deeper layers. Deep layer axons project locally to innervate layer four.

In addition pyramidal neurons are responsible for the majority of non-local projections, to other cortical areas and sub-cortical structures. The large pyramidal neurons found in the lower layers project sub-cortically.

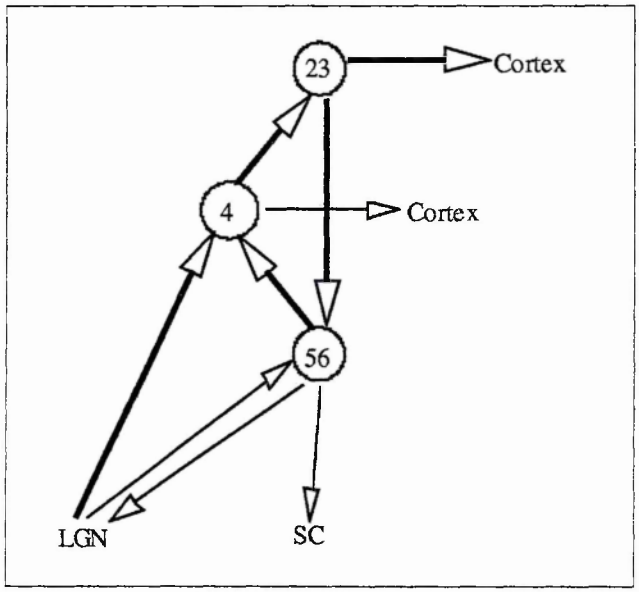

Figure 2.1 Principle intracortical connections of spiny cells in cat striate cortex (simplified from Gilbert (1983 pp 229-230) Lateral geniculate nucleus LGN, Superior colliculus SC, weight of arrows indicates relative density of connectivity. The strongest thalamic input is to layer 4. A local circuit is formed by the projections via the upper layers (1-3), to the lower layers (5 6) and back to layer 4.

2.1.2b Aspiny neurons

Around 20% of the neuron population are aspiny. The class of aspiny cells has a greater variety of morphological types than the spiny class. Aspiny cells make symmetrical synapses on their targets. The GABAergic action of the synapses made by identified aspiny cells has been demonstrated (for example, Kisvarday et al 1987). A working assumption is made that these smooth neurons have an inhibitory effect on their targets.

The morphologies of aspiny neurons have been extensively recorded. Different classes of IPSPs have been identified and associated with the GABAa and GABAb receptors. However it is not clear if a particular pre-synaptic aspiny neuron morphology is associated with a distinctive post-synaptic electrochemistry.

Common types of aspiny cells exhibit differences in their laminar distribution and the laminar distribution of their postsynaptic targets. The dendritic and axonal

arbourisation of aspiny neurons is typically extensive in the local cortical column, extending vertically to cells in other layers. The axonal and dendritic arbourisation of bipolar cells project vertically, apparently within the cells 'home' column. The arbourisation of chandelier cells is also local. In contrast, large basket cells, which are present in the upper and lower layers, possess axons which arbourise laterally to distances of several millimetres. The basket neurons' pattern of patchy lateral arbourisation is similar to that of pyramidal cells. The local connectivity of the cortex, although complex, is not amorphous at the scale of local vertical and lateral connections (reviewed by Lund 1988).

The population of inhibitory aspiny neurons has a more local projection than the spiny types. 'Exceptions' to this generalisation are : the small spiny stellates of layer 4 which project vertically to the upper layers ; the large aspiny basket neurons which arbourise laterally. The functional role of the inhibitory neurons does not seem to be a mirror image of the excitatory cell population.

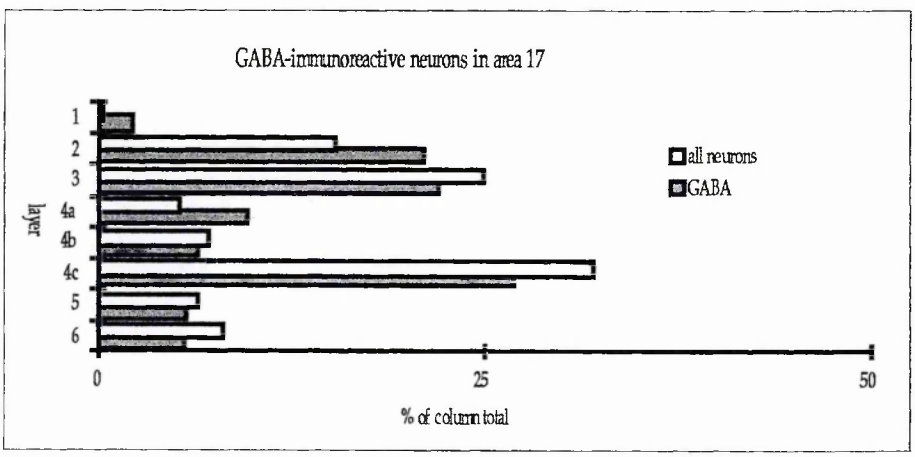

Figure 2.2 Proportions of inhibitory cells in visual cortex (adapted from Hendry 1987). The histogram indicates the fraction of the column total within each layer. The column total of GABA immunoreactive cells is 19% of the column total of all neurons.

Hendry et al examine the distribution of GABA-immunoreactive neurons in Macaque neocortex. In the visual cortex around 20% of neurons are GABA-immunoreactive (Hendry et al 1987). The upper layers have higher numbers of GABA-immunoreactive cells than the lower layers, and the GABA-immunoreactive cells in the upper layers

are a somewhat higher proportion of the neuron population within each layer (Figure 2.2).

Hendry et al compare different cortical areas and find GABA-immunoreactive cells in higher densities in the layers receiving the main concentrations of thalamocortical axon terminations (layers 4a and 4c in area 17). All areas display a high concentration of GABA-immunoreactive neurons in layer 2.

Hendry et al find a rather lower proportion of all neurons in the lower layers compared to the cell counts of O'Kusky and Colonnier (1982). But their overall estimate for unit volume neuron density is similar ($120x10^3$ mm^3).

2.1.3 Functional columns

Functional columns may be characterised by the gradation in receptive field (RF) properties. A column is defined where similar RF properties are found through the depth of the cortical layers. Iso-orientation columns are found in the primary visual cortex. The population of neurons in a vertical column, through the cortical layers, responds optimally to stimuli moving through the visual field at a certain angle. Adjacent columns exhibit a gradation in orientation preference (a classic paper by Hubel and Wiesel 1963).

Neurons differ in their particular RF properties within a column. Simple RF properties are associated with the small stellate neurons of the middle layers (thalamocortical recipient layer). Complex properties such as 'end-stopping' are associated with pyramidal neurons, especially the larger pyramids, found in the upper and lower layers. Despite these differences the orientation preferences of the different neurons within the column is similar.

In the primary visual cortex the iso-orientation preference columns are arranged in a 'pinwheel' hypercolumn where all orientations are represented (figure 2.3 below). These pinwheel hypercolumns tile the whole area of the primary visual cortex. Other RF properties are often arranged in the form of repeating stripes.

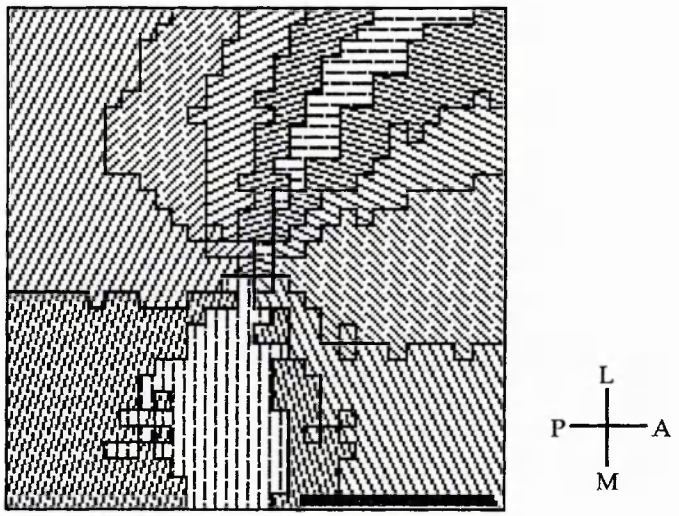

Figure 2.3 Orientation preference in visual cortex (after figure 2c in Bonhoeffer and Grinvald 1991). Scale bar 300mm, A anterior, P posterior, L lateral, M medial. Hatching indicates similar orientation preference to a resolution of 15°. Iso-orientation patches are ordered so that similar orientations are adjacent. The patches occur around orientation foci forming a 'pinwheel' pattern which tiles the surface of the visual cortex.

It may be noted that the scale of columnar organisation is of the same order of distance as the proximal radius of the dendritic arbourisation of typical neuron types. A radius of 150-300μm would contain the dendritic arbour of small neurons such as the spiny stellates of layer 4 and types such as the larger pyramids (for example figures in Gilbert and Wiesel 1981; Gilbert and Wiesel 1985).

A vertical cylinder of radius 300μm in macaque visual cortex contains a total of 52-57x10^3 neurons (185x10^3 neurons mm^{-2} sample CM187 in Hendry et al 1987, approximately 200x10^3 neurons mm^{-2} O'Kusky 1982). Of these around 10-11x10^3 will be GABAergic and 42-46x10^3 will be spiny cells, mostly pyramids. A column of this volume cannot possess all to all connectivity. O'Kusky finds a mean of 2.4x10^3 synapses per neuron indicating sparse connectivity at distances corresponding to the local dendritic arbourisation of typical neurons. Nicoll and Blakemore (1993) estimate a higher total of synapses per pyramidal neuron. However they estimate that the total number of functional synapses received by an individual pyramid to be around 1.2x10^3

(allowing a mean of 10 anatomical synapses contributing to one functional connection between a pair of pyramids).

2.2 Local connectivity

The morphology of an individual neuron, especially its dendritic and axonal arbourisation, gives some indication of its role in the local cortical circuit. Studies, using electrical and focal chemical stimulation, have investigated local functional connectivity. This chapter considers studies which examine direct pathways between neurons, with no mediating connections via intermediate neurons (known as 'mono-synaptic transmission'). In some cases the connectivity of a morphologically identified cell type has been established. Ideally a map of the local circuit might be compiled, identifying the role of particular neuron types. However, this information is partial. Relatively little is known about the detailed functioning and connectivity of the smaller inhibitory cells. More is known about local connections between larger pyramidal neurons. Differences in connectivity within and between layers is represented in the model network implemented in chapter 6.

2.2.1 Upper layers in the neocortex

Mason et al (1991) investigated synaptic transmission between individual pyramidal neurons in layers 2/3 of the rat visual cortex in vitro. A connection probability of 9% was found between cells separated by 50μm to 340μm. The excitatory post synaptic potentials (EPSPs) had short latency and fast rise times. All of the recorded cells that were successfully stained had typical pyramidal cell morphology.

Keeling et al (1996) compare PSPs evoked in layer 2/3 pyramidal neurons from lateral and vertical sites of stimulation. Excitatory PSPs are evoked from stimulation sites up to 150μm laterally (80% of PSPs). At greater lateral separations (250μm - 700μm) up to 80% of PSPs are inhibitory.

These findings, within the same layer, are consistent with the view that the effect of action originating in the 'home column' is on balance excitatory and action originating

in the neighbouring columns is inhibitory (redolent of a competitive network architecture). Excitatory PSPs prevail in the recorded layer 2/3 when the stimulation site is located in layer 4 (91% of PSPs). In contrast stimulation of layer 5 evokes 40% inhibitory PSPs in the upper layer pyramids.

Hirsch and Gilbert record PSPs evoked in layer 2/3 cells. An electrical shock is used as the stimulus at lateral and vertical sites (Hirsch and Gilbert 1991). This method activates many afferents and the recorded PSP may be complex as it results from the action of multiple synapses from different pre-synaptic neurons. With the stimulus within the home column in either layer 2/3 or layer 4, a triphasic PSP is evoked comprised of fast excitatory, fast inhibitory and slow inhibitory parts (fEPSP, fIPSP and sIPSP respectively). The triphasic PSP is still found after undercutting layer 2/3, thus isolating it from ascending afferents. This indicates that the various PSPs are intrinsic to the local layer and column. Lateral stimulation at wide separations (900μm to 3000μm) evokes fEPSP and fIPSP, but sIPSPs were not found. It seems then that the sIPSP is a feature of local inhibition within a column.

Van Brederode and Spain compared IPSPs in the upper and lower layers of cat motor cortex (van Brederode and Spain 1995). A stereotypical triphasic PSP was evoked in the upper layer neurons when local electrical stimulation was applied to upper or lower layers. EPSPs were suppressed by glutaminergic blockade to examine activity solely mediated by IPSPs. Following the application of glutaminergic blockade, both fIPSPs and sIPSPs are evoked in the upper layers during electrical stimulation of the upper layers. However, during glutaminergic blockade, no IPSPs could be evoked in the upper layer neurons by the stimulation of the deep layers. This reveals an absence of direct inhibitory connections from the deep layers to the upper layers.

2.2.2 Lower layers 5 and 6

Van Brederode and Spain found that IPSPs in the lower layers are weak and are only clearly revealed following the suppression of EPSPs by glutaminergic blockade. In the majority of recorded layer 5 neurons only fIPSPs were found. Both fIPSPs and sIPSPs were evoked in the remaining neurons, however the sIPSPs were relatively feeble.

Stimulation of the upper layers evoked proportionately more sIPSPs in the lower layers than a stimulation sited in the lower layers. It can be concluded that inhibitory neurons in the upper layers directly innervate lower layer pyramids.

Nicholl et al investigate the laminar differences in fIPSP inputs to pyramidal neurons in rat neocortex (Nicoll et al 1996). They also find that lower layer IPSPs are weaker than those evoked in upper layer neurons. In addition within the lower layer they find a class of pyramid (intrinsically bursting) that is significantly more weakly inhibited (a lower occurrence of evoked IPSPs) than other layer 5 pyramids.

Thomson and Deuchars investigate functional connectivity between pairs of layer 5 pyramidal neurons in neocortex (review Thomson and Deuchars 1994). They find pyramid to pyramid connections within a column or between neighbouring columns to be strong and large EPSPs are evoked which are capable of eliciting post-synaptic spikes. Pyramids that are laterally more widely separated have weaker synaptic connections and EPSPs are smaller and slower. Histological reconstructions of the connections between recorded pairs of neurons reveals that strong functional synaptic contact between two pyramids involves a number of anatomical synapses.

Nicoll and Blakemore (1993) estimate the probability of functional connectivity between pyramids in the neocortical layers. Connections between pyramidal neurons in the upper layers are individually weaker than between pyramids in the lower layers, but upper layer connections are more frequent. The median amplitude of a single connection EPSP in the upper layer pyramids is 0.4mV and in layer 5 pyramids EPSP median amplitude is 0.8mV. However the connection probability for pairs of neurons at separations up to 300μm is 8.7% between layer 2/3 pyramids and 1.5% between layer 5 pyramids.

2.3 Individual Synapses

Connections of the same synaptic type exhibit different timecourses (PSP shapes) and amplitudes at the soma. In addition a number of factors contribute to the variability of PSP shapes resulting from a single synaptic connection.

Synaptic connections between different neurons occur at different positions on the dendritic tree. The variability of PSP timecourse is presumably due to the different electrotonic positions of these different connections. It appears that the more distal synapses have a slower somatic PSP rise times than proximal synapses of the same type.

A single connection between two neurons exhibits some degree of PSP transmission variability. Connections which evoke higher amplitude PSPs tend to be more reliable than low amplitude PSPs. It is assumed that the collective probability of transmission at a number of synapses mediating a single functional connection contributes to a more reliable and greater amplitude PSP. One or a few synapses contributing to a low amplitude PSP have a low collective probability of transmission. Low amplitude PSPs are more variable in amplitude and transmission may fail completely (Thomson and West 1993).

Other factors influence somatic PSP shapes. Active conductances, which are especially likely when pulse transmission occurs via the apical dendrite, introduce further variability in somatic PSP shape. Postsynaptic electrochemistry may further modulate PSP shape. For example NMDA facilitation of glutamergic synapses enhances excitatory PSP amplitudes.

2.3.1 The functional synapse

Thomson and Deuchars (review 1994) propose the idea of a functional synapse which corresponds to a set of multiple anatomical synapses connecting two neurons in parallel. Where several presynaptic axon collaterals and several dendritic branches are in a connection between two pyramids, all the anatomical synapses appear to be at a

similar electrotonic distance on the dendritic tree of the postsynaptic neuron. These synapses contribute to a single 'functional synapse' possessing a distinctive somatic PSP timecourse. Other workers find a clustering of synaptic boutons that suggests a narrow range of possible timings for the functional synapse PSP (Freund et al 1989). (Note that the the 'functional synapse' proposal, a 'functional synapse' is comprised of many individual synapses connecting two neurons in parallel, corresponds to 'mono-synaptic' functional connectivity. This 'functional synapse' does not involve transmission via intermediate neurons, and the 'functional synapse' does not correspond to studies of general neural 'functional connecticvity' which includes indirect connections via multiple synapses in series.)

2.3.2 Synapse types

Connors et al (1988) studied inhibitory postsynaptic potentials (IPSP) in the upper layers of somatosensory cortex in vitro. Slow (sIPSP) and fast (fIPSP) types were found. The sIPSP was associated with the GABAb receptor type and fIPSP was associated with the GABAa receptors. The rise time of fIPSP was found to be in the order of 8ms, only a little slower than excitatory PSPs (EPSP) evoked by a common stimulus. The sIPSP time to peak was found to be in the order of 100ms (figure 1 pp447). Connors et al contrasted the inhibitory roles of the two IPSPs. The fIPSP greatly increased a pyramid neuron's firing threshold and abolished or substantially reduced the production of a spike train during the application of a strong excitatory stimulus. The sIPSP increased the firing threshold and reduced the firing rate in a spike train, but the pyramid's response to a strong transient stimulus was unimpaired. Hirsch and Gilbert have also investigated IPSP types in layers 2 and 3 of cat visual cortex (Hirsch and Gilbert 1991). Their findings echo those of Connors et al. They find that fIPSPs are associated with the GABAa receptor and sIPSPs are GABAb-ergic.

The reversal potential of the fIPSP is around the typical resting potential of a pyramidal neuron (eg -75mV). The fIPSP is only clearly revealed at more depolarised potentials, for example at a potential close to the action potential threshold. The sIPSP has a more negative reversal potential (eg -90mV, Connors et al 1988).

2.3.3 Laminar differences of functional synaptic types

The time courses and laminar differences in PSP types have been reported by other workers (below table 2.2 after van Brederode and Spain 1995, fIPSP by Nicoll et al 1996, fEPSP by Mason 1991, fEPSP and fIPSP by Komatsu et al 1988). The PSP rise times found for a particular synaptic type are variable and a wide range has been reported by different workers. fIPSP 10-90% risetimes are reported by some to be in the order of 10 mS (van Brederode p1153, Nicoll p114) and others as fast as ~2ms (Komatsu p361). fEPSP risetimes are generally reported to be in the order of a few mS and sIPSP risetimes are in the order of 100ms.

Layers	time to peak mS	
upper	fEPSP	<5
	fIPSP	16
	sIPSP	~140
lower	fEPSP	<5
	fIPSP	9
	sIPSP	~100

Table 2.2 PSP rise times after van Brederode and Spain (1995), Nicholl et al (1996), and Mason (1991).

These workers find that fIPSP amplitudes are larger in the upper layers. Brederode and Spain find that fIPSPs are generally able to terminate fEPSPs in layer 2-3 neurons, but the EPSP dominates in most layer 5 cells. They find that sIPSPs are very weak or absent in the lower layer cells. In the upper layers single sIPSPs have lower amplitudes than fIPSPs. However, sIPSPs are long lasting and temporal summation of sIPSPs results in a sustained depression of the excitability of upper layer neurons.

2.3.4 Estimation of relative conductances of synapse types

The relative conductance of a particular synapse type can be estimated from the relationship between peak PSP and post synaptic membrane potential.

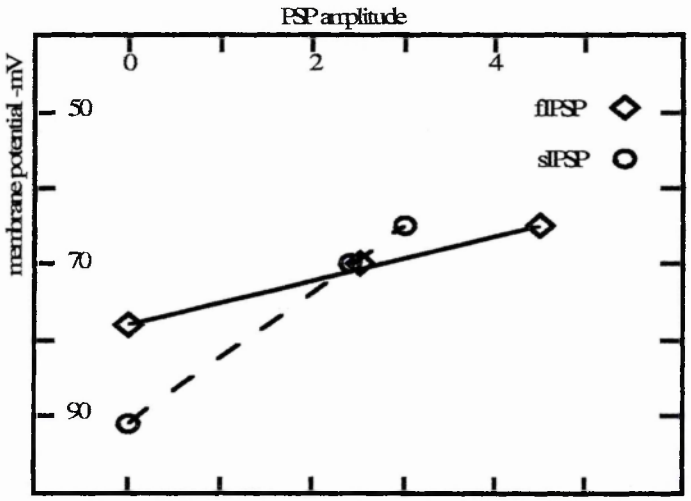

Figure 2.4 IPSP amplitudes and membrane potential in layer 2/3 pyramids. Stimulation site in upper layers (values estimated from figures 1A and 1D p1155 van Brederode and Spain 1995).

Assuming that PSP achieved is proportional to the synaptic current, then PSP amplitude is a function of the potential 'driving force' (the difference between the neuron's membrane potential and the synaptic current's reversal potential) and the conductance of the activated synapse. (The reversal potential is the equilibrium point where no current flows through the activated receptor.)

The effectiveness of different synaptic types may be compared using values of PSP amplitude, membrane potential and estimation of synapse current reversal potentials. The three PSP types considered here have different synapse current reversal potentials (fEPSP ~0mV, fIPSP ~79mV, sIPSP ~93mV).

The sketch graph in figure 2.4 above uses IPSP values found by van Brederode and Spain (1995) in the upper layer pyramid neurons in rat neocortex. Assuming that PSP amplitude is proportional to peak synaptic current, the ratio of gradients in the figure indicates that the fIPSP/sIPSP conductance ratio is approximately 3. Connors et al (1988) report a fIPSP/sIPSP conductance ratio of 6 (for rat neocortex layers 2/3 with stimulation of layers 5/6 table 1 pp448 1988). However, van Brederode and Spain examined IPSPs in layer 2/3 which were evoked by the stimulation of the upper layers, they do not report values for pharmacologically isolated upper layer IPSPs with

the stimulation site in layers 5/6. Brederode and Spain do report that the upper layer triphasic PSP, evoked by stimulation of layers 2/3, is different from the upper layer PSP evoked when the site of stimulation is in layers 5/6. They find a relatively stronger fIPSP and weaker sIPSP in layers 2/3 when the site of stimulation is in the lower layers, hence their observations are at least qualitatively similar to Connors et al.

Conductance ratios for the synapse types and different layers can be estimated in a similar fashion. Table 2.3, below, presents conductances calculated from pharmacologically isolated PSP data reported by van Brederode and Spain. The most striking feature is the variable and weaker fIPSP and nearly absent sIPSP conductances of layer 5 pyramids. Often no sIPSP was found in a layer 5 pyramid. Where an sIPSP was found in layer 5, it was only revealed by strong stimulation and pharmacological blockade of EPSPs (the EPSP blockade avoided the generation of action potentials and their afterpotentials which would have eclipsed the IPSPs, in this instance the relative EPSP conductance presented in the table is estimated from other cases). The last three rows of the table are included for comparison with the conductances reported by Connors et al. Estimates, based on the triphasic PSPs reported by van Brederode and Spain, allow for the interaction of fEPSP and fIPSPs.

Layers	Stimulation site	fEPSP	fIPSP	sIPSP	Comment
2/3	1/2	1.0	2.0	0.6	
5	5/6	1.0	0.45	0.0	
5	5/6	(1.0)	0.47	0.037	(estimate)
2/3	1/2	(1.0	1.5	0.5)	(estimated from
2/3	5/6	(0.67	1.5	0.3)	triphasic PSP)
2/3	5/6	~	1.5	0.25	f/s= 6 Connors et al

Table 2.3 Synapse conductance ratios. Based on van Brederode and Spain (1995), last row Connors et al (1988).

It should be noted that PSPs were evoked using electrical stimulation of a local neuron population and so conductances result from a population of synapses impinging on the recorded neuron. The relative 'connection' strengths represent collective synaptic action, not individual synapses (nor single functional synapses). The relative conductance values are approximate and should be regarded as a qualitative guide to laminar differences. These values, indicating relative connection strengths in the local neural population, are used as a guide for the network models implemented in chapters 5 and 6.

2.4 Neuron types

Many morphological types of neocortical neurons have been identified. A series of studies have related differences in electrophysiology to some common morphological types. Simple models of the impulse generation of these neuron types are introduced in chapter 3.

2.4.1 Neuron electrophysiology

In the sensory neocortex three main types of neurons have been described according to their electrophysiology (Connors et al 1982). These neurons are fast spiking, regular spiking and intrinsically bursting (FS, RS, IB). These were later identified as smooth stellates, pyramidal and large pyramidal cells, respectively (McCormick et al 1985). Layer 4 spiny stellate neurons exhibit RS type behaviour.

The regular spiking neuron (RS) responds to a suprathreshold tonic stimulus by an initial high frequency of firing which declines to a much slower rate (firing rate adaptation). The initial interspike interval (inverse of initial firing rate) reduces proportionately as the stimulus amplitude increases.

Fast spiking neurons (FS) have been difficult to record. The spike produced by a FS neuron has a depolarisation rate comparable with the other types, but the rate of repolarisation is faster resulting in a 'thin' spike of approximately 0.5ms duration. The

afterhyperpolarisation period ('refractory' period) is relatively brief. The response of the FS cell to a tonic stimulus is distinctive in that no, or very little, adaptation of spike train frequency occurs. The FS neuron sustains a firing rate proportional to stimulus strength up to high frequencies.

Intrinsically bursting neurons (IB) differ from the response of RS neurons. Characteristically several spikes occur in clusters or 'bursts' in the initial response to a tonic stimulus. As the stimulus is sustained repetitive bursts may continue or be replaced by a train of single spikes. The spike frequency within a burst is very high and is a product of the cell's intrinsic membrane properties. The frequency of burst repetition is an order of magnitude slower (eg 250Hz/12Hz intra/inter-burst frequency, review Connors and Gutnick 1990). IB neurons appear to be restricted to layer 5 and some have been identified as large pyramidal neurons with thick apical dendrites arbourising in layer 1 (Mason and Larkman 1990). Kasper et al find that the majority of the bursting pyramids project to the superior colliculus (SC) and do not project to the contralateral cortex. Every layer 5 pyramid that projected to the opposite visual cortex was a non-bursting type with a thin apical dendrite terminating in layers 2/3 (rat visual cortex, Kasper et al 1994).

2.5 Discussion of the local neocortex

This section summarises aspects of cortical physiology with the intention of developing a simplified view of the local functional circuit. Studies showing layer differences of neuron distribution and connectivity are used to inform the neural circuit models examined in subsequent chapters.

The organisation of the neocortex into layers and columns may be taken as a starting point when considering local functioning. The distribution of cell types and the connectivity of pyramidal neurons has been extensively studied. Local differences in the functioning of smooth neuron types is less well established.

Relative frequencies of neuron types is summarised in table 2.4 below.

Layers	Type	%
upper	RS	80
	FS	20
lower	RS	80
	FS	15
	IB	5

Table 2.4 Proportions of neuron types in upper and lower layers.
FS number after Hendry 1987. IB proportion estimated from Kasper et al 1994.

Layer	Local Pyramid Connectivity lateral	vertical
upper	9% at <300μm between pyramids strong lateral EPSPs patchy arbourisation to several mm	innervation of 5/6, receive many axons from layer 4
lower	1.5% at <300μm, strong functional synapses patchy axonal arbourisation to several mm	innervation of 2/3 evokes 60% EPSPs, 40% IPSPs

Table 2.5 Summary of local pyramidal connectivity

In the local neocortex the upper layer pyramids project horizontally, with patchy axonal arbourisation to several millimetres, and vertically to innervate the deep layers. Differences in the axonal arbourisation of layer 5 pyramids have been reported. Local axonal projections of IB pyramidal neurons mostly target layers 5/6. In contrast, layer 5 RS neurons possess vertical axon collaterals which arbourise in the upper layers (in rat neocortex, Chagnac-Amitai et al 1990). The distant projections of these two pyramid types also differ. IB neurons project subcortically to the superior colliculus

(SC). The axons of RS pyramids project to ipsi- and contra-lateral cortices (Kasper et al 1994). The local connectivity of pyramidal neurons is summarised in table 2.5 above.

The most striking characteristics of local inhibition are that upper layers are more strongly inhibited than the deep layers and sIPSPs are restricted to the 'home' column (summarised in table 2.6 below). In addition there is some evidence that IB neurons receive weaker IPSPs than other layer 5 pyramids.

	Local inhibitory action	
Layer	lateral	vertical
upper	strong lateral fIPSPs <800μm absent sIPSPs patchy arbourisation to several mm by large cells	smooth population 20% spike vetoing by fIPSPs strong modulation by home column sIPSPs direct inhibition of 5/6
lower	patchy axonal arbourisation to several mm by large cells	smooth population 15% weak and variable fIPSPs variable and absent sIPSPs indirect inhibition of 2/3 evokes 40% IPSPs

Table 2.6 Summary of aspects of local inhibition.

It is not known if the differences in the fIPSP and sIPSP types is correlated with the morphological type of the (inhibitory) presynaptic neuron. GABAa receptors generate fIPSPs and GABAb receptors generate sIPSPs but both bind the same species of transmitter molecule (GABA) and so in principle a presynaptic release of GABA may evoke both fIPSPs and sIPSPs. However, sIPSPs appear to be restricted to vertical columnar projections (<300μm laterally) which suggests some association with a morphological type.

The extent of IPSPs in inhibitory neuron types has not been investigated. However, smooth neurons have been observed to synapse on other smooth cells in the neocortex (Kisvarday et al 1985).

2.5.1 The local neocortical circuit

By combining the classification of the functioning of 'typical' neuron types and the studies of functional connectivity a tentative sketch of the functional local neural circuit may be proposed. In figure 2.5, below, layer 4 is lumped in with the population of the upper layers. Connections between and within subpopulations are sparse. The indicated self innervation of the layers and reciprocal connections between populations does not represent the directly reciprocal connections between pairs of neurons. (Reciprocal connections between closely neighbouring pyramids occur infrequently. Thomson et al 1993 record, in 2/56 connections, pairs of layer 5 pyramids where both evoke EPSPs on the other, but in such cases they find the involvement of a third neighbouring pyramid.)

This simplified local circuit is rich enough in detail to prevent any easy predictions of its dynamic behaviour. The localisation of sIPSPs to the 'home' column might indicate some form of 'gain control' of the reciprocal circuit between upper and lower layers. Weak lateral inhibition might indicate a cooperative interaction with neighbouring columns, strong lateral inhibition should favour a competitive interaction, from this consideration interactions between neighbouring columns is ambiguous. Strong fIPSPs, evoked in the upper layers by lateral stimulation, support the idea of a competitive interaction with adjacent columns. However the weak fIPSPs of the lower layers and the presence of rhythmic IB neurons may result in cooperative recruitment across columns. These behaviours are not exclusive, and could occur at the same time, but at different ranges.

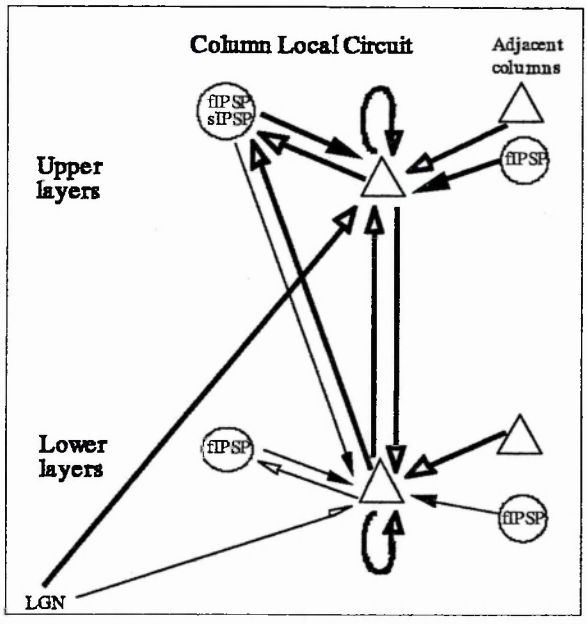

Figure 2.5 Sketch of simplified column circuit with inputs from adjacent columns.

Triangle represents a pyramid population, circle represents smooth cell population. Weight of arrows indicates relative density of connectivity. Open arrowhead fEPSP on target, solid arrowhead IPSP on target. Non-local input shown from lateral geniculate nucleus LGN. Not shown: deep layer exhibit some weak sIPSPs; upper and lower layers have significant reciprocal connections with distant cortical areas; subcortical projections of layer 6 to LGN and layer 5 IB projection to Superior Colliculus.

The ability of the deep layers to evoke strong fIPSPs in the upper layers is intriguing. Neurons within a column share RF preferences. Since RF properties are similar a circuit involving upper and lower layers must fit a model of cooperative behaviour. Hence, it would seem, fIPSP inhibition of upper layer neurons, evoked from deep layer neurons, is part of a mechanism that supports a cooperative response. Perhaps fIPSPs contribute to the controlling of the phase of neuronal action, and so enhance a cooperative dynamic between upper and lower layer neurons. If this is the case, then lateral inhibitory projections, supporting strong fIPSPs, may be an indication of cooperative phase behaviour rather than competitive inhibition. Further, if a columnar cycle exists, the effect of any lateral connections will depend on the origin of the lateral innervation in the cycle of columnar activity. Inhibition in phase with excitatory activity will have an inhibitory effect. Inhibition out of phase with excitatory activity contributing to an oscillation may reinforce the oscillation. In addition, differences in the intrinsic dynamics of neuron types (FS, RS, IB) will also contribute to a phase trajectory of the local circuit. The dynamic role of these different

aspects of the local neocortex may be explored by modelling. Chapter 6 examines a model implementing layer differences in a representation of a single neocortical column; chapter 7 discusses the extension of this model to include adjacent columns and more distant inputs.

2.6 Modelling aspects of local neocortex.

This study is limited to examining aspects of the local neocortex which may contribute to collective oscillations. Model dynamics need to encompass the range of time periods reported for the observed behaviours of oscillation and synchronisation (see chapter 1). The topology of the model neural network should take account of the typical pattern of neuron distribution and connectivity.

2.6.1 The neuron impulse and synaptic transmission

The time constants associated with different synapse types and the distinct dynamics of FS and pyramidal neurons are especially relevant. This thesis uses a phenomenological approach to modelling. Empirically reported values are modelled by 'curve fitting' rather than the explicit simulation of a physiological process. It is intended to reconstruct the qualitative behaviour of the local neocortical circuit. "Each neurone is a spatially extensive, complicated, system. However, what is biologically significant is not the spatio-temporal pattern of activity in a neurone but when this influences other cells." (Holden et al 1992). The task in this thesis is to model and test the dynamics of impulse time series and their transmission across a volume of nodes forming a network. Chapter 3 examines simple models of the neuron excitable membrane and post synaptic potential shapes.

The various values for neuron and synapse types reported above must be considered as approximate. In any case the partial nature of information about the local cortex means that various assumptions have to be made. Additional assumptions are introduced with the aim of simplifying the model to aid the interpretation of behaviours and reducing the computational load of the simulation of activity in a network.

Economy dictates that closely coupled processes are lumped together. For example the chain of events which evokes a PSP at the soma may be represented by a single function (an alpha function is used, see chapter 3) as a 'good enough' first approximation.

As a further measure of model parsimony, additional terms for PSP latency are not introduced. Axonal transmission (in the pre-synaptic neuron) introduces some delay before the initiation of a PSP. However, here it is only intended to model local circuits with sub-millimetre axonal length. This implies a maximum variability of axonal latency in the order of one millisecond. It is proposed that the variation in somatic PSPs time to peak (of the same transmitter type) will be dominated by variation in dendrite-soma electrotonic distance, which can be adequately modelled by the alpha function giving risetimes in the order of several to tens of milliseconds.

The alpha function model of PSP shape has a number of weaknesses. It is not a good model of weak synapse functioning as low quanta release probability is not modelled. However strong functional synapses exhibit transmission reliability, so the generic alpha function may be considered to be appropriate for modelling strong neuronal connections. This introduces an economy of modelling, only one functional synapse between source and target needs to be modelled in place of several anatomical synapses.

An additional postsynaptic simplification is introduced. It is assumed that PSPs will sum linearly at the soma. Nonlinear PSP interactions, for example shunting, are not considered in this thesis. This is justified by the empirical in-vivo observations by Ferster and Jagadeesh (Ferster and Jagadeesh 1992). The linear summation of PSPs were observed at 'in-vivo' levels of synaptic activity. Although, it is noted that non-linear effects such as dendritic saturation have been investigated (Bush and Sejnowski 1994).

The effect of neuromodulators or slow processes of facilitation or depression fall outside the scope of this investigation. In some cases, at least, this may be justified by the time scale of the phenomena. For example NMDA facilitation takes many seconds to develop (Thomson et al 1993).

2.6.2 Neocortical layer differences

Cortical areas differ in detail. The visual cortex is denser and possesses subdivisions of the layering scheme, for example functionally distinct subdivisions are found in layer 4. In contrast the motor cortex lacks the granular layer 4. Yet, cortical areas share generalised features of the distribution of neuron types and column and layer topography. This investigation attempts to include stereotypical features of local neocortex but finer detail is omitted. Neuron and synapse types are each reduced to three. Basic layer and column differences are qualitatively represented by a topography that distinguishes just an upper and lower layer. These simplifications allow a generalised model of a cortical column to be sought. Chapter 6 implements a representation of neocortical layer differences.

The apical dendrite, the archetypal feature of pyramidal neurons, is common to all neocortical areas. However, this stereotypical apical dendrite is not explicitly modelled, even in a simplified form. It may be argued that the empirical data for PSP and neuron excitability (discussed above) is derived from whole pyramidal neurons and so the apical dendrite, or active currents on other parts of the dendritic tree, is included at a phenomenological level. In addition, since it is intended to model local neuronal interactions, the proximal dendrites may be considered more important than the distal dendritic arbour supported by the apical dendrite. If the function of the apical dendrite is passive, it simply reduces the electrotonic distance from the distal dendrites, and so there is no need for a separate model to characterise the action of the apical dendrite.

But there is some evidence for the presence of active conductances on the apical dendrite. In this case, an active apical dendrite may perform a gating function to more distal PSPs. Synapses which impinge on the shaft of the apical dendrite may perform

an important role in this regard (Deuchars et al 1994). The omission of an explicit model element representing the apical dendrite is serious if the apical dendrite acts to modulate a significant proportion of local PSPs. Connors et al demonstrate the presence of active currents on the trunk of the apical dendrite and the modulation of distal EPSPs by the action of the apical dendrite (Connors et al 1994). The apical dendrite may act as a coincidence detector. The back-propagation of an action potential into the apical dendrite coinciding with distal excitatory input can induce the pyramid to fire a burst of 2 or 3 more spikes (Larkum et al 1999).

An alternative modelling approach, which develops a compartment model including explicit physiological processes, may adequately portray the apical dendrite. However the distribution of active conductances over the surface of the apical dendrite is not well established, hence a such a modelling exercise is likely to be protracted and the subject of a thesis in its own right. The omission of a model representing an active apical dendrite may not be serious, at the attempted level of simulation. If the function of the active apical dendrite is to modulate input from distant neurons (cortico-cortical synapses on the apical tuft in layer 1) then it may be omitted from a model of purely local activity. In vivo, locally evoked PSP action does not appear to be subject to strong non-linear effects (Ferster and Jagadeesh 1992, discussed above). The models introduced in this thesis do not include modelling of the active apical dendrite. This omission is reconsidered in chapter 7, together with the consideration of other modelling simplifications.

2.7 Summary

The functional physiology of the local neocortex is reviewed as a guide to the development of a local circuit model of short term behaviour. It is observed that different cortical areas share a general pattern of organisation into layers and columns.

Three neuron types are defined by their intrinsic properties of excitability. These are identified as regular spiking (RS), intrinsically bursting (IB) and fast spiking (FS). RS

and IB neurons are found to be pyramids. FS neurons are smooth. Pyramidal neurons evoke excitatory PSPs (EPSP) on their targets and smooth neurons evoke inhibitory PSPs (IPSP).

Three PSP types are distinguished. These contribute to the typical triphasic PSP found in upper layer pyramids following local electrical stimulation. A fast EPSP (fEPSP) is evoked by a presynaptic RS or IB neuron. Fast and slow IPSPs (fIPSP and sIPSP) are evoked by a presynaptic FS neuron.

For the purposes of modelling, the established classification of six cortical layers are simplified to just two: upper and lower layers. RS neurons are found in all layers (except the traditionally classified layer 1) and comprise around 75% of the neuronal population. IB cells are only found in the lower layers. FS cells occur in all layers (around 20%), but with a lower frequency in the lower layers.

The upper layers exhibit much stronger collective IPSPs than the lower layers. The IPSPs of the lower layers are relatively weaker than the reduced lower layer FS frequency would suggest (lower layer collective fIPSP conductance is around one third or a quarter of the upper layer value), and sIPSPs are weak or absent in lower layer pyramids. Upper layer fIPSPs are capable of terminating EPSP depolarisation and effectively abolishes the generation of an action potential. Lower layer fIPSPs are less effective. Upper layer sIPSPs produce an effective and lasting (hundreds of milliseconds) hyperpolarisation which substantially reduces firing rates.

Stimulation sited laterally evokes strong fEPSPs and fIPSPs, but sIPSPs are not evoked in the upper layers. Stimulation of the lower layers evokes strong fIPSPs and fEPSPs in the upper layers. However stimulation of the lower layers do not directly evoke IPSPs in the upper layers. In contrast, upper layer FS cells directly innervate lower layer pyramids.

A phenomenological modelling approach is proposed. Qualitative models representing the neuron and synapse types are presented in the next chapter. Small circuits,

connecting these elements according to the anisotropies observed in neocortical layers and columns, are examined in subsequent chapters.

3 Simple properties of model elements

This chapter introduces and examines the model components that will subsequently be used to construct networks representing local circuits. The models chosen are intended to reflect some basic properties of the transmission of neural activity.

Two simple generic models are presented. A 'synapse' model portrays the process of transmission between neurons to evoke a post synaptic potential (PSP). The generation of a neural impulse is characterised by an excitable membrane or somatic 'neuron' model. Three types of impulse firing behaviours are modelled, representing fast spiking, regular spiking and intrinsically bursting neurons.

Both excitable membrane and synapse models are based on curve fitting which approximates the physiological behaviour. This approach may be contrasted to biophysical modelling where the physics which form the foundations of a behaviour are explicitly modelled.

3.1 A simple synapse model

The basic time course or shape of the somatic PSP is modelled using an alpha function. The alpha function has a single time constant which controls the rise time and exponential decay (see figure 3.1a, below).

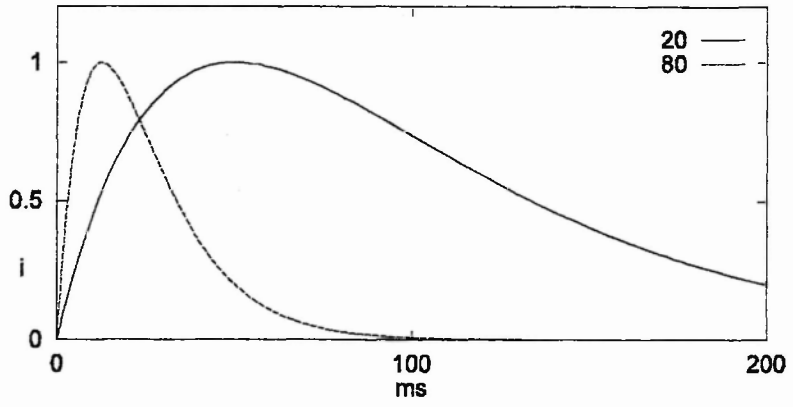

Fig 3.1a The unit current alpha function is defined by the equation $i_{psc} = e \cdot \frac{1}{e^{\alpha}}$

Solid line α=20 and dashed line α=80. The initial rate of increase and the exponential decay is determined by the single parameter α. The rise time is inversely proportional to α.

In the simulation, below, the alpha function unit shape is used as a conductance term in the calculation of a post synaptic current (PSC):

$$PSC_j = f_{\alpha(t_i)} \times w_{ij} \times (x_j - r_i)$$ synapse i acting on membrane j

$f_{\alpha(t)}$	alpha function
w_{ij}	connection weight
x_j	membrane potential of jth cell
r_i	reversal potential of ith synapse
$(x_j - r_i)$	'driving force'

The unit amplitude is multiplied by a weighting factor representing the synaptic connection strength. The driving force is the potential difference between the postsynaptic membrane potential and the synaptic current reversal potential. This PSC term is added to the differential equation which defines the rate of change of membrane potential on an excitable cell model. The resulting post synaptic potential is both a function of the alpha function shape and the dynamic of the excitable membrane system. (The reversal potential is the membrane polarisation which exactly balances the concentration gradient of a particular ion species, so that no current flows through the activated channel.)

Three parameter sets are chosen to portray typical somatic PSP types (table 3.1 below). Empirically observed rise times for somatic fEPSPs and fIPSPs are in a similar range; 2-20ms (reviewed in chapter 2, Mason et al 1991; Nicoll et al 1996; van Brederode and Spain 1995). The post synaptic membrane potential rise time is related reciprocally to the alpha function parameter. The PSP changes by an integral of the post synaptic current, this is process is limited by the current-voltage relationship in the FS neuron impulse model (the dynamics of this model are examined in section 3.2 below). The reciprocal of α for the fEPSP model would suggest a rise time of 1.8ms, however the rise time achieved by the somatic fEPSP model is 5ms. Slower synapse models achieve somatic PSP rise times nearer $1/\alpha$.

The synapse implementation here and in network models in subsequent chapters is represented schematically in figure 3.1b

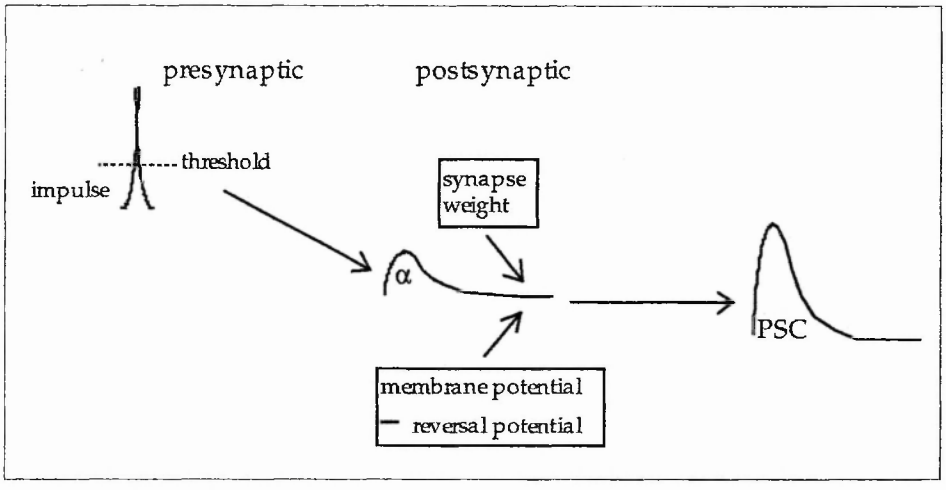

Figure 3.1b Schematic of model synapse. The presynaptic input signal for the alpha function is a thresholding function applied to the presynaptic neuron impulse. The postsynaptic process applies the synapse weight and driving force (membrane potential minus reversal potential) multipliers to the alpha function to find the PSC.

Model current reversal potentials (model rv) are estimated based on the equilibrium points of the neuron impulse model (equilibrium points are examined in section 3.2.1) and observed physiological resting and threshold potentials (reviewed in chapter 2, values for pyramidal neurons taken from Connors et al 1988; Hirsch and Gilbert

1991; van Brederode and Spain 1995). If it is assumed that the subthreshold range of the membrane potential of the impulse model (from resting point A to 'threshold' equilibrium point B in figure 3.6), linearly approximates that of a typical neuron, the biological reversal potentials may be scaled to impulse model values. The model fIPSP reversal 'potential' is set near the membrane potential (model x value) for the resting equilibrium point. The sIPSP reversal is set to a more negative, hyperpolarised, value. The fEPSP reversal potential is selected to approximate the biological 0mV.

synapse type	$\alpha_{(conductance)}s^{-1}$	PSP rise time mS	reversal potential mV	(model rv) x
fEPSP	555	5	0	(0.3)
fIPSP	125	11	-70	(-1.4)
sIPSP	10	107	-90	(-1.8)

Table 3.1 Synapse model parameters

The fIPSC rise time is set to 8mS (=1/α). This is a compromise value based on the empirical studies of van Brederode and Spain (1995) and Connors (1988). These studies record compound IPSPs arising from the simultaneous action of multiple inhibitory synapses. Komatsu et al obtained measurements from the action of a single inhibitory synapse, and found a considerably faster fIPSP rise time of 1 to 2mS (Komatsu et al 1988). This difference may arise from the collective action causing a different dendritic behaviour (ie active conductances), but this consideration is beyond the scope of this thesis. Models in this thesis use the 8mS fIPSC rise time as it is considered to be representative of the conditions that the models are attempting to simulate (with the exception of model 5f in chapter 5).

3.1.1 Synapse simulation

The model's responses to a test signal is examined. The simulation has three parts; a white noise signal source, the alpha function 'synapse' and a target 'cell body'. A noise signal, simulating uncorrelated multiple inputs, is applied to the alpha function via a sigmoid threshold function. The PSC is calculated from the 'conductance' term of the alpha function (using a reversal potential and weighting multipliers) and then added to a sub-threshold excitable cell model (FS impulse model introduced below in section

3.2.1). This current injection evokes the PSP on this target 'cell'. The time series of these PSPs are then compared to the noise series.

The noise input has a high rate of activity. This is intended to simulate the uncorrelated activity in a large number of pre-synaptic sources ($20x10^3$ pre-synaptic input events per second). Hence the 'synapse' simulated here represents a large number of functional synapses but with the same characteristic time constant.

3.1.1a Synapse model results

Simple transmission properties are revealed by the PSP frequency spectra and PSP to input cross-correlations.

All frequencies are equally present in the white noise input signal, this yields a flat frequency power spectrum (not shown). The frequency spectra below show that the PSP models transmit low frequencies and attenuate higher frequencies (figs 3.2a c e). The attenuation of higher frequencies is in proportion to the inverse of the time constant for the particular model (table 3.2). Synapse models with the faster time constants allow the transmission of higher frequencies.

synapse type	Hz at -3dB	PSP rise time mS
fEPSP	25	5
fIPSP	10	11
sIPSP	1	107

Table 3.2 Approximate frequency at half the power of maximum transmission.

The input noise to PSP cross-correlations reveal the respective PSP alpha function shapes (figs 3.2b, d and f). The model synaptic transmission process is simply a convolution of the input series of noise events by the alpha function shape.

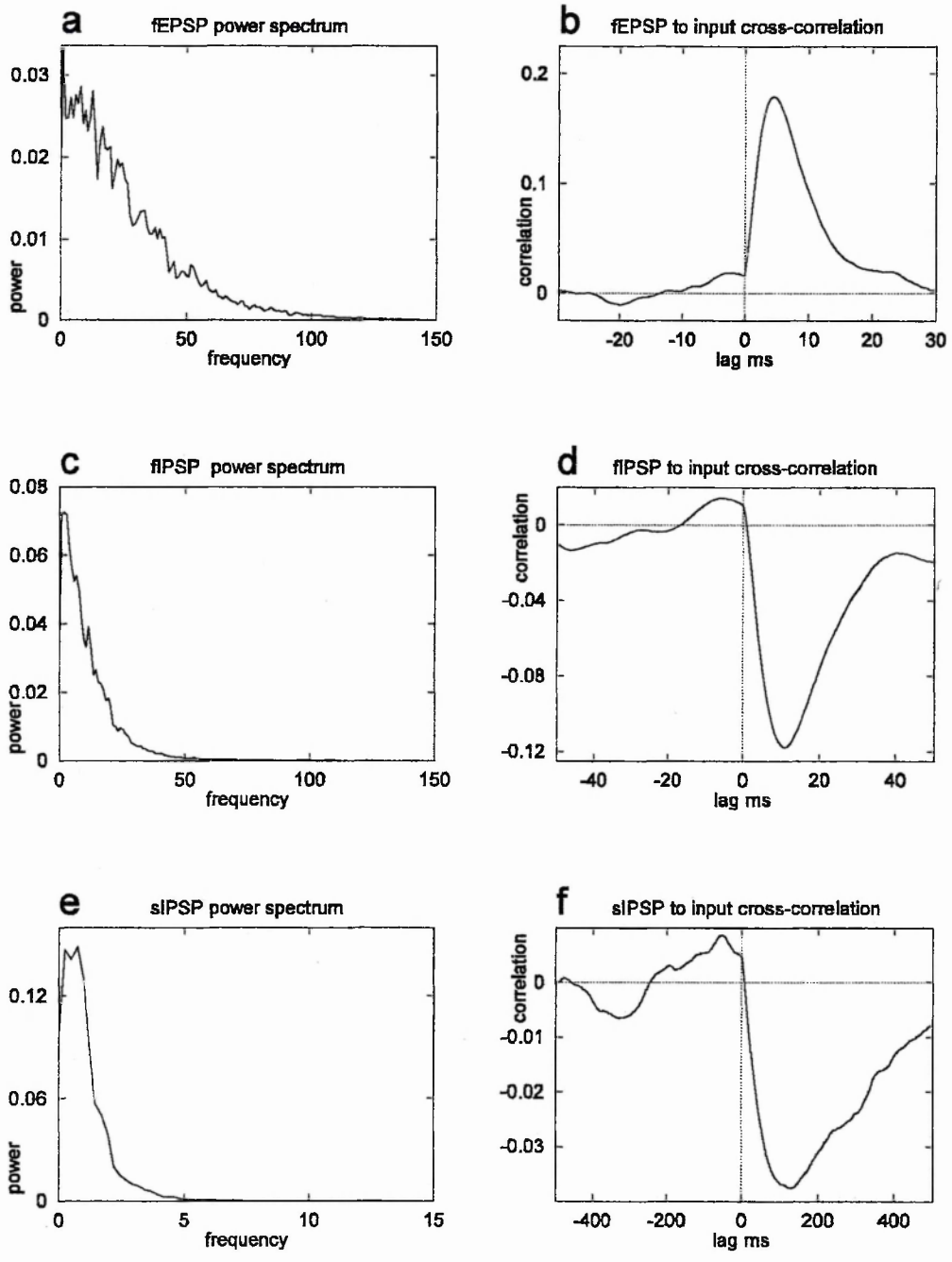

Fig 3.2a-f Responses of model synapses. Model parameters in table 3.1 . The frequency power spectra show that transmission at higher frequencies is strongly attenuated. Cross-correlations show that the lag of maximum response is the same as the respective model rise-time constants. Note the different frequency and time scales for the different synapse types.

Frequency spectra are estimated from the Discrete Fourier Transform of N points of the series h^k

$$H_n \equiv \sum_{k=0}^{N-1} h_k e^{2\pi i k n / N}$$

Correlation of two sampled functions gk and hk, at lag j, is defined by

$$Corr(g,h)_j \equiv \sum_{k=0}^{N-1} g_{j+k} \cdot h_k$$

3.1.1b Discussion

The generic PSP model behaves like a low pass or smoothing filter, the rate of cut-off of higher frequencies is determined by the time constant associated with the particular synaptic type. This high frequency cut-off is quite sharp. For example the 11ms risetime of the fIPSP model, above, may be considered to approximate the 1/4 wave period for a frequency of 25Hz. At this frequency the fIPSP model's transmitted power is around 10dB less than the power at 1Hz in its frequency spectrum (estimated from fig 3.2c). The transmitted power at 60Hz is -9.5dB of the power at 1Hz for the fEPSP model (estimated from figure 3.2a). This indicates that synapses with fast PSP rise times, in the order of a few milliseconds, are required to achieve the robust transmission of frequencies in the cortical gamma range of 40 to 60 Hz.

3.2 Neuron physiology and morphology

In the sensory neocortex three main types of neurons have been described according to their electrophysiology and morphology (reviewed in chapter 2, (McCormick et al 1985). These neurons are **fast spiking, regular spiking and intrinsically bursting (FS, RS, IB)**, identified as stellate inhibitory, pyramidal and large pyramidal cells, respectively. A generic model is introduced and adapted to imitate the qualitative differences in the impulse time series of these neurons. These different neuron model types are incorporated in the simulations of neuron population activity that are examined in subsequent chapters.

3.2.1 A generic excitable cell model

The classic Hodgkin and Huxley axonal model (1952) identifies the contribution of different ionic conductances to the production of an action potential. The desired properties may be built into a model by extending the Hodgkin and Huxley system. But this system is already mathematically complex with four coupled differential equations and six functions. Here it is intended to examine the transmission of activity in a network model. A sufficient neural impulse model is required to characterise the

impulse time series. An adequate model may be built upon a more abstract representation of the impulse dynamic than the Hodgkin and Huxley system. It is not necessary to explicitly separate the biophysical components.

Hindmarsh and Rose (1982) obtain a considerably simpler abstract model. They examine the voltage current relation, but do not explicitly separate the ionic conductances. Their generalised model is developed from some simplifying assumptions; the rate of change of membrane potential, x, is linearly dependent on intrinsic and electrode currents, y and q respectively, and is non-linearly dependent on membrane potential; function f(x) (equation hr1). The rate of change of the intrinsic current y is assumed to be non-linearly dependent on the membrane potential; function g(x), and an exponential decay of current is represented by the -y term in the equation (hr2).

$$\dot{x} = -f(x) + y + q \qquad \text{(hr1)}$$

$$\dot{y} = g(x) - y \qquad \text{(hr2)}$$

membrane potential x, intrinsic current y, clamping electrode current q

(time constants used in Hindmarsh and Rose 1982 are omitted)

They determined the form of the nonlinear functions f(x) and g(x) from a voltage clamp experiment. As a depolarising voltage step is applied an initial inward current occurs, as the voltage step is maintained a steady outward current develops. The initial and late currents are treated separately. Currents were determined for a range of voltage steps, producing an early current voltage curve and a late current voltage curve. These curves are used to determine the form of the functions f(x) and g(x). The shape of the function f(x) is taken from the early current voltage curve. In the resting state y=0 and upon the application of the voltage step the early current, q_0, develops. Assuming y remains 0 then the curve of the early current, q_0, is used to define f(x). The voltage is clamped, so $\dot{x} = 0 = -f(x) + q_0$ and $f(x) = q_0$ (from hr1).

The late current q_∞ allows g(x) to be set. The current is steady hence

$\dot{y} = 0 = g(x) - y$ (from hr2) and from hr1 $\dot{x} = 0 = -f(x) + g(x) + q_\infty$.

or $g(x) = f(x) - q_\infty$.

The variable y should be considered to portray a slow intrinsic or recovery current since the early current is represented by the function f(x).

A cubic function is used for f(x) and a quadratic fitted for g(x) (Hindmarsh and Rose 1984) giving the two variable system:

$$\dot{x} = y - ax^3 + bx^2 + I \qquad \text{(hr 3)}$$

$$\dot{y} = c - dx^2 - y \qquad \text{(hr 4)}$$

I external current, a b c d constants

This model may be adjusted to introduce various behavioural qualities. However, first it is useful to consider the nature of its operation. A time series is shown in figure 3.4 below (line HR). Trajectories drawn in the x-y phase plane indicate the coevolution of the two variables (figure 3.3), the system's null clines and equilibrium points are also shown.

The null cline identifies those points in the phase space (ie the x and y values) where that variable is not changing with respect to another. The intersections of null clines identify equilibrium points in a system as neither variable is changing. In one dimension an equilibrium point can be stable, like a ball in a hollow, or unstable, like a ball on top of a hill. In two dimensions three equilibrium types are possible; stable, unstable and saddle points. The two dimensional stable and unstable points are respectively stable and unstable in both dimensions. The saddle point is stable in one dimension and unstable in the other.

The Hindmarsh and Rose basic two variable model is attractive as it is parsimonious. It can easily be modified by the adjustment of the voltage or recovery current null clines which partition the voltage-current phase space (figure 3.3).

A characteristic of this model, termed by Hindmarsh and Rose as a 'narrow channel property', is the proximity of the x and y null clines in the area close to the label B in figure 3.3. The trajectory of the action potential cycle through this region is indicated (line labelled 'cycle'). Because of the proximity of the null clines the evolution of the system is at its slowest in this channel. This slower evolution corresponds to the inter-spike interval in the first time series in figure 3.4 (line 'HR').

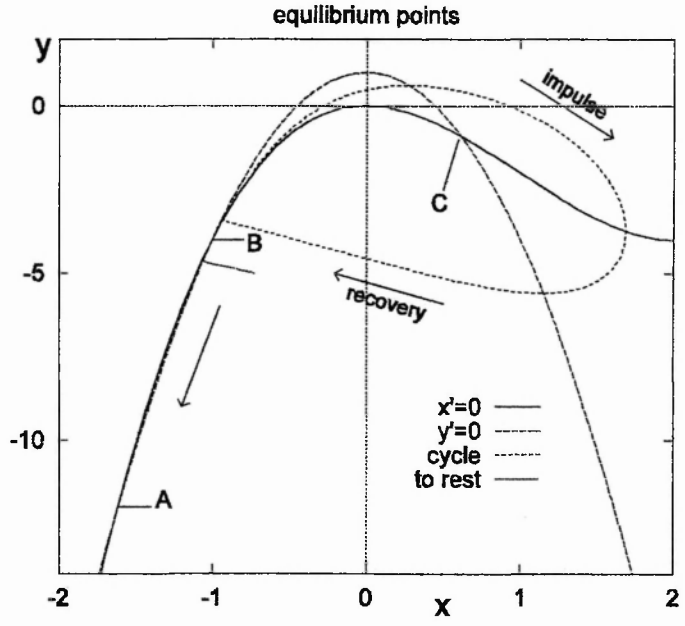

Figure 3.3 Phase plane of the Hindmarsh and Rose model (1984). Parameters {a,b,c,d,*I*} are {1,3,1,5,0}. Equilibrium points at the intersections of the x and y null clines are marked; A is stable, B is a saddle and C is an unstable spiral. The limit cycle trajectory is marked and its direction of rotation is indicated by arrows. This limit cycle corresponds to the first time series shown in figure 3.4. The 'to rest' trajectory starting at a point more negative than B is shown approaching the resting equilibrium point A, its direction is indicated by an arrow.

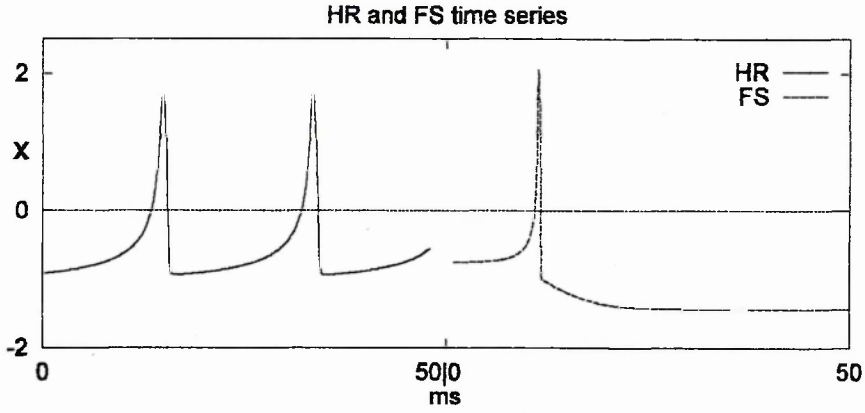

Figure 3.4 Time series of the Hindmarsh and Rose model (1984) and FS model. The limit cycle shown in figure 3.3 corresponds to the line labelled HR. The broken line indicates the FS model time course, corresponding to the trajectory in figure 3.5 .

3.2.1a Fast Spiking impulse model

Hindmarsh and Rose (1984) describe a property of 'triggered firing' in their two variable model, the model could be induced to fire indefinitely following an initial impulse. This is not wanted in the fast spiking (FS) and regular spiking (RS, described below) models. For these a response similar to a typical threshold model is desirable; a spike train is evoked when a supra-threshold input is applied, and the spike train ceases when the input is removed.

Figure 3.3 shows the equilibrium points of the Hindmarsh and Rose system with no external current input (I=0). The relative positions of the three equilibrium points support the 'triggered firing' behaviour. The unstable spiral equilibrium point labelled C is the focus of the limit cycle of a sustained spike train. The recovery side of the cycle (labelled 'recover') approaches the 'narrow channel' of the null clines at a more positive potential than the saddle equilibrium point, B, it enters the narrow channel and continues round, sustaining the cycle indefinitely. The point B may be considered to correspond to the threshold level in a simple threshold and fire model. But unlike a threshold model, once the 'threshold' has been exceeded, sustained firing occurs. If, however, the system is displaced and arrives at a more negative potential with respect to B, then the system evolves towards the rest or stable equilibrium point A (trajectory marked 'to rest' in figure 3.3). (The 'threshold' in this model is not the potential at B, it

is a two dimensional line or separatrix that divides the voltage-current plane and passes through B.)

The triggered firing behaviour is avoided in the FS model by a modification to the y null cline so that the equilibrium point B is more positive than the recovery side of the impulse cycle, so that a limit cycle cannot be sustained. The trajectory shown in figure 3.5 illustrates this. The recovery side of the impulse trajectory in the FS model crosses into a narrow channel between the points A and B. It then slowly evolves towards the resting equilibrium A.

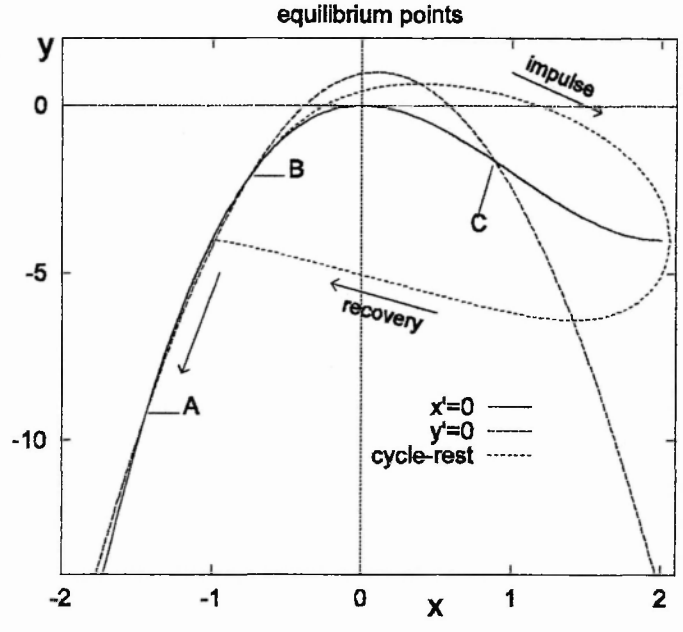

Figure 3.5 Phase plane of the FS model. Parameters {a,b,c,d,k,*I* } are {1,3,1,4.3,-0.1,0}. Equilibrium points at the intersections of the x and y null clines are marked; A is stable, B is a saddle and C is an unstable spiral. An impulse trajectory is shown, arrows indicate the direction of its evolution.

The equations for the FS system are

$$\dot{x} = y - ax^3 + bx^2 + I \qquad \text{(fs1)}$$

$$\dot{y} = c - d(k+x)^2 - y \qquad \text{(fs2)}$$

I external current, a b c d k constants

This modified system only differs from the Hindmarsh and Rose (1984) model by the addition of the constant k to the quadratic which defines the y recovery current rate of change.

The FS model sustains an impulse train with the addition of a tonic current. As I the input current is increased the x null-cline is displaced towards lower y values, the null cline intersections A and B converge and both are abolished. A sustained cycle develops, its frequency is a linear function of I, the current that determines the distance of separation of the null clines on the recovery side. When I is large the null cline 'channel' is no longer narrow and frequency then begins to be limited by the action potential part of the cycle.

3.2.1b Regular Spiking impulse model

The FS and Hindmarsh-Rose models described above achieve a constant impulse rate following the onset of a step current input. In contrast, regular spiking neurons show impulse rate adaptation when stimulated by a tonic current. At the onset of a current the firing rate is high but the impulse train slows or even stops as the current is maintained. Intrinsically bursting neurons also exhibit response adaptation, but the impulse pattern is more complex as initially bursts of impulses occur and as the input is maintained these bursts are replaced by a train of single impulses. Sustained bursting may occur when excitation is strong.

Hindmarsh and Rose (1984) propose a third variable, z, to introduce the property of adaptation. This variable acts as an inhibitory current on the model membrane potential. The rate of change of z is set to be linearly dependent on the membrane potential. Its rate of increase and decay is set by time constants r and s. The z reversal potential is set to the resting equilibrium potential of the system x_{ep}. Equations for the complete three variable system are ;

$$\dot{x} = y - ax^3 + bx^2 - z + I \qquad \text{(hr 3)}$$ hyperpolarising z current

$$\dot{y} = c - dx^2 - y \qquad \text{(hr 2)}$$

$$\dot{z} = r(s(x - x_{ep}) - z) \qquad \text{(hr 5)}$$

I external current, a b c d r s x_{ep} constants

The z rate of change is set to be slow compared to the impulse period, the constant r is set to a low value. Consider the case where an input $I > 0$ is applied. As x the membrane potential rises above the resting potential, z the adaptation variable slowly increases and in turn begins to have a hyperpolarising effect on x. Slowly z will increase to balance the input. If the current I is sufficient to initially evoke an impulse train, (the large depolarisations will make z increase somewhat faster) the adaptation current will start to oppose it. The impulse train will be slowed or stopped given the relative strength of I and the adaptation rate constants.

3.2.1c Intrinsically Bursting impulse model

Hindmarsh and Rose (1984) develop a model of triggered firing (described above in section 3.2.1), a short depolarising current can change a neuron from an initially silent state to a repetitively firing condition. They add an adaptation current, z, to limit this firing to a burst to model the observed action of a molluscan neuron. They find that the model exhibits periodic bursting when a steady current is applied and so is a simple model of oscillatory bursting.

This bursting rests on two features of their model; firstly the triggered firing property (in the two dimensional model) and secondly, the slow rate of adaptation with respect to the impulse cycle. Triggered firing may be explained by considering the relative positions of the equilibrium points in the model's phase space (discussed in section

3.2.1). Starting from rest a transient depolarising current is required to initiate firing. Subsequently a hyperpolarising current is required to terminate firing. In terms of the afferent current a hysteresis exists between an 'on' threshold and a more negative 'off' threshold. In the three dimensional model a slow adaptation, z, current allows many impulse cycles before z grows sufficiently to achieve the 'off' current threshold and terminate the burst. A relatively fast z current will terminate the 'burst' quickly (one impulse is generally not considered to be a burst). The IB model has the same form as the Hindmarsh and Rose three variable bursting model (1984), with the addition of a time constant to balance the relative rates of adaptation current and limit cycle.

3.2.1d Impulse model summary

The FS model shares two general equations with the RS and IB models excepting that the FS model has no z current (hence z==0). The adaptation current z has the same form as in the three variable model of Hindmarsh and Rose (1984).

$$\dot{x} = (y - ax^3 + bx^2 - z + I)\,\tau \qquad \text{(fs3)} \quad \text{(FS model z==0)}$$

$$\dot{y} = (c - d(k+x)^2 - y)\,\tau \qquad \text{(fs4)}$$

$$\dot{z} = r(s(x - x_{ep}) - z) \qquad \text{(hr 5)}$$

I external current, a b c d k r s x_{ep} τ constants

The time constant τ is introduced to adjust the rate of evolution of the impulse model. McCormick et al (1985) report impulse widths of around 1.7ms to 0.7ms (spike width at base for RS and FS cells). The τ value is chosen so that one time unit in the model approximates one physiological millisecond for the above threshold region where an exponential increase culminates in an impulse. The FS impulse can be seen to be 'thinner' than the unmodified Hindmarsh Rose model impulse in figure 3.4 above.

	a	b	c	d	k	r	s	x_{ep}	I	τ
Fast Spiking (z==0)	1	3	1	4.3	-0.1	-	-	-	0.25+input	3
Regular Spiking	1	3	1	4.3	-0.1	0.08	5	-1.5	1.7 +input	3
Intrinsically Bursting	1	3	1	5.0	0.0	0.02	5	-1.5	1.7 +input	3

Table 3.3 FS, RS and IB impulse model parameters

The FS and RS models' x and y parameters are the same. The adaptation rate r of the RS model is faster than that of the IB model. The triggered firing property is retained in the IB model (parameter k=0).

3.2.2 Impulse models simulation

3.2.2a Method

A noise input, simulating current from multiple uncorrelated sources, was directly applied to the rate of change of x, the models membrane potential. A tonic input was also applied to evoke a train of impulses.

3.2.2b Results

Qualitative differences may be seen by inspection of the raw time series for the three excitable cell models.

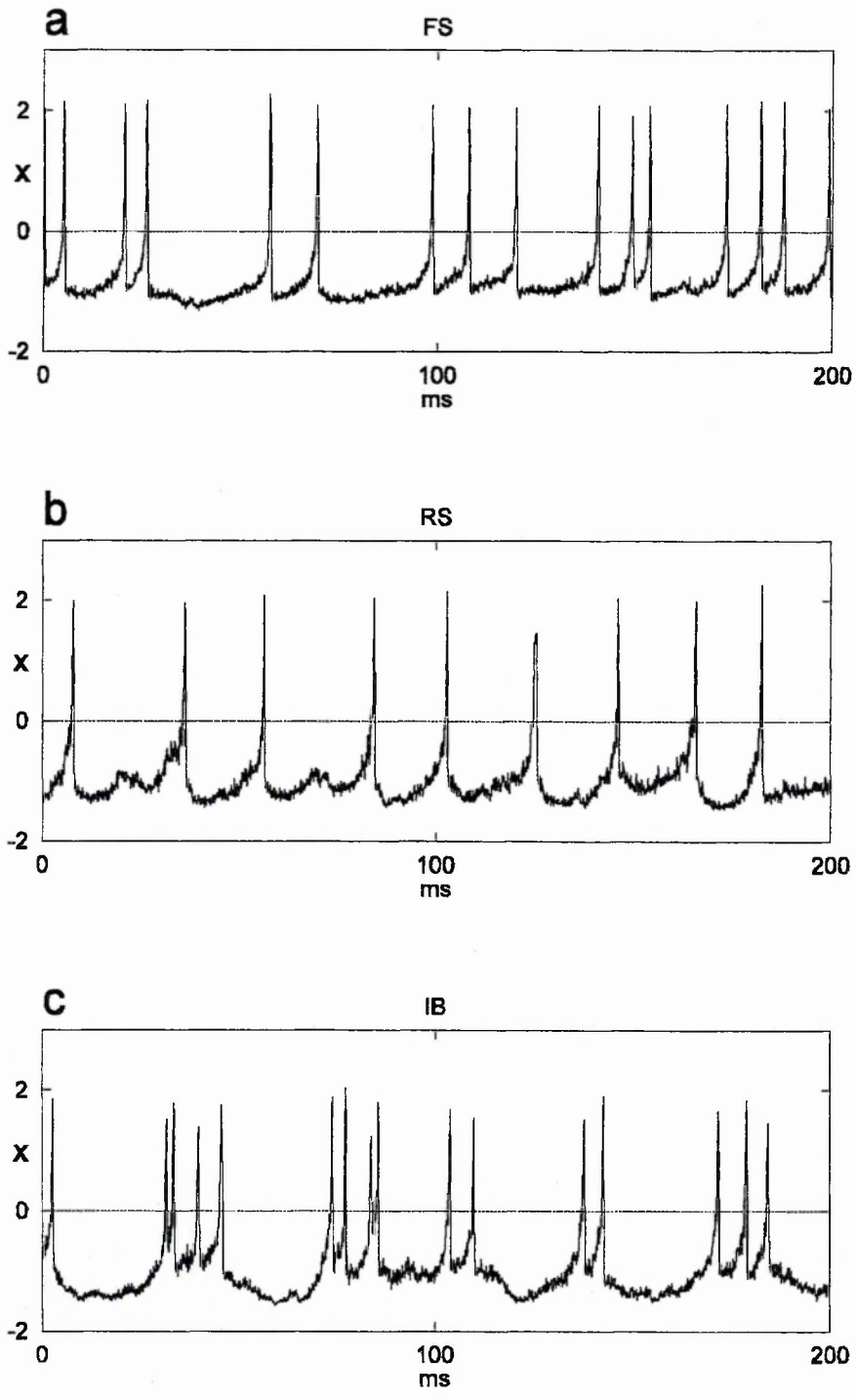

Figure 3.5 a-c Short impulse time series **a** FS, **b** RS, **c** IB responding to a noise input. Parameters in table 3.3. The impulse time series of the RS model appears more regular than that of the FS model. The IB model exhibits a clustering of impulses, evidence of bursting behaviour is limited to two impulse doublets near 30 and 90ms.

The cross-correlation of the RS impulse time series is shown in figure 3.6. There is a modulation of impulse probability at positive lags. However this tendency is not very clear. The impulse time series are very sparse (pulse widths are around 2ms and

impulse frequency is in the range 40-80Hz so the impulse series is non-zero for around 0.05~0.025 of the time series). The resulting cross-correlation is quite 'noisy' (not shown, FS and IB cross-correlations showed no clear trend).

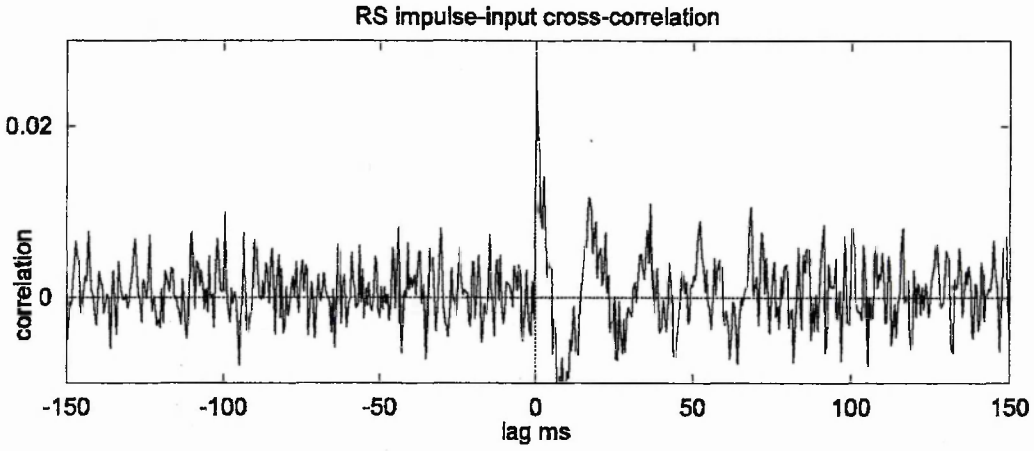

Figure 3.6 Cross-correlation of noise input to RS impulse series.

The auto-correlation of the RS impulse series (in figure 3.7d, below) shows a clearer response structure that is otherwise qualitatively similar to the lag side of the cross-correlation (figure 3.6, above).

In figures 3.7a and 3.7b, below, the FS impulse power spectrum is nearly flat, with both low and high frequencies well represented. The auto-correlation of FS impulse activity shows a short refractory period of around 2 mS following an initial impulse. The firing probability rebounds to be slightly enhanced around a delay of 10 mS, subsequently the probability of firing remains constant with increasing delay. This characteristic is reminiscent of a leaky integrator threshold impulse model. A step change of tonic input evokes a simple change in the sustained FS model impulse firing rate (not shown).

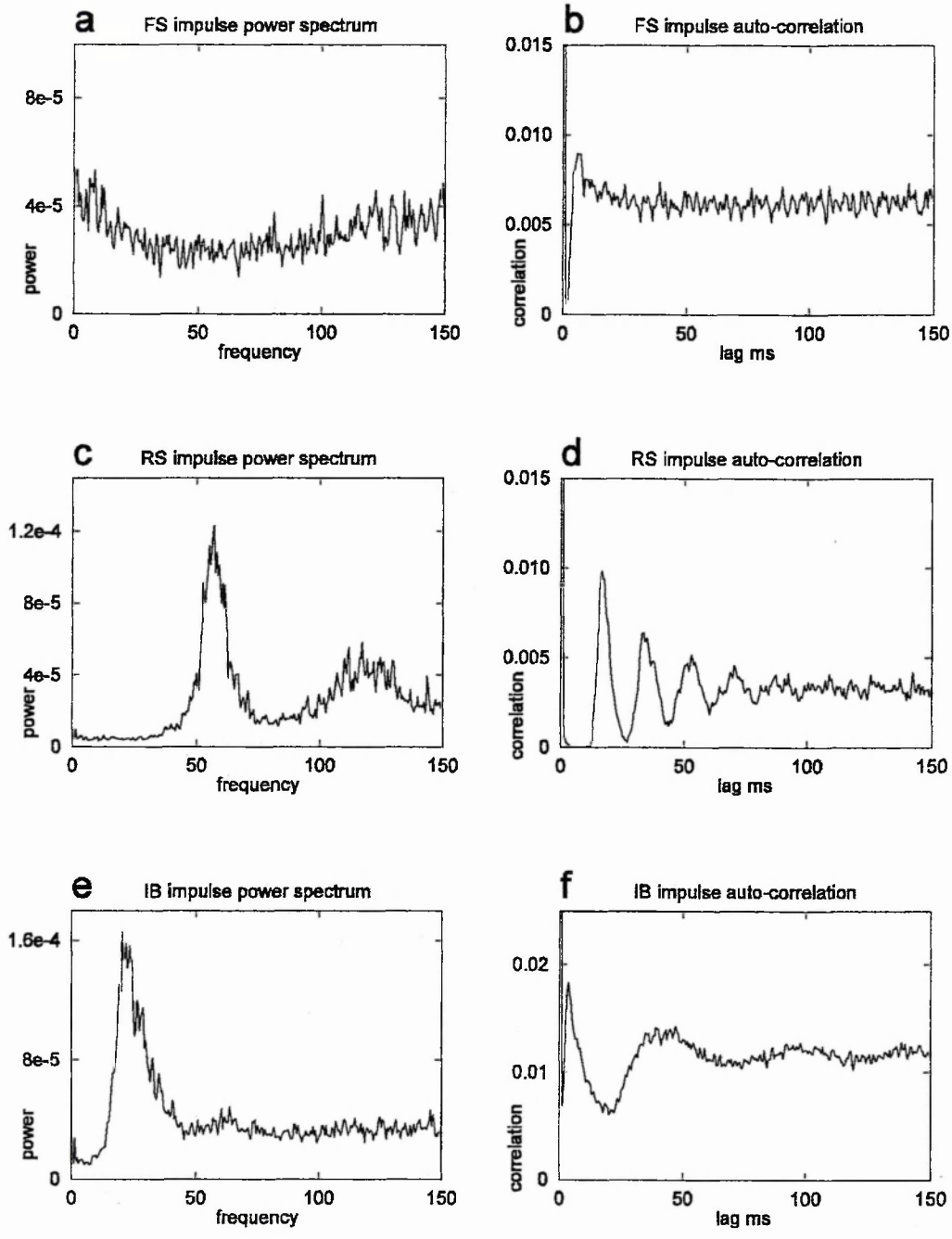

Figures 3.7a-f Impulse transmission spectra and auto-correlations for FS, RS and IB models.

The RS model exhibits a very different power spectrum. Low frequencies are nearly abolished and there is a large peak in power spectrum at approximately 56Hz and a weak peak around 120Hz. The auto-correlation of the probability of firing is low for 12ms following an initial impulse, subsequently inhibited and enhanced probabilities of firing occur at intervals with a period of 17.5ms which corresponds to the period of the frequency peak in power spectrum.(In figures 3.7c-d.) Thus the RS model has an

intrinsic frequency of activity. A step increase in the tonic input results in an initially fast firing rate that slows as the adaptation process comes into effect (where the increase is large enough, not shown).

The pattern of response of the IB model is similar to the RS model, but slower (figures 3.7e-f, above). The autocorrelation indicates that following an initial impulse and a brief refractory period (~3ms) firing probability is immediately enhanced, subsequently inhibited and then enhanced again around a lag of 42ms. The power spectrum shows peak around 22Hz, this denotes the lower intrinsic frequency of the IB model. Unlike the RS model the IB model has an enhanced firing probability at a very short delay of 4ms following the initial impulse. The impulse doublets in figure 3.5c. are instances of this short delay firing, this is due to the burst firing property. The IB model responds to a step increase in tonic input with an initial impulse burst. As the adaptation process comes into effect subsequent bursts contain fewer impulses (where the tonic step increase is large enough, not shown).

3.2.2c Summary of results

The neuron impulse models are compared in table 3.4. The FS model has a simple impulse firing response where the rate of impulse firing is sustained following the onset of a tonic input (or step input). In contrast, a step input to the RS and IB models, evokes an initially high rate of impulse firing that slows. The adaptation process governs the sustained impulse firing rate in the RS and IB models. Both the RS and IB models exhibit an intrinsic firing rate that is related to the adaptation process.

Model	Variables	Impulse train characteristic	Frequency Hz (in range 1-100)
FS	2	threshold with brief refractory period sustained impulse firing rate	variable
RS	3	adaptation of impulse firing	~56
IB	3	adaptation of impulse burst firing	~22

Table 3.4 Comparison of impulse firing models

Note that the indicated characteristic frequency applies to the chosen parameter sets

3.2.2d Discussion

The neuron impulse models transmit higher frequencies in contrast to the alpha function model synapses. The FS model transmits a broad spectrum and its responsiveness seems only limited by the refractory period of the impulse cycle. High frequencies are passed by the RS and IB models at nearly the same power level as that achieved in the FS model. It is notable that both the RS and IB models have characteristic resonance frequencies and responses at lower frequencies are nearly abolished. The resonance and the attenuation of lower frequencies is a consequence of the action of the third variable, the adaptation current z, in these two models.

These different properties, the intrinsic resonance in the RS and IB models and the contrasting low-pass ability of the FS model (or lack of low frequency attenuation), indicate very different roles for these elements in the phase behaviour of a network.

3.3 Alternative modelling approaches

The above models retain some of the temporal properties of neurons and synapses and their simplified form contribute to the tractability of larger scale network modelling. The synapse model represents a simplification of pre and postsynaptic processes; a further simplification of the alpha function synapse model does not seem reasonable. The FS model is a two variable system based on the Hindmarsh and Rose (1982) impulse model. Any further simplification of the neuron models leads to a consideration of single variable models.

Kistler et al develop a single variable 'spike response' model neuron (SRM) as a simplification of the Hodgkin and Huxley system (Kistler et al 1997). This model includes a response function to represent the impulse and after-potential, and response kernels to account for membrane voltage variation due to inputs. Spike trains resulting from noisy inputs are compared to the spike train series produced by the Hodgkin and Huxley system (HH). The SRM model successfully predicts 90% of the HH spikes; an integrate and fire model achieves 43%; and integrate and fire with moving threshold

achieves 70% of the HH spikes (estimated from figure 8, coincidence measure by Kistler et al). Kistler et al suggest that modelling adaptation of the firing rate might be obtained by including a function that integrates previous episodes of afterpotential hyperpolarisation. However the derivation of the response kernels is non-trivial (the response kernels are found by analysis and numerically); finding the response kernels to include adaptation and burst firing, to allow modelling of RS and IB neuron responses, is likely to require an extended study. Higher order kernels include many terms, and although a reduced variable system may be obtained, it is unclear if a network simulation would be more computationally efficient.

Fitzhugh proposes a two variable model that represents some of the properties of the excitable membrane (FitzHugh 1967). This is a somewhat simpler system than the two variable Hindmarsh and Rose model and may be less computationally demanding in a network simulation. The Fitzhugh abstract oscillator model would require some adjustment to represent the different firing patterns for FS, RS and IB neurons.

Chay examines a three variable model of an excitable membrane (Chay 1985). This includes an adaptation current and is comparable to the Hindmarsh and Rose (1984) three variable model (HR3). The Chay model is a simplification of the HH system and explicitly retains HH terms for certain conductances. As a result the Chay system is more computationally expensive than the HR3 equations.

More detailed models of synapse, postsynaptic and neuron functioning are available. For example, postsynaptic transmission over the dendritic tree may be implemented. Rall et al consider the passive transmission of PSPs in a model of the dendritic arbour of a pyramidal neuron. They point out the contribution of the cell's morphology to the postsynaptic response (Rall et al 1992). The passive compartment model represents the dendritic tree as a network of connected RC compartments (resistor and capacitor). The spatio-temporal pattern of activation of synapses contributes to the PSP shape that is achieved at the soma. Such properties introduce temporal signal processing properties.

The intention of network modelling in this thesis does not require a detailed representation of the (passive) dendritic tree. An implementation that includes a range of alpha function rise times may be considered to represent the effect of different synapse positions, sufficient for a model including 'local' connectivity.

Compartment models which implement active conductances have been investigated. Rhodes and Gray model a large layer 5 pyramidal neuron (Rhodes and Gray 1994). A detailed compartment model includes the distribution of active conductances on the dendrites. Dendritic calcium impulses are found to contribute to the generation of bursts of impulses.

The models in this thesis only implement the active conductances that achieve an impulse in the soma or axon. This is justified (chapter 2, section 2.6) on the basis that local connectivity is less likely to involve the more distal dendritic synaptic inputs and the empirical whole cell recordings lump the synaptic and dendritic transmission together, so the model implicitly includes these processes. Following the results of the network simulation in chapter 6, the importance of active dendritic conductances is reconsidered in chapter 7.

The Hindmarsh and Rose models (1982 and 1984) are abstract models of impulse generation and are the basis of the FS RS and IB neuron models presented in this chapter. The impulse model is mathematically represented as a point process (these impulse models do not explicitly model the surface of a neuron), and may be compared to a single compartment in a compartment modelling system. The alpha function synapse model may be considered as acting in a separate compartment, linked to the neuron compartment by an input current term. These simplified neuron and synapse models may be compared to the model elements used by Bush and Sejnowski (1996) in a simulation of local cortical activity. The Bush and Sejnowski neuron models are reduced compartment models. The soma has active conductances and other compartments are passive. Alpha function synapses are made onto various neuron compartments, so there is a variation of somatic PSP shape due to differences in dendritic (passive) conduction. This variation is not great as Bush and Sejnowski do

not implement the distal dendrites and they implement an electrotonically 'compact' cell (length constant $\lambda = 2.97$, reported range of dendritic λ is 0.5 to 2, (Segev 1992). In the absence of an explicit model of the passive dendritic tree this variation of somatic PSP shapes might be achieved by implementing a wider range of model synapse time constant values (so lumping the synaptic and dendritic conduction processes together). This 'lumped synapse' approach is used in the models presented in subsequent chapters. Although the detailed compartment modelling of Bush and Sejnowski is omitted, a qualitatively similar model is obtained. The Bush and Sejnowski pyramidal neuron models place HH type conductances, with an adapting conductance, in one 'somatic' compartment to achieve a bursting behaviour. This is qualitatively similar to the IB model presented in this chapter. Similarities between the modelling approach of this thesis and the modelling of Bush and Sejnowski is discussed further in chapter 5.

The simplified synapse and impulse models presented in this chapter are intended for a limited application; the modelling of fast oscillatory activity in a 'local neocortical circuit'. The scale of the modelling is restricted, and simplifications are made to increase the computation tractability of the model, whilst retaining certain characteristic neocortical features. Inclusion of other features of neurophysiology would require extensions to the modelling elements, or a different modelling approach. Where further biophysical detail is required, but computational efficiency is important, other methods are available (Destexhe et al 1994). Kinetic models which define the rates of reaction between states may be implemented efficiently, and the state transition models, containing the set of the states and their possible transitions, can be obtained by analysis or curve-fitting.

3.4 Summary

Qualitative models of post synaptic potential and neuron impulse are introduced. Parameters allow the implementation of the different types of synapses and neurons with contrasting transmission properties.

PSP models are based on the alpha function. These model synapses function as passive low-pass or smoothing filters. Neuron impulse models are based on modified Hindmarsh and Rose phase plane models (the triggered firing property is retained in the IB model, but RS and FS do not support triggered firing). The two variable fast spiking (FS) model transmits a broad frequency spectrum including the high frequencies. The three variable regular spiking (RS) and intrinsically bursting (IB) models transmit high frequencies as effectively. Both the RS and IB models have a band-pass characteristic where their response is enhanced at an intrinsic resonant frequency. The transmission of lower frequencies is effectively abolished in these two models.

The interaction of these models is examined in the next chapter. Small circuits are studied, as an initial step in the development of larger scale simulations in the subsequent chapters.

4. Properties of simple local circuits

This chapter examines simple circuits which combine the model elements presented in chapter 3. These demonstration circuits serve to link the simple models in chapter 3 to their incorporation into larger scale networks where population activity is studied in chapters 5 and 6. Here, the interaction of a few model neurons and synapses and neurons is examined in a 'feedforward' circuit and a reciprocal circuit. The form of these circuits is guided by empirical results regarding local cortical receptive field (RF) functioning and local connectivity.

A functional feedforward description of local connections has been given to account for the RF properties of neurons in the visual cortex (Hubel and Wiesel 1962). This early proposal for the functional role of local connectivity is sufficient for a minimum account of the different RF properties; successive layers of a feedforward circuit achieves more complicated RF properties by a combination of responses from a previous layer. In the pathway from thalamus to layer 4 to layer 3: a line of LGN centre-surround responses are amalgamated to achieve a simple orientation preference RF in a layer 4 neuron; a layer 3 complex RF response (for example orientation preference with end-stopping) is achieved by a combination of layer 4 responses. This functional proposal was made in the knowledge of the presence of a far more complex local connectivity, however it succeeds in giving a basic account of these RF properties.

Subsequent studies have built on the early contribution of Hubel and Wiesel. It is observed that the orientation tuning of layer 4 cells is sharper than can be accounted for by their direct LGN inputs (review Sompolinsky and Shapley 1997). It is proposed that lateral feedback inhibition contributes to this (based on in-vivo suppression of lateral inhibition (Crook et al 1998a). Local lateral inhibition is an important factor in achieving RF responses.

Stratford et al conclude that intracortical afferents provide most of the excitation input to the simple cells in layer 4. They find that layer 4 spiny stellate cells receive most of their inputs from other layer 4 cells and layer 6 pyramidal cells (both with restricted lateral range). The volume of local cortical connections compared to thalamic afferents suggests that the interlaminar vertical recurrent circuit has an important role in shaping RF properties (Stratford et al 1996). The functional contribution of the local vertical circuit to RF properties is not extensively studied.

A purpose of this thesis is the examination of fast temporal behaviours in the cortical local circuit. It is not intended to construct circuits which reproduce RF properties. However it is reasonable to study representations of local feedforward and recurrent circuits, justified as being biologically probable and relevant to explanations of RF properties.

4.1 Two circuits

This chapter examines two basic circuit configurations. A simple feedforward chain model allows a study of the timing of 'feedforward' impulse transmission between different neuron types. This chain model could be considered to represent the 'forward' propagation of activity from layer 4 to 3 or the lateral intralaminar propagation between adjacent columns. A reciprocal circuit is presented, including features representing the interlaminar vertical circuit of an upper and lower layer.

These simple model circuits are implemented with just one model neuron acting as a distinctive element in the circuit (one neuron of each type in each layer). Accordingly the interpretation of the behaviour of these circuits is limited, the circuits do not achieve a good representation of the actions of populations of neurons. However, strong functional synapses that are capable of recruiting an impulse on the postsynaptic pyramidal neuron have been observed (observation of large EPSPs and disynaptic EPSPs in layer 5 pyramids (Thomson et al 1993) and so the activity in the

model circuits may be considered to represent the early local propagation via strong synapses before large numbers of neurons are involved.

4.1.1 Chain circuit

This model is based on simplified descriptions of local connectivity that emphasise the feedforward propagation of activity (for example layer 4 to 3, figure 1 in (Martin 2002), with the omission of any 'feedback' connections between the 'layers'. The chain model includes connection weights which represent the typical ratio of post synaptic conductances (PSC) in the upper layers of the neocortex (discussed in chapter 2). Each stage of the full chain model includes a pair of FS and RS excitable membrane models with associated alpha function synapses. Within a stage the RS FS pair are reciprocally connected. The FS element makes both fIPSP and sIPSP connections to the RS model and receives a fEPSP from the RS model element. The chain has a feedforward configuration, RS_1 and FS_1 elements project onto the elements in the next stage, RS_2 and FS_2. Later stages do not project back to an earlier stage. A schematic of the chain model is shown in figure 4.1a. The configuration in 4.1d implements feedforward transmission between two RS elements for comparison with the model including FS neurons.

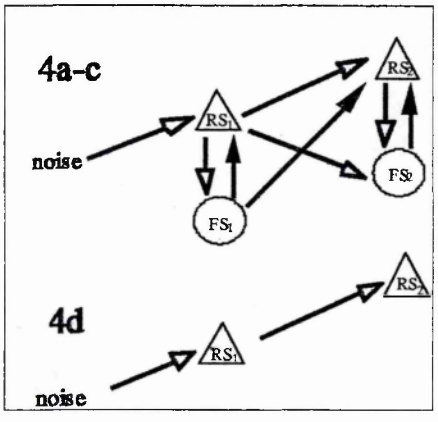

Figure 4.1 Chain model circuit. **a** Full chain model includes RS and FS (conditions 4a-4c) , **d** RS only chain for comparison (condition 4d). Triangle RS , circle FS , open arrowhead fEPSP innervation, solid arrowhead fIPSP and sIPSP innervation. FS and RS elements receive weak independent disturbance signals (not shown).

A noise input (independent Poisson time series, activating a alpha function model synapse) is implemented. This represents an external, uncorrelated input, for example LGN input to layer 4.

4.1.2 Reciprocal circuit

The reciprocal circuit includes weights and connections which represent the differences found between upper and lower neocortical layers (figure 4.2). A simplified configuration of two layers is studied.

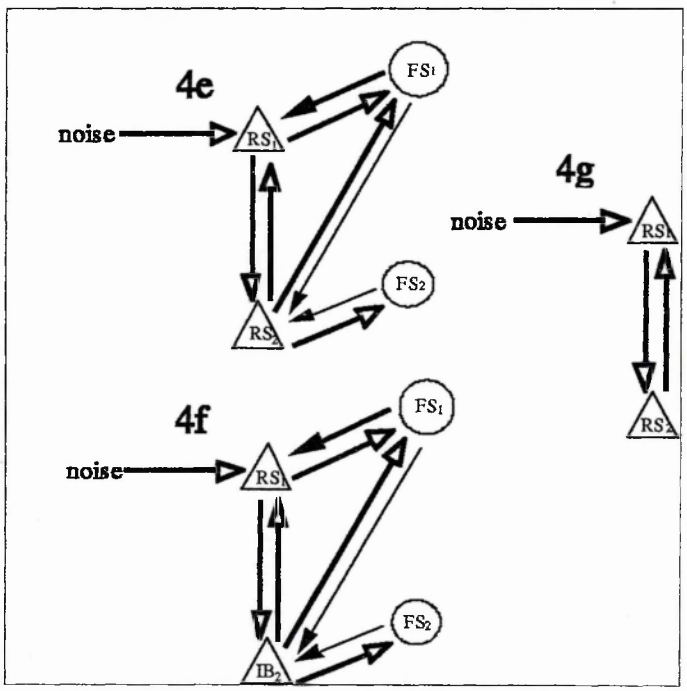

Figure 4.2 Reciprocal model circuit. Upper layer RS_1 and FS_1, lower layer RS_2 and FS_2. **4e** Full reciprocal model includes RS and FS. **4f** RS-IB reciprocal model, lower layer includes IB_2 element in place of RS_2. **4g** RS only reciprocal model for comparison. Triangle RS, circle FS, open arrowheads fEPSP and solid arrowhead is both fIPSP and sIPSP innervation, connection strength indicated by weight of arrow. FS and RS and IB elements receive weak independent disturbance signals (not shown).

Each layer is comprised of a FS and RS pair. The upper layer RS_1 element is more strongly inhibited than the lower layer RS_2 (4e). The configuration includes reciprocal connections between the model elements with the exception that the lower layer FS_2 element does not target the upper layer elements (neocortical laminar differences are

discussed in chapter 2). Again a comparison configuration is implemented which includes no FS elements (4g). In addition, a reciprocal circuit model with a IB element in the lower layer is implemented (4f).
Each layer is comprised of a FS and RS pair. The upper layer RS_1 element is more strongly inhibited than the lower layer RS_2 (4e). The configuration includes reciprocal connections between the model elements with the exception that the lower layer FS_2 element does not target the upper layer elements (neocortical laminar differences are discussed in chapter 2). Again a comparison configuration is implemented which includes no FS elements (4g). In addition, a reciprocal circuit model with a IB element in the lower layer is implemented (4f).

An external input (independent Poisson time series, activating a alpha function model synapse) is placed on the RS_1 in the upper layer to represent a distant input (for example LGN input to layer 4).

4.1.3 Model limitations

The parameter values chosen for individual 'synapse' and 'neuron' elements are estimated from results in neurophysiology where local neocortex sub-populations have been studied (see chapter 2, section 2.3.4).

A single model element represents a nominal neocortical subpopulation. The simple scheme of connections includes reciprocally connected elements. In the local neocortex subpopulations are reciprocally connected, however identified pairs of neurons have a low probability of direct connection and directly reciprocal innervation is rare. The dynamics of the model may be compromised by the implementation of directly reciprocal connections, but only low rates of activity have been simulated in an attempt to minimise this problem.

The alpha function 'synapse' implemented in these model circuits should only be considered as a reasonable approximation of the PSP achieved by a strong functional synapse. The model 'synapse' element does not include a model of release probability of transmitter quanta, and so is not a good model of the weaker PSPs. Due to the lower

probability of transmitter release, weaker synapses are also less reliable. In addition PSPs are assumed to sum linearly and no active dendritic currents are modelled.

Axonal and dendritic transmission contribute latency and shape to the PSP, however, the alpha function does not model these as separate processes. A 'local' circuit can be considered to include distances in the order of 300µm, implying an axonal delay of <0.3mS (assuming an axonal transmission rate of $1mS^{-1}$ approximately). The PSP model ignores this delay, as it is small compared to the PSP rise time. In addition, van Brederode and Spain(1995) (see chapter 2 section 2.3) record PSPs using clamp electrodes on the pyramidal cell body, hence the recorded PSP shape includes dendritic transmission from more peripheral synaptic sites. The alpha function parameters are based on these empirical values (Chapter 3 table 3.1).

4.2 Methods

Parameters used are the same as in Chapter 3 (tables 3.1, 3.3) and elements are combined in various configurations to represent the different circuits. The excitable cell input has a tonic part (table 3.3; I) and a variable part. In the circuit models, the variable input is implemented as a weighted sum of the different alpha function 'synapse' inputs together with a 'synapse' noise signal. The presynaptic input 'signal' for the alpha function model synapse is a thresholding function applied to the presynaptic excitable membrane model.

Where more than one synapse of the same type occurs on a single excitable membrane element (for example, figure 4.1a, FS_2 receives two fEPSP connections in the full chain model) the conductance weight is divided equally to preserve the conductance ratio of the different synaptic types.

A strong simulated synaptic noise signal was applied to the 'input' element of each circuit model (RS_1). Weak disturbance signals, comprised of mixtures of independent noise signals, were applied to other neuron elements (0.1 the level of the input signal).

The noise process was implemented as an independent Poisson event series with a mean interval of 5mS. This noise event time series was filtered with an alpha function to simulate the fEPSC shape and then applied to the input element. Moderate spike rates were obtained by applying a constant bias level or 'tonic' input to the neuron elements. Spike trains, in the order of several hundred events, were recorded for each neuron element (recording simulations for 200 to 300 S of simulated time).

Certain parameters were varied to examine the behaviour of the circuits under different conditions. Tables 4.1 and 4.2 summarise the different conditions for the two circuit models.

4.2.1 Chain model conditions

	RS1 noise input	Tonic input				comment
		RS1	RS2	FS1	FS2	
4a	0.2	2.5	3.1	0.14	0.14	
4b	0.6	2.5	3.1	0.14	0.14	noise input+
4c	0.2	2.7	3.1	0.18	0.18	FS fast
4d	0.2	1.2	1.4	-	-	RS only

Table 4.1 Chain model conditions : input weights

4a Moderate noise input, tonic input levels set to achieve a spike rate of $10S^{-1}$

4b Strong noise input to RS_1

4c FS tonic input increased to achieve a faster spiking rate.

4d RS only chain.

The different conditions for the chain model were: 4a moderate level input signal; 4b strong noise input signal; 4c moderate input with FS biased to achieve a faster spike rate; 4d moderate input to chain of RS only (table 4.1). The tonic levels were set to achieve an average spiking rate of around $10S^{-1}$ for the moderate input case and RS only cases.

4.2.2 Reciprocal model conditions

	RS1 noise input	Tonic input				comment
		RS1	RS2/IB2	FS1	FS2	
4e	0.2	2.7	1.55	0.14	0.12	
4f	0.2	2.9	0.8	0.14	0.14	IB2
4g	0.2	1.1	1.55	-	-	RS only

Table 4.2 Reciprocal model conditions; input weights

4e Moderate input to RS_1

4f IB element in the lower layer

4g RS only reciprocal circuit.

The reciprocal model was tested in three configurations each with a moderate input signal level: 4e the full model; 4f the RS only comparison; 4g RS-IB where an IB element replaces the RS_2 element (figures 4.2a, 4.2b, 4.2c). Tonic levels were chosen to achieve average spike rates in the order of $10S^{-1}$ (table 4.2).

4.3 Results

Spike time series were recorded for all the model neurons in the different model circuit conditions.

4.3.1 Chain model

Time series for the first stage of the chain model are shown below in figures 4.3a and 4.3b (condition 4a). The impulse series of the RS1 model neuron is irregular. The rate of impulse activation is much lower than the intrinsic frequency of the RS model (due to the action of the adaptation variable). The RS_1 neuron shows a sub-threshold variation due to the strong noise input. In addition there is a tendency for a damped sub-threshold oscillation (for example figure 4.3a, following the impulse after 1500mS). The time series of the FS_1 model neuron closely follows the RS_1 series.

Where two RS_1 impulses occur close together, a burst of FS_1 impulses are induced (for example figure4.3b, around 1200mS and 1900mS).

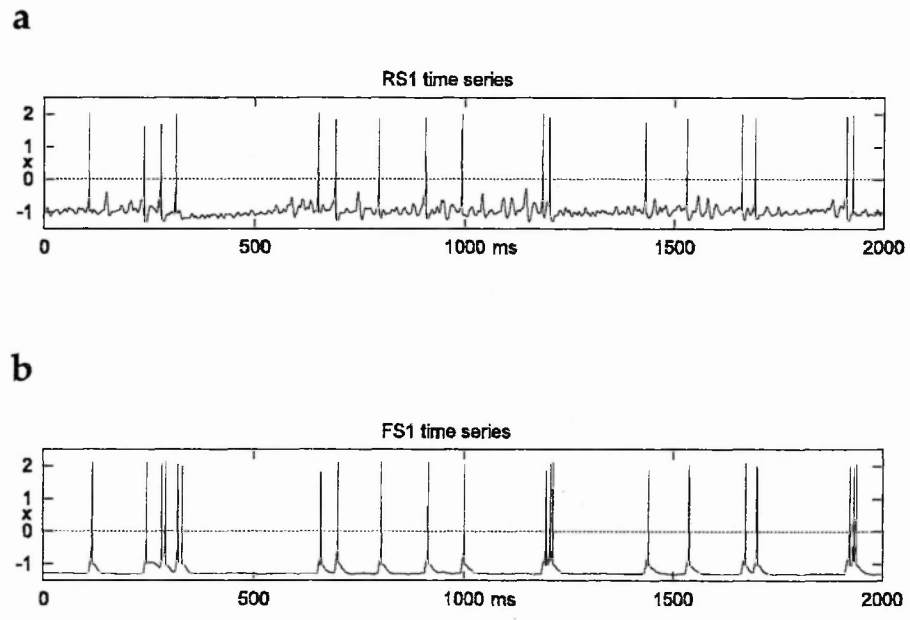

Figures 4.3a and 4.3b Chain model time series, condition 4a

Other individual model neuron impulse time series are similar (not shown). Many RS_2 impulses closely follow an initial impulse on the RS_1 model neuron. When an impulse is not recruited a clear EPSP is seen in the RS_2 model neuron time series. Following an impulse on the RS_2 model neuron, a damped sub-threshold oscillation is evident.

Rates of activity of individual model neurons under the different circuit conditions are compared in the table 4.3 below.

Condition	Spike rate S^{-1}			
	RS_1	RS_2	FS_1	FS_2
4a moderate noise input	8.5	10.9	9.4	10.1
4b strong noise input	13.9	6.0	16.7	8.3
4c FS biased fast	4.5	4.6	13.5	13.0
4d RS only	11.5	10.2	-	-

Table 4.3 Chain model spike rates under different conditions

The strong input signal (condition 4b) was weighted to be three times the moderate signal (condition 4a). The strong input evokes a higher spike rate in the first stage of the chain (RS_1 and FS_1). However the second stage of the chain (RS_2 and FS_2) is relatively inhibited and the RS_2 element achieves a spike rate of $6S^{-1}$. The inhibitory influence of the FS neurons is powerful and limits the response to an increased input signal, so that the RS_1+RS_2 spike total is similar in the two cases.

In condition 4c the tonic input to FS model neurons maintains the FS neurons close to their threshold. The tonic input increase is not great enough to obtain FS spiking without the fEPSP input from the RS neurons, but the bias favours FS activity and reduces the RS activity rate.

Table 4.4 summarises information from a number of correlograms (selected correlograms are shown in the figures below). The magnitude and lag of the first peak in the particular correlogram is recorded. In the case of a cross-correlogram of the spike series of two model neurons this indicates the timing of an increase in firing probability on the second element, following an initial spike on the first element.

Condition	Spike event correlation magnitude @ lag		
	RS_1-RS_2	RS_1-FS_1	RS_2-FS_2
4a moderate noise input	28 @ 4mS	34 @ 9mS	13 @ 10mS
4b strong noise input	17 @ 4mS	15 @ 10mS	16 @ 9mS
4c FS biased fast	44 @ 4mS	38 @ 7mS	23 @ 6mS
4d RS only	25 @ 5ms	-	-

Table 4.4 Correlation of spike events in the chain model under different conditions. Magnitude and lag of the first peak in the cross-correlogram. One cross-correlation unit is the chance level of spike coincidence.

Despite the differences of signal input strength and differences in FS activity, the relative timing of RS spikes remains similar. The cross-correlation of spike events shows similar lag values for the various RS element pairs under different conditions

(table 4.4). The firing of RS_1 evokes a spike on RS_2 at a lag of 4 or 5mS. This timing is preserved even in the RS only case (4d) where no IPSPs are present. The relative timing of spikes on FS units is more flexible.

RS elements evoke a spike on FS elements at a lag of around 10mS, again under different input signal conditions (4a and 4b). However in the case where the tonic input was increased to bias the FS units to achieve a higher average rate of firing (4c), the cross-correlation lag between RS and FS was reduced, indicating that the RS evokes a shorter latency spike on the FS element in the order of 6 or 7mS (condition 4c FS biased fast, table 4.4).

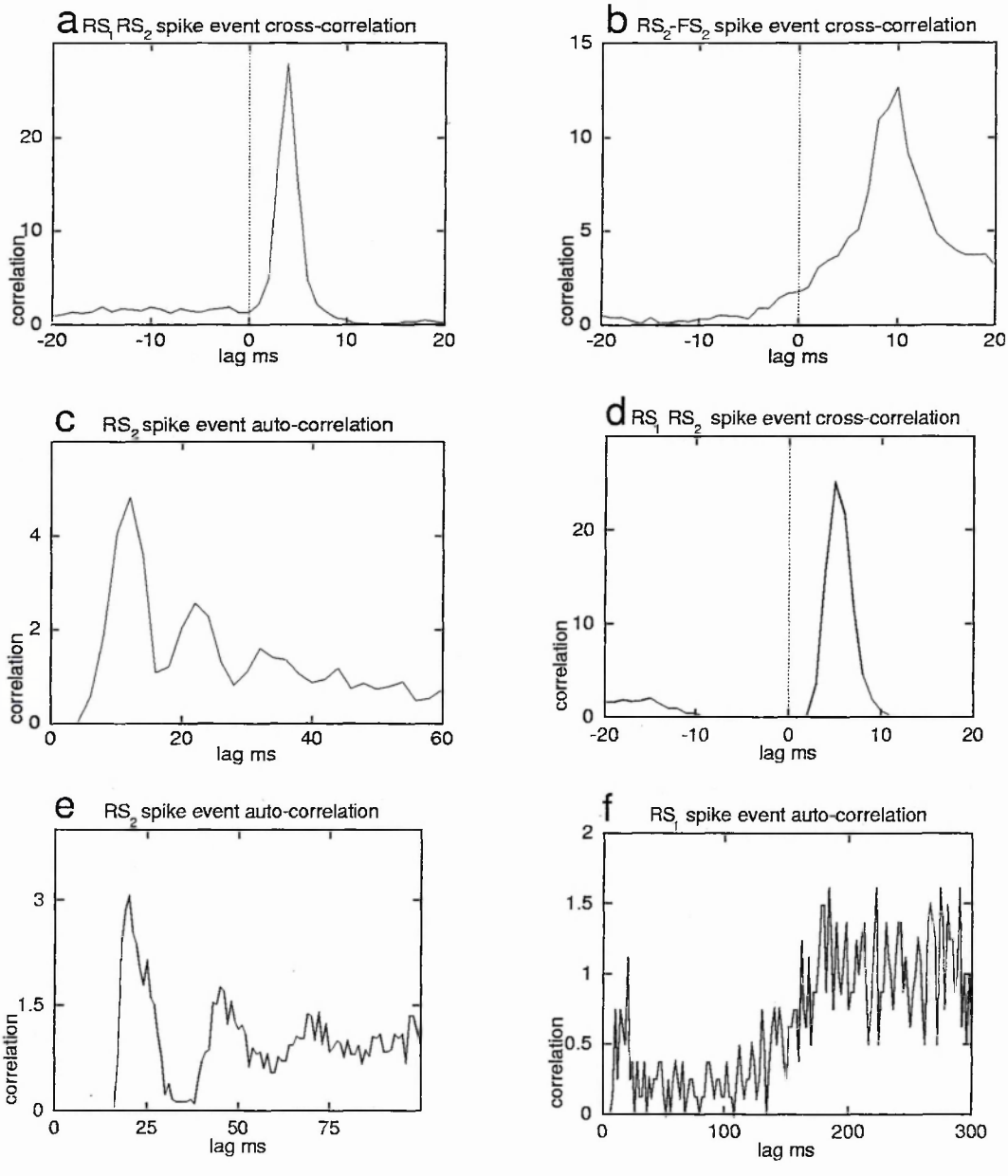

Figures 4.4 a-f Correlations of spike event series in RS FS chain (figure 4.2). One correlation unit is a chance level of spike coincidence..

Condition 4a moderate noise input spike rates: RS_1 8.5 s^{-1}, RS_2 10.9s^{-1}, FS_1 9.4s^{-1}, FS_2 10.9s^{-1}

a Cross-correlation of RS nodes. RS_1 leads by approximately 4mS. **b** Cross-correlation of RS_2 and FS_2 nodes. RS_2 leads by approximately 9mS (not shown: RS_1 and FS_1 show a similar pattern of cross-correlation). **c** Auto-correlation of the RS_2 exhibits a damped periodic response. This is similar to the response of the RS model in chapter 3 (figure 3.7d).

Condition 4d figures 4.4d and 4.4e

d RS only condition 4d, cross-correlation of RS_1 and RS_2 .

e RS only condition 4d, auto correlation of RS_2 .

Condition 4c figure 4.4f

f FS biased fast condition 4c, RS_1 auto-correlation is below chance level until >180mS lag.

Selected cross and auto-correlograms are shown above. Figure 4.4 shows the spike timings for the chain model with moderate input (4a). Spike timing, resulting from the input of a strong noise signal, exhibits very similar time shapes of cross and auto-correlograms, although actual correlation peak values differ due to different firing rates achieved in the two cases (condition 4b correlograms not shown).

The chain model RS only configuration (4d) has a similar RS to RS lag as the full model (compare figures 4.4d and 4.4a). RS_2 spike auto-correlation may be compared in figures 4.4c and 4.4e. Following an initial spike, subsequent firing probability of the RS_2 unit traces a damped oscillation. However, in the RS only case (4d) the RS_2 spike auto-correlation indicates a period of around 20mS of recovery of firing following an initial spike compared to 12mS in the full RS-FS model (4a).

In the faster FS condition (4c), the RS_1 auto-correlogram (figure 4.4f) exhibits firing probability that is relatively depressed. However the general pattern of an initial recovery in firing probability around a lag of 14mS, followed by a reduced firing probability until lag > 180mS is similar for auto-correlations of RS elements in all three conditions for the full model under the different input conditions (condition 4a moderate noise input, 4b strong noise signal input, 4c FS biased faster) (4a and 4b not shown).

In summary: the recruitment of impulses on the RS_2 model neuron following an initial impulse on the RS_1 neuron is similar under different conditions; FS activity stabilises or reduces RS activity as conditions are changed (4b and 4c).

4.3.2 Reciprocal model

Tonic inputs were chosen to set spike rates around $10S^{-1}$ for all RS, IB and FS elements. The spiking rate of the RS only configuration (4g) was very sensitive to input level and it achieved a spike rate of around $10S^{-1}$ with only a low tonic input level. Firing rate changed from nil to approximately $100S^{-1}$ as a small increase in the tonic input level was applied.

The burst firing of the IB element was effective at evoking FS spikes, effectively inhibiting the upper layer RS_1 element (condition 4f). The tonic input to the IB element was set to a lower level than in the RS_1-RS_2 model, to achieve around a $10S^{-1}$ spiking rate in the RS_1 element. As bursts of spikes were evoked on the IB unit the neuron model's spike rate was still in the order of $10S^{-1}$.

In the reciprocal circuit, following a spike on RS_1 a spike is evoked on RS_2 at a lag of around 5mS under different conditions. The cross-correlogram also indicates that the RS_2 element leads the RS_1 by around 5mS but with a lower probability (figure 4.5a). This reciprocal relationship is seen more strongly in the RS only case. Apart from some truncation of the peak around -5mS lag, the RS only RS_1-RS_2 cross-correlogram appears symmetrical, and so it resembles an auto-correlogram (figure 4.5e).

In the full RS-FS reciprocal circuit model (condition 4e) the auto-correlograms of the RS elements are not clearly oscillatory in comparison to the chain model (4.5c and 4.5d compared to 4.4c). The 'upper layer' RS_1 exhibits a peak of firing probability at a lag of 12mS in contrast to the sharp peak at 17mS lag found in the 'lower layer' RS_2 spike series. In the RS only model (condition 3), RS auto-correlograms show at best a weak, damped oscillatory pattern, and the initial period of recovery of firing probability is around 25mS lag for RS_2 (figure 4.5f) and 36mS for RS_1 (not shown).

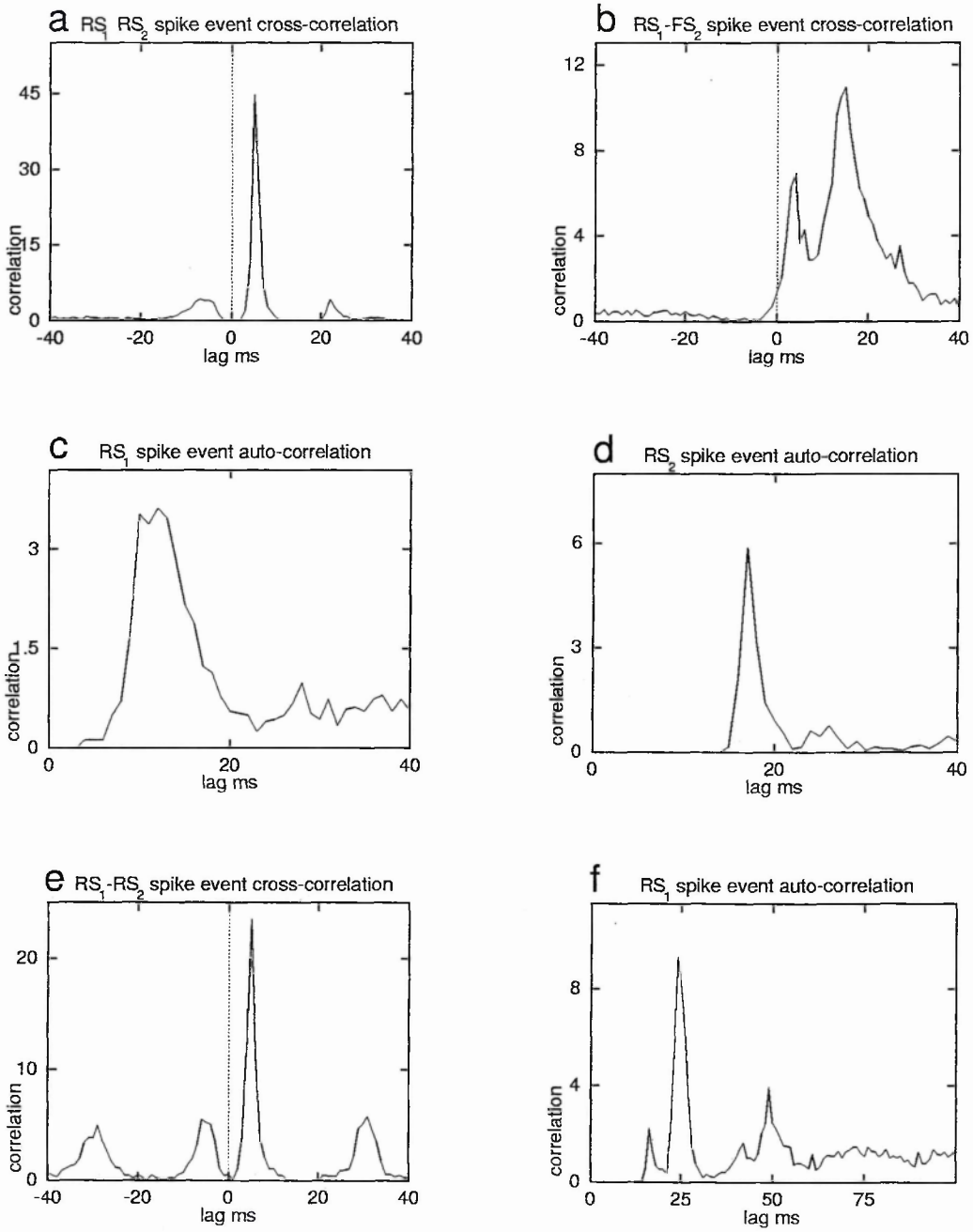

Figures 4.5 a-f Spike correlation in reciprocal RS-RS circuit model.

Condition 4e Figures 4.5a-4.5d

a Cross-correlation of RS_1 and RS_2 spike trains., RS_1 leads by around 5mS

b Cross-correlation of RS_1 and FS_1 spike trains. **c** Auto-correlation of RS_1 spike train.

d Auto-correlation of RS_2 spike train.

Condition 4g Figures 4.5e and 4.5f

e cross-correlation of RS_1 and RS_2, RS_1 leads by around 5mS.

f auto-correlation of RS_2 spike train.

The RS-FS pattern of cross-correlation is similar for 'upper' and 'lower' RS-FS pairs (condition 4e RS_1-FS_1 shown in figure 4.5b, other RS-FS cross-correlograms are similar but are not shown). An initial peak in firing probability occurs at a lag of 4mS followed by a larger peak at 15mS. Firing probability remains above the chance level up to 30mS lag.

Correlograms for the reciprocal RS-IB circuit are shown below (condition 4g, figures 4.6a-d). The 'upper layer' RS auto-correlogram (4.6c) is similar in shape to that found in the RS-RS reciprocal model (4.5c), but the correlation magnitude around the 13mS peak is greater. The RS-IB cross-correlation (4.6a) has a large peak at a lag of 6mS which is comparable to the RS-RS cross-correlation maximum value at a lag of 5mS (condition 4e, figure 4.5a). However the RS-IB cross-correlogram differs in that it exhibits an above chance correlation from around a lead of 10mS to up to a lag of 20mS. Subsequently RS-IB spike correlation values remain depressed until they recover to around chance levels at lags greater than 170mS (not shown).

The 'lower layer' IB auto-correlogram shows a strong initial peak around 6mS (4.6d). Later firing is depressed until a lag of around 170mS, which is consistent with the RS-IB cross-correlation values found at these longer intervals. The in-circuit IB element may be compared to the isolated IB model in chapter 3 (figure 3.7f). The IB in-circuit element's initial burst response is similar but the longer period intrinsic frequency is not clearly evident. IB in-circuit firing probability does recover to around the chance level at a lag of approximately 50mS which is consistent with an intrinsic frequency in the order of 20Hz. The bursting behaviour of the IB element is evident in its initial recovery of firing probability at 6mS. This contrasts with the RS-RS reciprocal model lower layer RS_2 recovery of firing probability around a lag of 17mS (auto-correlogram 4.5d).

Upper RS-FS and lower IB-FS cross-correlation patterns are broadly similar (RS-FS correlation in figure 4.6b). The peaks in the IB-FS cross-correlation occur at somewhat shorter lags (not shown).

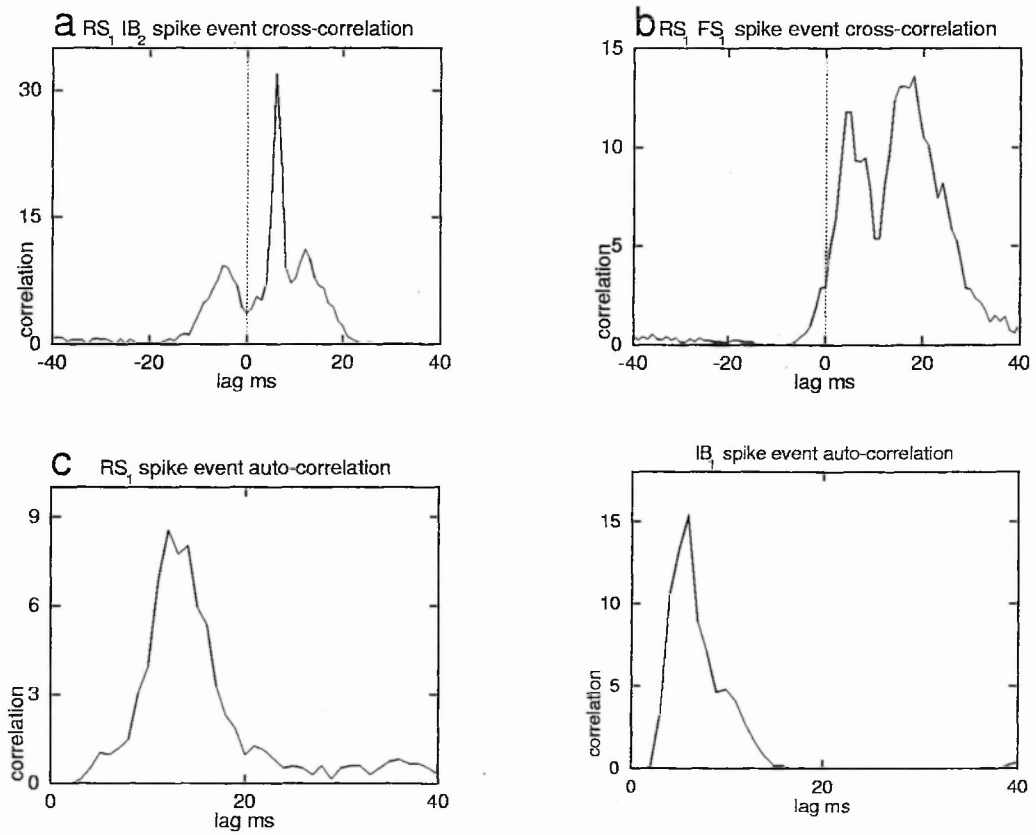

Figure 4.6 a-d Condition 4f Spike correlation in reciprocal RS-IB circuit model.

a Cross-correlation of RS_1 and IB_2 spike trains., RS_1 leads by around 5mS

b Cross-correlation of RS_1 and FS_1 spike trains. **c** Auto-correlation of RS_1 spike train.

d Auto-correlation of IB_2 spike train.

In summary, the reciprocal model achieves: a graded average impulse rate occurs due to the negative feedback of the FS neurons (in the absence of FS model neurons, the RS only reciprocal circuit tends to self excite to result in the maximum RS to RS rate of activity).

4.4 Summary of results

4.4.1 RS to RS spike latency

The timing of RS to RS impulse recruitment appears to be robust. Following a spike on the pre-synaptic neuron model, a spike is evoked on the post-synaptic RS or IB neuron at a lag of around 5mS. This latency is robust under different configurations and conditions (tables 4.4 and 4.5).

Model configuration		Spike event correlation magnitude @ lag		
		RS_1-RS_2	RS_1 auto-corr	RS_2 auto-corr
chain (4a)	RS - RS	28 @ 4mS	1.2 @ 14mS	4.9 @ 13.5mS
reciprocal (4e)	RS - RS	45 @ 5mS	3.4 @ 12mS	5.9 @ 17mS
reciprocal (4f)	RS - IB	32 @ 6mS(IB)	8.5 @ 13mS	15 @5.6mS (IB)

Table 4.5 Comparison of reciprocal and chain models. Lag of first peak in correlogram, one correlation unit is a chance level of spike coincidence.

4.4.2 FS negative feedback

Feedback from FS model neurons tends to stabilise the average RS impulse firing rate. In the chain circuit an increase in FS activity reduces the RS impulse rate (4b and 4c). In the feedforward case the balance between RS and FS activity will determine if a sustained chain of activity can be achieved. In the reciprocal circuit FS model neurons also act to moderate the RS activity rate (4g.adjusted tonic input, section 4.3.2).

4.4.3 RS intrinsic oscillation

In the chain model a pattern of damped oscillation of RS firing probability follows an initial impulse (condition 4a, figure 4.4c). The reciprocal model exhibits a similar primary period of recovery, however subsequent firing probability does not clearly show an oscillatory pattern (condition 4e, figures 4.5c and 4.5d).

4.4.4 IB element burst firing

The RS-IB (condition 4f) differs from the RS-RS reciprocal model (condition 4e) in the bursting behaviour of the IB model neuron in the lower layer. The IB neuron has a high probability of firing a subsequent spike at a shorter latency compared to the RS_2 elements in a similar circuit position (table 4.5). The response timing of the upper layer RS neurons appear to be similar in both conditions (4e and 4f).

4.5 Discussion

Two generalisations, relevant to the behaviour of the local neocortex, may be drawn. First, the timing of RS to RS impulse recruitment appears to be robust under different conditions. Second, IPSP feedback by FS model neurons moderates the average rate of spiking by RS neurons.

The use of negative feedback to control the gain of a circuit is well established, and so the influence of FS model neurons in reducing the average rate of activity was predictable. Yet some of the results may seem counter-intuitive, for example: RS neurons in the reciprocal circuit appear to be 'less oscillatory' than those of the feedforward chain model. This discussion will initially consider the basic properties of the isolated model elements and then attempt an explanation of the circuit model results.

4.5.1 RS transient response

A transient input is effective at evoking a RS impulse where the rate of change of the input is short compared to the adaptation process. A sub-threshold tonic input makes little contribution to rise time to threshold, a transient input is more effective at approaching the spiking threshold. The RS-RS impulse timing is seen to be relatively robust under different conditions as the adaptation process has time to oppose tonic or slowly varying inputs. The constant input factor is the high fEPSP rate of change which evokes an impulse in the postsynaptic RS model neuron at a consistent latency (tables 4.4 and 4.5).

4.5.2 Reciprocal circuit masks RS intrinsic frequency

The RS and IB neuron models have an intrinsic frequency of action associated with the adaptation current (see chapter 3). The in-circuit RS model neuron exhibits some evidence of oscillatory behaviour in the chain model (figures 4.4c and e). However, in the reciprocal model the transmission of spike activity in the circuit is sufficiently powerful to mask the intrinsic frequency of the RS or IB neurons and RS auto correlograms do not appear oscillatory (figures 4.5c and d).

4.5.3 sIPSPs moderate average spike rates

The sIPSP rise time constant implemented in the models is 100mS. Given the FS impulse rate of approximately $10S^{-1}$, the successive sIPSPs merge to form a tonic inhibitory input to the RS elements. This inhibitory feedback moderates the RS average impulse rate.

4.5.4 IB spike timing more variable than RS

The RS-IB and RS-RS reciprocal circuits support broadly similar patterns of activity. It is possible that the bursting behaviour of IB pyramidal neurons is associated with their sub-cortical projection (see chapter 2). However the RS-IB cross-correlogram indicates that the short period timing of the IB spike is less constrained by the RS_1 element. Compared to the RS-RS case, the RS-IB relationship is relatively movable and so it may be considered that IB neurons may play a different role in the behaviour of the local cortical circuit compared to RS neurons.

4.5.5 Other models

Douglas and Martin implement small cortical circuit models (1991; 1992; 1994). Their intention is to examine the cortical response to thalamocortical afferents. They examine the response of upper and lower model layers (representing a simplification of cortical layers) to a thalamocortical afferent pulse stimulus. They do not examine the sustained response or consider the emergence of oscillatory activity. They implement compartment models to represent the passive dendritic conduction of morphologically described pyramidal and interneuron cells. Their model (1991) is

implemented with three model neurons representing three subpopulations of neurons in the 'microcircuit'. The model upper layer 'population average neuron' represents the pyramidal and spiny stellate neurons in layers 2 to 4, the lower layer model neuron represents the pyramidal neurons in cortical layers 5 and 6, an inhibitory model neuron acts on both the upper and lower layers (self excitation and inhibition is allowed). Active conductances that generate action potential impulses are not implemented (p764 1991). The model assumes that population average rates of activity are represented by the depolarisation of the membrane potentials of the (non-spiking) model neurons. Douglas and Martin implement a stronger level of inhibition acting on the lower layer, contrasting with the implementations in this thesis. (Their assumptions leading to this implementation of inhibitory levels are discussed in chapter 5, section 5.4.4 .) Although the Douglas and Martin model differs in many respects from the models implemented in this thesis, their work is of interest because of their recognition of functional layer differences in the local circuit.

4.5.6 Model limitations

The exact pattern of transmission of spike activity in this chapter's circuit models is not a realistic representation of local circuit activity due to the limited number of neurons in the model circuits. The case of the RS only reciprocal circuit illustrates this (4g). RS elements in the reciprocal model supported a $100S^{-1}$ firing rate when tonic levels were set too high (see section 4.3.2). This rate corresponds to the RS-RS return impulse recruitment time of 2x5mS. This sustained high frequency behaviour was not explored as it was considered to be a poor representation of the biological case.

The exploration of local circuit dynamics requires the implementation of a more complex model with longer circuit paths. The limitations of the above models flow from the inadequate representation of the numbers of neuronal elements within local sub-populations. Subsequent chapters will explore the behaviour of model networks including hundreds of neurons and synapses.

Given that the probability of pyramid to pyramid innervation in a local volume is around 9% (chapter 2) it can be expected that most local circuit return paths would

involve at least one more neuron (discussed in chapter 5). The transmission of activity through a population representing a local neuronal volume will be explored in the next chapter.

4.5.7 Conclusions

Two general conclusions may be drawn from these results, despite the limited nature of the model circuits. Inhibitory feedback by FS elements reduces average circuit rates of activity, but the transient response of RS elements is not impaired. The timing of RS to RS spike recruitment appears similar under different conditions.

Both these features would seem to facilitate a reliable local circuit response to a time varying signal. However the models' assumption of PSP reliability contributes to the similarity of RS to RS spike transmission times. A strong functional synapse (comprised of a number of anatomical synapses, see chapter 2) reliably achieves a PSP of a certain amplitude. In the case of a reliable EPSP, the model may reasonably reflect the reliability of spike latency on a postsynaptic RS neuron.

Empirically observed weaker PSPs are less reliable in amplitude, even though the rise time of a particular functional synapse is constant. Variation in weaker PSP amplitude also implies a variability in the postsynaptic impulse recruitment (since RS neurons respond to rate of change). Simply put, reliable RS to RS impulse transmission times can be expected for the stronger synapses where EPSP amplitudes are reliable (given the assumption of passive PSP integration).

4.6 Summary

Simple models combining elements of the neocortical local circuit are considered. The relative timing of activity is examined using impulse event cross-correlograms.

RS to RS (regular spiking neurons) impulse recruitment is similar under different conditions and circuit configurations. The model is appropriate for RS to RS

transmission involving a strong functional synapse. Weaker unreliable synapses, leading to less reliable spike timing, are not well modelled.

Inhibitory feedback by fast spiking (FS) elements tends to stabilise the average RS firing rate. The relative timing of spiking of the intrinsically bursting element (IB), included in the lower layer of the reciprocal circuit, is more variable than the spiking of the lower layer RS element.

The interpretation of the behaviour of the model circuits presented in this chapter must be cautious. The detail of the behaviour exhibited by these circuits is subject to the caveat that as low numbers of neurons and synapses are modelled, the circuits are not good representations of the typical local connectivity where each neuron receives many thousands of synapses. This chapter serves as a pilot exercise in developing more realistic network models which include representative populations of model neurons and synapses.

5 Local networks in upper layers of neocortex

This chapter examines the behaviour of a model network, representing an assembly of upper layer neurons. The network comprises 80 Regular Spiking (RS) and 20 Fast Spiking (FS) units, interconnected by model 'synapses' representing the fEPSP, fIPSP and sIPSP synapse types (as described in chapter 3). The network is sparsely and randomly connected.

The model is based on in-vitro results which find relatively strong inhibitory PSPs in the upper layers (discussed in chapter 2). Although the upper layers are differentiated, this model makes the simplification of treating these layers as a homogeneous assembly. It is intended to address the question of the extent that local activity contributes to neocortical synchronisation and oscillation. An independent noise input initiates impulse activity in the network. The noise input represents uncorrelated inputs, representing the state of the local assembly and its afferents before the emergence of oscillatory activity. The noise input also acts to disturb the model network activity as collective oscillation begins to be established.

The patterns of activity in a number of networks are compared. The networks have the same general scheme of connectivity, but some connection parameters are varied: the relative strength and time constants of different synapse types; tonic and noise input levels. Models 5a to 5d explore the variation of parameters that affects the balance of RS and FS activity and collective oscillations. Models 5e and 5f change inhibitory synapse parameters, to allow a comparison with the published model of Bush and Sejnowski (1996).

The full model network (5a) does not exhibit a strong oscillatory pattern of activity. It was found that removing sIPSP connections produced a network that sustains oscillatory activity more effectively (5e). In addition, oscillatory network activity is made more regular by setting fEPSP and fIPSP risetimes to similar values (5f).

However, such a reduced model does not correspond to the biophysics reported for an assembly of upper layer neurons, as the upper layers exhibit sIPSPs that are stronger than those found in the lower layers (discussed in chapter 2, section 2.3).

5.1 Method

The neuron network model is based on in-vivo and in-vitro results (discussed in chapter 2). The sparsely connected network is implemented with a variation of the parameters of individual model neurons and synapses to represent the variation of a neural population.

5.1.1 Neuron model parameters

The FS and RS models are based on those introduced in chapter 3 (section 3.2.1, parameter table 3.3). A network of units with identical parameters could introduce a sharp response at a specific frequency. To avoid this artifact, the adaptation rate parameter for each RS was randomised (parameter 'r' , see chapter 3 section 3.2.1.b). A multiplier, taken from a uniform random distribution in the range 0.7 to 1.3 , was applied to the adaptation rate. This range results in the fastest RS unit producing nearly twice (1.86) as many impulses as the slowest RS unit for the same tonic input. The RS unit population mean impulse rate remains approximately the same.

5.1.2 Synapse model parameters

Parameters for the model synapses are based on empirical studies reviewed in chapter 2 (sections 2.3.3 and 2.3.4). The generic alpha function synapse model does not separate out pre and post-synaptic conduction; axonal and dendritic transmission are not explicitly modelled. However, parameters are chosen to achieve a PSP rise time appropriate for the type of model synapse (section 3.1 table 3.1). Empirical studies give a range of PSP rise time values. To reflect this, a random multiplier is applied to the PSC time constant for each synapse in the model network. The multiplier is taken from a uniform random distribution in the range 0.8 to 1.2.

It may be noted that the achieved PSP rise time is a function of the action of the conductance impulse (PSC) on the model excitable membrane (RS or FS model neuron). Although the PSC time constant for the fEPSP is multiplied in the range 0.8 to 1.2 (mean α^{-1}= 1.8mS, range from 1.4 to 2.2mS), the achieved PSP rise time is limited by the dynamics of the excitable membrane model and remains approximately 5mS (note these PSP rise times are estimated when the membrane model is in an epi-threshold condition). In contrast the slower PSC risetimes of the IPSP models (fIPSC α^{-1}= 8mS, sIPSC α^{-1}= 100mS) determine PSP time courses approximately proportionally.

5.1.3 Conductance weights

Synapse model 'connection' weights were assigned in a ratio to preserve the overall conductance ratios appropriate to the upper layers (section 2.3.4 table 2.3). These conductance values represent the effect of populations of synapses on the target neuron. Accordingly the conductance ratio is apportioned according to the number of each synapse type on the target model neuron unit. For example each RS neuron receives 15 fEPSP and 5 IPSP inputs. The individual synaptic weights are therefore 1/15 of the population fEPSP and 1/5 of the population IPSP weights respectively. Each conductance weight assigned to a particular connection is randomised within a band by a multiplier taken from uniform random distribution in the range of 0.8 to 1.2.

5.1.4 Network activity and conductance ratios

A preliminary examination of the contribution of network inputs to evoking impulse activity was made. The model neurons receive inputs from a noise source, a tonic input and the network's synapses intrinsic connections. Parameters are selected to achieve a moderate rate of impulse activity averaged over the network.

The noise input is intended to simulate a set of external inputs that are independent of the network's intrinsic activity. The noise source is implemented as a Poisson noise process, where each noise event activates a model synapse with a fEPSP time course. The noise synapse is weighted and each conductance weight is randomised within a band by a multiplier taken from uniform random distribution in the range of 0.8 to 1.2.

The inverse of the Poisson interval gives the mean noise event rate. The Poisson interval and weight are chosen so that the product of the noise weight and event rate is similar to the level of fEPSP activity on a network model neuron. For example a Poisson interval of 12.5mS gives a noise rate of $80S^{-1}$, this rate, weighted by 0.1, achieves a noise input activity level of 8 S^{-1} per neuron. Network RS mean impulse activity of $40S^{-1}$, with an individual PSC synapse weight of 0.013 gives a comparable fEPSP input activity level of $7.8S^{-1}$ per neuron (with 15 fEPSPs acting on one model neuron).

The tonic input parameter is set to maintain the model neurons close to an impulse threshold level (parameter *I*, see chapter 3 section 3.2.1.d).

The conductance weight for fEPSP model synapse and the networks intrinsic rate of activity is used to set the level of noise input as described above. Conductance weights for fIPSP and sIPSP model synapses were initially set according to the conductance ratio estimated from the results of van Brederode and Spain (1995) (approximate conductance ratio fE : fI : sI 2:3:1 for upper layer neurons, discussed in chapter 2, section 2.3.4).

It was found that the model network cannot support sustained RS impulse activity when implemented using this conductance ratio. As input weights are increased an initial burst of RS impulse activity can be evoked but sustained RS activity is not achieved. As inputs are increased further this burst terminates in the 'excitatory death' of the model neuron. The RS neuron model x variable (see chapter 3, section 3.2) recovers to less hyperpolarised levels (x variable more positive) after successive impulse cycles, until the x variable remains above the impulse threshold. This level would not be consistent with the survival of a biological cell.

5.1.5 Adjustment of synapse conductance ratio

Changing the balance of the conductance ratios, increasing the relative contribution of the excitatory conductance, allows the model network to achieve sustained RS activity. A conductance ratio fE : fI : sI of 4:3:1 was found to achieve a balance of

impulse activity, with comparable average rates of impulse activity on RS and FS model neurons. In addition inhibitory conductances for synapses on FS neurons are reduced to achieve a higher rate of FS action. The relative IPSC values are based on the lower layer conductance ratio reported by van Brederode and Spain.

The working model conductance ratio (4:3:1 approximately) doubles the contribution of the excitatory conductance compared to the fE : fI : sI conductance ratio estimated from the empirical results of van Brederode and Spain (ratio 2:3:1 see chapter 2 section 2.3.1). This discrepancy may have arisen due to a number of factors.

The morphology of FS neurons differs from typical RS neurons (pyramidal neurons). Also the pattern of innervation of FS neurons may differ from typical RS neurons. In the empirical study, differences in physiology and morphology may affect the recruitment of neurons local to the stimulation site (stimulation of a population of presynaptic neurons is by extracellular electrode). Possibly, the experimental conditions may have over recruited FS neurons, resulting in relatively larger IPSPs in comparison to IPSPs achieved by naturally occurring rates of activity.

In addition, the limited accuracy of estimation of conductances from empirical measurements contributes to inaccuracies. Given these uncertainties, the adjustment of the conductance ratio is unsurprising.

5.1.6 Network configuration

Each network model contains 100 model neurons, comprising 80 RS and 20 FS model neurons. In the neocortex a functional column contains many thousands of neurons (chapter 2, section 2.1.3). The size (upper limit) of the model network is chosen to ensure that the calculation of network activity is tractable. Consideration of preserving some of the statistics of population activity guides the minimum network size. Given the restricted network size, the model network is over connected compared to the local connection probability of the natural neocortex (discussion in chapter 2, section 2.2).

This allows the implementation of a larger number of synapse inputs innervating each model neuron, preserving some statistical function over these inputs.

Connectivity between the model neurons is sparse and random (reciprocal connections are excluded):

80 RS model neurons, each receives ;

15 fEPSP connections from other RS,

5 fIPSP and 5 sIPSP connections from FS

20 FS model neurons, each receives;

15 fEPSP connections from RS,

5 fIPSP from other FS,

giving a network total of 2400 model synapses across the whole network. (Note sIPSPs removed for some model networks, see table below.)

On RS neurons the model synapse conductance ratio fE : fI : sI is maintained at 3:2:1 . The absolute conductance value is varied for different model networks (see table 5.1 below). Inhibitory conductances on FS model neurons were set at lower levels.

The noise process interval and input weight is adjusted so that the weighted noise activity level is approximately 0.67 of the sum of the fEPSC weighted activity level received by a neuron. (The same weight is applied across the model network.)

The set of inputs, applied across the model network, is adjusted to obtain a mean rate of impulse activity of 20 S^{-1} to 40S^{-1} per model neuron. In this activity range, a majority of model neurons are involved in each population peak of activity. At lower input levels it was difficult to obtain sustained network activity.

5.1.7 Network Models

Network parameters and configuration were varied to explore the model's behaviour. The variation in network parameters is set out in table 5.1 below.

The balance of synaptic conductances implemented in the models is based on empirical results (and subsequently adjusted; section 5.1.5 above). However the 'absolute' weight of a synapse is less well defined. A rough estimate of the absolute strength of a single functional synapse may be made for a particular instance. In-vitro, for example, Thomson and Deuchars (1993) measure large single axon EPSPs between pyramidal neurons in layer 5. The amplitude of a large pyramid to pyramid EPSP is in the order of 9mV and these functional synapses are capable of eliciting an action potential in the postsynaptic pyramid.

From an estimate of somatic surface area and electrical characteristics (depolarisation, membrane resistance and capacitance) the peak current (PSC amplitude) may be estimated to be in the order of 100pA. This value is then scaled to the 'single point' process of the RS model, to give an estimate for the required amplitude for a strong model PSC, and the model synapse weight required to achieve the PSC amplitude. Fortunately confirmation for this rough estimate can be obtained by considering the strong EPSP amplitude (for example 9mV) in relation to the approximate threshold for impulse firing and the EPSC reversal potential and the model equivalent values. These different approaches give estimates for a 'strong' individual excitatory synapse weight in the region of 0.1 to 0.15 model units.

Brederode and Spain (1995) find collective EPSPs achieving amplitudes that are not greatly different in scale compared to the single EPSPs found by Thomson and Deuchars (estimated from their figure 1A, p1152, EPSP amplitudes evoked by stimulation in same layer: upper layer 7.5mV; lower layer 15mV).

The precise 'absolute' level of synaptic weights implemented in the model networks cannot be specified from a consideration of the in-vitro recordings; a limited exploration of network behaviour at different synapse weights is justified. Model 5a implements a collective EPSC weight of 0.2, which is divided amongst the individual excitatory synapses. Model 5b implements a collective EPSC weight of 0.3 to examine the case where synapses may be stronger. (In model 5b the tonic input to RS model neurons is increased to balance FS and RS activity.)

Tonic input levels are initially set to place model neurons close to their impulse thresholds as a modelling expedient. In pilot network simulations these levels are adjusted as other parameters are changed in order to approximately balance the rates of impulse activity of the RS and FS model neurons. The use of a tonic input level may be justified by the in-vivo observation of background activity that maintains a tonic depolarisation level (Destexhe and Pare 1999). Ideally tonic levels might be based on in-vivo measurements, however available data is limited (especially for a state just before local oscillations occur). Model network 5c implements increased tonic inputs to RS and FS neurons. Model 5d increases the tonic input to the RS neurons only, unbalancing the RS and FS activity.

The role of IPSPs is changed in models 5e and 5f, to allow comparison with the Bush and Sejnowski column model (1996). sIPSPs are omitted from model 5e, note that the RS tonic input level is reduced to maintain the balance of FS and RS impulse activity. Model 5f sets the fIPSP rise time to fast rate for comparison with Bush and Sejnowski model.

Model		RS PSC total weights			RS tonic	FS PSC total weights			FS tonic
	comment	fE	fI	sI	*I*	fE	fI	sI	*I*
5a		0.2	-0.15	-0.06	2.5	0.25	-0.09	-0.006	0.17
5b	increase PSC	0.3	-0.225	-0.09	2.6	0.3	-0.09	-0.009	0.17
5c	increase I	0.2	-0.15	-0.06	2.75	0.25	-0.09	-0.006	0.185
5d	increase RS I	0.2	-0.15	-0.06	2.75	0.25	-0.09	-0.006	0.17
5e	no sIPSP	0.2	-0.3	none	1.7	0.2	-0.1	none	0.14
5f	no sIPSP *fast fIPSP	0.2	-0.3*	none	1.7	0.2	-0.1*	none	0.14

Table 5.1 Individual synapse conductance weights equal the total conductance divided by the number of synapses innervating a neuron and multiplied by a value in the uniform random interval 0.8 to 1.2. *fIPSC time constant set same rate as fE (α^{-1} = 1.8mS). Individual model synapse PSC time constants are multiplied by value in the uniform random interval 0.8 to 1.2 . Noise input Poisson interval is 12.8mS, noise weight is 0.1 and 0.02 on RS and FS model neurons respectively. Individual noise inputs are multiplied by value in the uniform random interval 0.8 to 1.2 .

In summary, model 5a provides a baseline of network behaviour. Synapse PSC weights are increased in model 5b. Increased tonic inputs are implemented in Model 5c and PSC weights are set at the same level as 5a. Network model 5d has an increased tonic input level acting on RS neurons (level as 5c), but the tonic inputs to FS neurons are set to the lower 5a level. In models 5e and 5f sIPSPs are omitted to allow comparison with a published column model. In addition, model 5f sets the time constant for fIPSPs to the same value as fEPSP model synapses.

The noise input represents non-oscillatory inputs that are not correlated to the local activity. The synapse weight of the noise input is set to achieve a similar power (activity rate multiplied by weight) to the collective network model 'internal' fEPSPs. This may be considered to represent inputs to a local neural assembly before local oscillatory activity is established. It is intended to examine the collective oscillation properties of model network. The noise input initiates impulse activity in the network, but it also serves to deflect network activity and may weaken periodic or collective oscillatory activity.

5.1.8 Simulation method

The network was specified as an array of partial differential equations. The state of the network was evolved using an adaptive step algorithm based on Richardson Extrapolation and the Bulirsch-Stoer Method described by Press et al (1992). This method is appropriate for smooth systems and allows control of calculation error. The calculation of network activity scales approximately linearly with the number of variables and is dominated by the number of model synapses.

Initial states for the neuron elements of the network were randomly chosen from a lookup table of time series of RS and FS models. Synapse model variables were initialised within a uniform random distribution around a time averaged mean, found from trial runs of a network with moderate levels of activity (the slow time constant of the sIPSP model ensures that it is moderately active at the start, fIPSP and fEPSP show little activation at the start). A settling time of 500mS was used before 1000mS of network activity was recorded. The model simulations ignore initial activity

occurring at the onset of a stimulus. Due to the initialisation of variables and settling period, sustained network activity is recorded.

5.2 Results

5.2.1 Network Model 5a

The time series of network activity is shown as impulse rates per millisecond in figures 5.1a and 5.1a detail, below. The mean rates of activity are $32S^{-1}$ per RS model neuron and $30S^{-1}$ per FS model neuron. A large proportion of the neurons in the network contribute to each population activity peak (figures 5.1.a and 5.1.a detail). The collective action of FS units typically lag the RS units by 10ms or so. The pattern of activity is not strongly oscillatory (auto and cross-correlations of activity are examined in section 5.3.1 below).

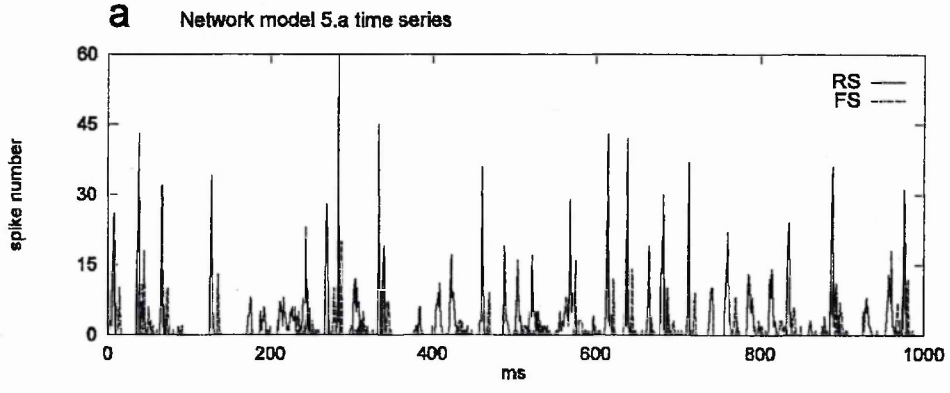

Figure 5.1a

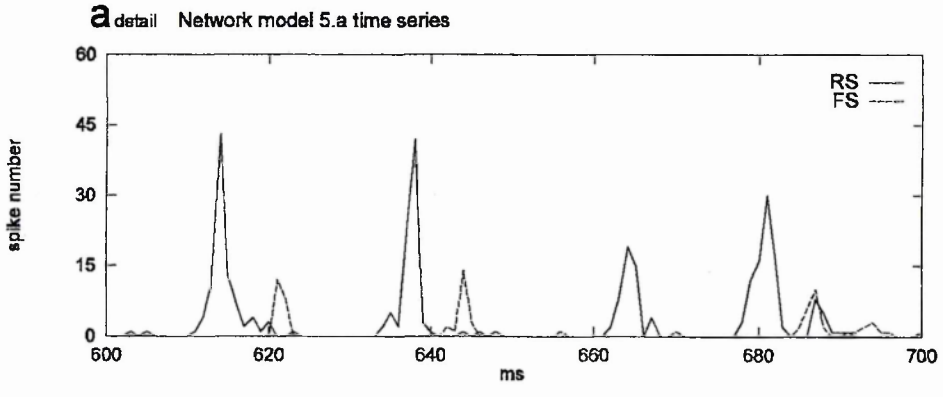

Figure 5.1a detail

5.2.2 Network Model 5b

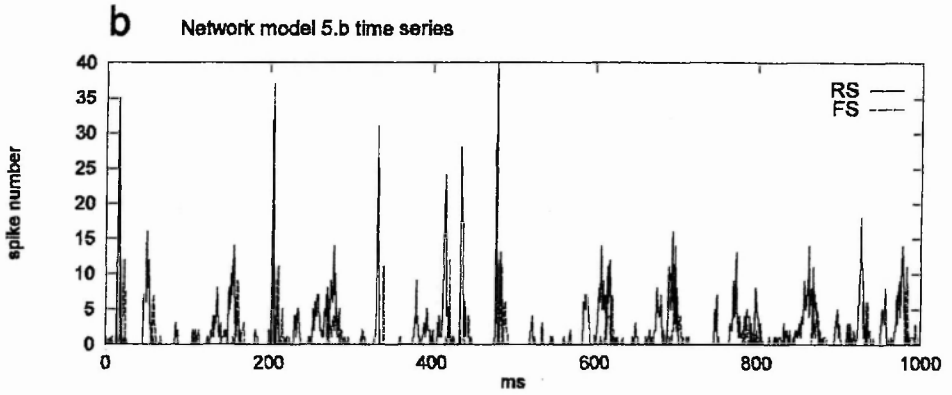

Figure 5.1b

Network 5b has stronger model synapse innervation of RS model neurons than the 5a model. The overall impulse rates for RS and FS neurons are somewhat reduced ($24S^{-1}$ and $23S^{-1}$ respectively), compared to the 5a model. Each population activity peak involves a large proportion of the model network's neurons. The general pattern of population activity appears a little less regular than that shown by the 5a model.

5.2.3 Network model 5c

Compared to 5a, model 5c retains the same level of synapse innervation, but the tonic inputs to RS and FS neurons are increased.

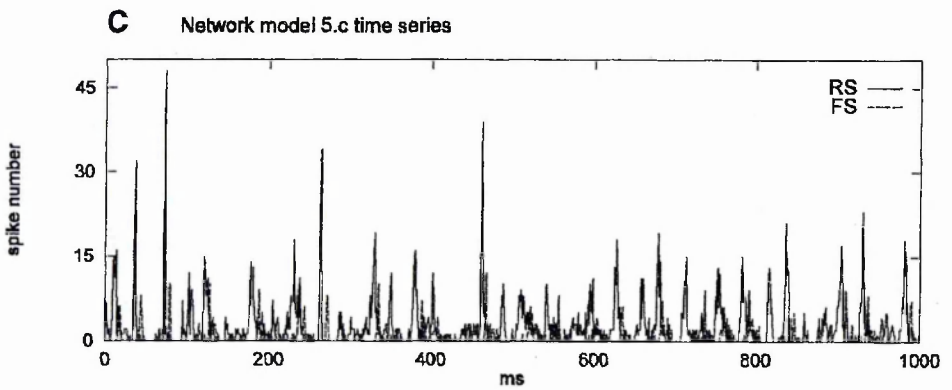

Figure 5.1c

Mean rates of impulse activity are similar to those of the 5a model: RS $33S^{-1}$ and FS $33S^{-1}$. The general pattern of activity is also similar to that of the 5a model, however

the RS activity peaks have tended to spread over 3-4ms compared to 1-2ms in the 5a model.

5.2.4 Network model 5d

The tonic input to RS neurons is increased, other inputs are at the same level as model 5a.

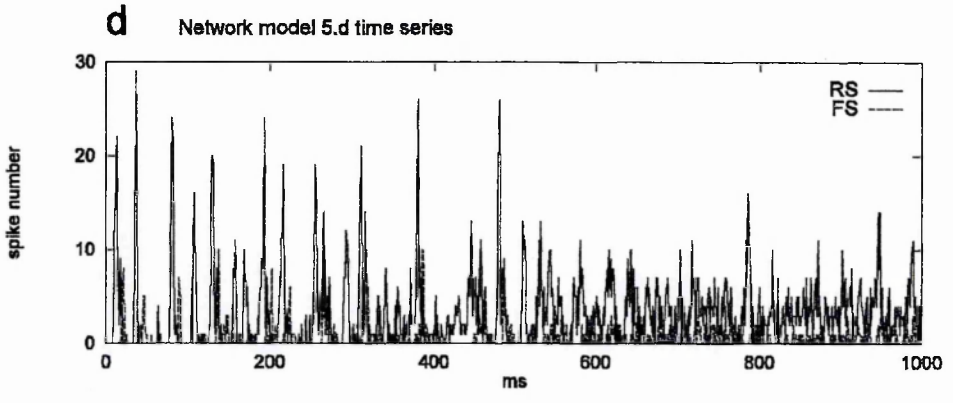

Figure 5.1d

Model 5d population activity is less regular than the pattern shown by 5a, especially in the second half of the time series. Mean rates of impulse activity are RS $42S^{-1}$ and FS $34S^{-1}$.

5.2.5 Network model 5e

The 5e network lacks any sIPSP, also synapse weights and tonic levels differ from the 5a model.

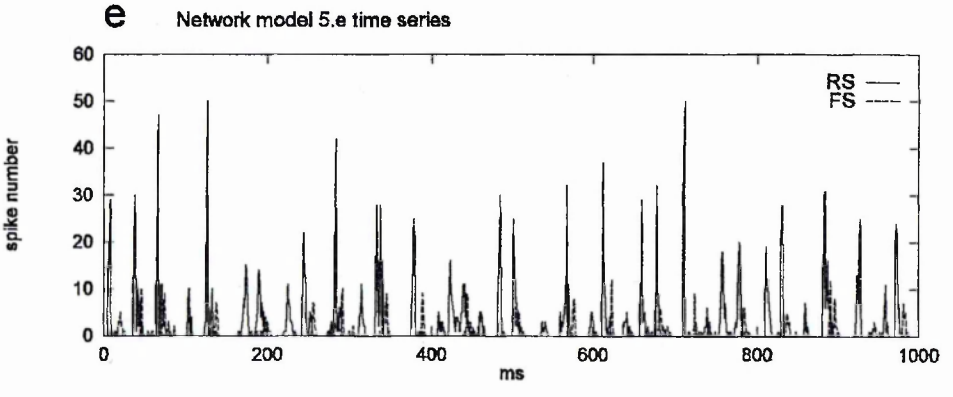

Figure 5.1e

Network model 5e achieves the mean activity rates: RS $32S^{-1}$ and FS $24S^{-1}$. The general pattern of activity appears similar to that of 5a.

5.2.6 Network model 5f

The fIPSP time constant is set to achieve a faster risetime than the other network models. Other parameters are set to the same levels as model 5e.

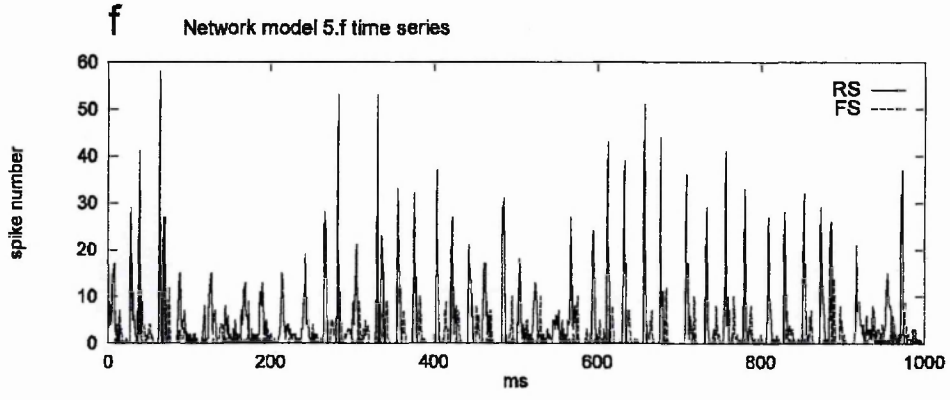

Figure 5.1f

The population activity of model 5f appears more regular than 5e. The mean rates of activity per neuron are higher: RS $46S^{-1}$ and FS $51S^{-1}$. In common with the other model networks, peaks of population activity include a large proportion of neurons.

5.3 Correlation of impulse activity

Time series correlations give an indication of the relative contribution of the neuron types and noise input to the activity pattern of the network models. Correlograms allow the examination of the correlation of the activity of network elements at different time lags.

5.3.1 Model 5a

The impulse time series of network model 5a (section 5.2.1, figure 5.1a) exhibits synchronised RS activity, but this activity is not clearly regular.

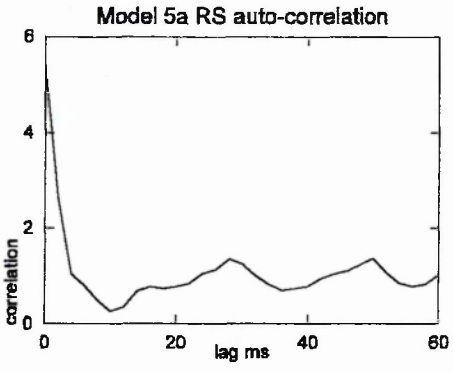

Figure 5.2a

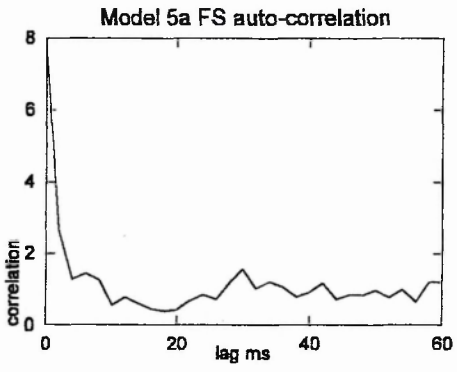

Figure 5.3a

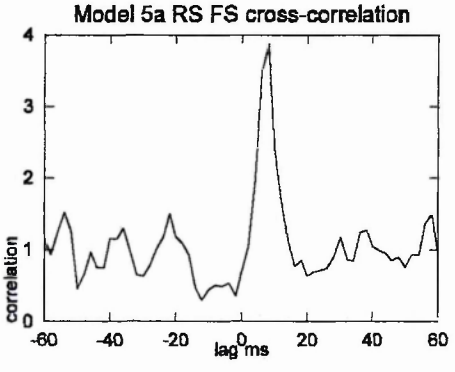

Figure 5.4a

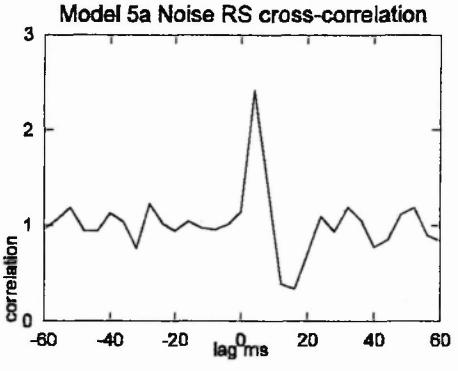

Figure 5.5a

In the impulse existence correlograms, one correlation unit is the chance level of correlation. Some of the variation in the correlograms can be ascribed to the limited duration of the data series, for example the noise-RS correlogram Fig 5.5a. shows variation in the region -60ms to 0mS lag. In this region RS activity leads the noise event, hence the expected correlation is the chance level of one unit.

5.3.1a RS impulse autocorrelation figure 5.2a

The time series of RS neuron population activity in model network 5a shows peaks of activity which involve many of the RS neurons (section 5.2.1, figure 5.1.a). RS impulse activity is broadly synchronised but not clearly oscillatory. This pattern is confirmed by the RS impulse existence autocorrelogram. Following the initial RS impulse (0mS lag), there is a depression of firing probability reaching a minimum at 10mS lag. The first minimum is 0.27 times the chance level of autocorrelation, indicating a strong depression of firing probability. Firing probability recovers to reach a maximum at 28mS. This and variation of firing probability at greater lags is consistent with a weakly oscillatory pattern. Following the first minimum, subsequent

maxima and minima reach 1.35 and 0.7 times the chance level of autocorrelation, respectively.

5.3.1b FS impulse autocorrelation figure 5.3a

The autocorrelogram shows a depression and recovery of FS impulse firing probability to above chance by a 30mS lag. This modulation is relatively weak compared to the RS pattern of activity. At greater lags, the correlogram does not show a strong pattern of modulation.

5.3.1c RS - FS impulse cross-correlation figure 5.4a

Following a RS impulse, FS model impulse firing probability is greatly enhanced at a lag of 8mS; the RS FS impulse existence cross-correlogram shows a strong maximum peak at 8mS lag. In addition the RS FS impulse cross-correlogram shows a strong minimum in the region -12mS to -2mS lag (ie a lead), minima are 0.3 to 0.36 times the chance level of cross-correlation. This indicates that RS firing probability is strongly depressed following a FS impulse.

5.3.1d Noise event to RS impulse cross-correlation figure 5.5a

The correlogram exhibits a first maximum at 4mS lag, followed by a minimum at 16mS. This may be interpreted as the recruitment of a RS impulse by the noise event, followed by a depression of RS firing probability.

The effect of the data series length on the variability of correlation values can be seen. The noise RS correlogram shows a random variation where RS impulse leads the noise event (negative lags). If the network simulation time series were extended, the cross-correlation of the independent noise process and RS impulse time series would approach the chance level of one unit in the negative lag region of the correlogram.

5.3.2 Model 5f

The RS impulse time series of network model 5f appears more regular than the activity of 5a (section 5.2.1, figures 5.1.f and 5.1.a respectively).

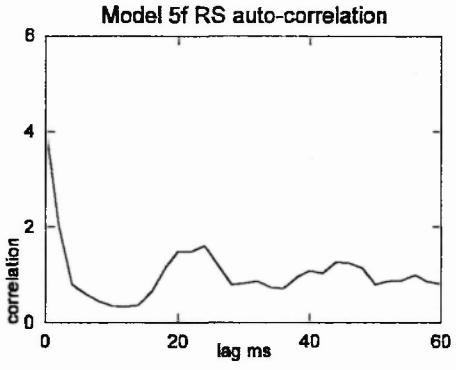

Figure 5.2f

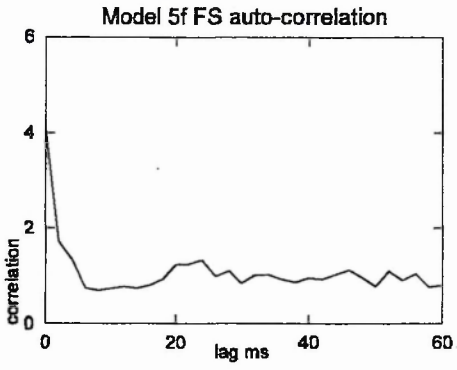

Figure 5.3f

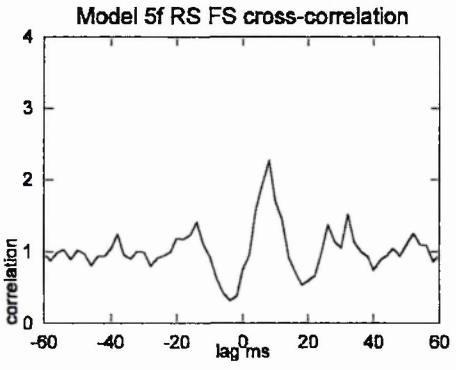

Figure 5.4f

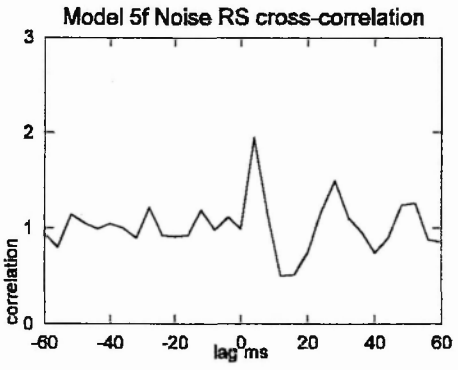

Figure 5.5f

5.3.2a **RS impulse autocorrelation** figure 5.2f

The general pattern of the model 5f RS impulse existence autocorrelation is similar to that exhibited by 5a. However a stronger modulation of RS impulse activity is indicated by the greater difference between the first correlation minimum and maximum at 12mS and 24mS lags, respectively. The recovery of RS firing probability is stronger than in the 5a model. This is consistent with the apparent regularity of the impulse time series of network 5f (figure 5.1f above).

5.3.2b **FS impulse autocorrelation** figure 5.3f

The modulation of FS impulse probability is weak. There is a weak depression and recovery up to about 24mS, at greater lags the autocorrelogram shows little variation around the chance level.

5.3.2c RS FS impulse cross-correlation figure 5.4f

The correlogram shows a sharp maximum at a lag of 8mS indicating the enhanced FS impulse probability following an initial RS impulse. There is some modulation of the correlation level at greater lags, echoing the strong modulation of RS activity. The depression of RS firing probability following an initial FS impulse is indicated by the correlogram lead minimum at 4mS. This is a 'sharp' minimum it does not extend over many mS, in contrast the lead minimum in model 5a (figure 5.4a above) extends from -2mS to -12mS. Similarly FS lead minimum extends from -4mS to -12mS in model 5e RS FS cross-correlogram (not shown).

5.3.2d Noise event RS impulse cross-correlation figure 5.5f

Following a noise event, RS impulse probability reaches a maximum at 4mS lag. RS firing probability is depressed to minimum at a lag of 12mS. The noise RS correlation is modulated at greater lags, echoing the strong modulation of RS activity as in figure 5.4f above.

5.3.3 Comparison of network models 5a to 5f RS autocorrelations

Figures 5.2a to 5.2f are presented below for comparison. Impulse existence correlation variation and timing is summarised in table 5.2 below.

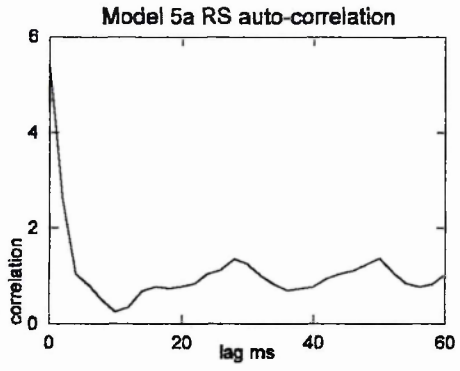

Figure 5.2a

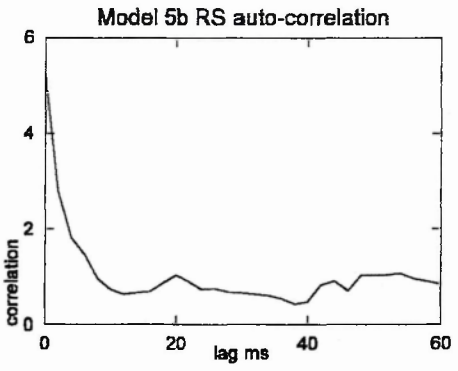

Figure 5.2b

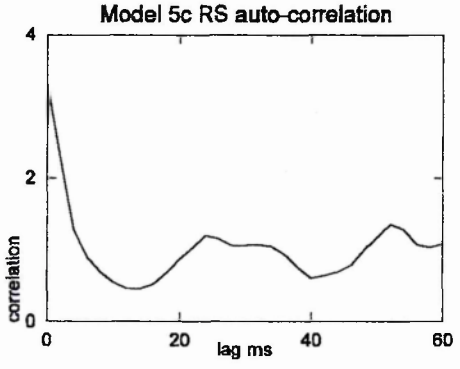

Figure 5.2c

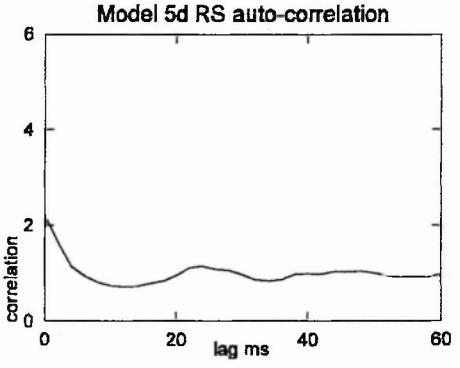

Figure 5.2d

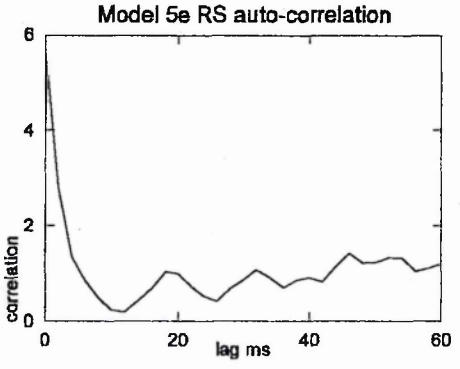

Figure 5.2e

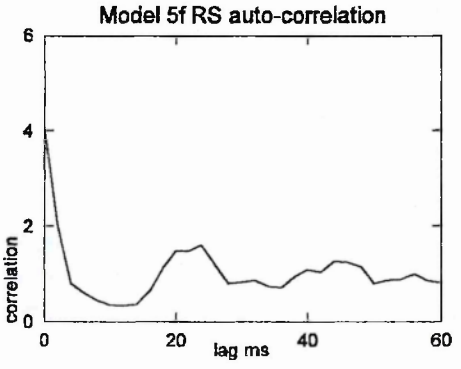

Figure 5.2f

Figures 5.2a-f Comparison of network models RS autocorrelations

Network model	Impulse existence autocorrelation @ lag mS					
	max @ 0 mS	1st minimum	@ lag mS	1st maximum	@ lag mS	max-min
5a	5.48	0.27	10	1.35	28	1.08
5b	5.32	0.54	12	1.03	20	0.49
5c	3.33	0.45	14	1.19	24	0.74
5d	2.23	0.72	12	1.15	24	0.43
5e	5.69	0.20	12	1.03	18	0.83
5f	4.10	0.33	12	1.61	24	1.28

Table 5.2 RS collective impulse existence autocorrelation comparison.
Precision of correlation timing is limited by 2mS data bin size.

The magnitude of the difference between the first maxima and minima may be considered as a rough indicator of the regularity of the RS population activity (last column in Table 5.2). This measure indicates model 5f as the most oscillatory, and model 5d has the least regular RS population activity.

Model 5a exhibits a moderate oscillation of RS impulse activity. Model 5c has increased tonic input levels, however RS and FS rates of activity are barely changed, but RS collective activity is somewhat less regular. Model 5b has increase synapse weights (noise input unchanged), impulse activity rates are reduced, and collective RS activity is less oscillatory. Model 5d has an increased tonic input to RS neurons, RS impulse activity is greater than the rate of FS activity and RS collective activity is the least oscillatory. This limited exploration of network behaviour indicates that the model is sensitive to the balance of inputs (intrinsic synapse weights and tonic input level) and the balance of RS and FS activity. In addition the collective RS neuron impulse oscillation is not very pronounced in the 'best' configuration, model 5a (however it should be recalled that the noise input is relatively strong, and will tend to disturb a collective activity cycle).

Model 5f exhibits a strong collective RS oscillation, evident in the raw time series and the RS autocorrelogram (figures 5.1f and 5.2f respectively). Model 5f omits sIPSP synapses and implements a fast fIPSC rise time and so is comparable with the Bush and Sejnowski model (1996). Model 5e omits sIPSP synapses, but retains the same fIPSC rise time as the previous models 5a to 5d. Model 5e achieves a pattern of RS impulse activity that is similar to the 'moderate' collective oscillation of 5a.

5.3.4 Results summary

Given the limited exploration of the models' parameters space it is appropriate to consider the broad differences between the behaviours exhibited by the models. Small differences in behaviour might be abolished by a small adjustment of parameters (for example the regularity of RS collective activity in models 5a and 5e).

Common behaviour of network models

Peaks of activity in the RS neuron population involve a majority of the RS neurons. The probability of RS action is depressed to a minimum at around 12mS following initial collective activity, recovering to above chance levels by 20mS. The recovery of RS impulse probability is at a maximum at 24mS (mean of all network models 5a to 5f). Innervation from the 'external' noise process recruits impulses in RS model neurons after a delay of around 4mS. Impulse activity by RS model neurons recruits FS impulses at around 8mS.

Contrasts in behaviour of network models

The 5a network model does not sustain a strong oscillatory action, although RS autocorrelation reveals a weak periodic component. Model 5b, 5c and 5d implement parameter changes and demonstrate the sensitivity of the network as all of theses changes reduce the regularity of network activity. The 'unbalanced' change in model 5d results in the average RS neuron activity rate being higher than the FS rate, and the least regular collective action. These upper layer models (5a to 5d) do not appear to support the strong oscillatory action observed in-vivo (see Chapter 1 discussion).

Models 5e and 5f differ from 5a by omission of sIPSP model synapses. Despite this, model 5e achieves a time series which appears similar to 5a. The population activity in 5a is supported by a relatively higher tonic input level (reducing 5a tonic input to the 5e level abolished nearly all RS impulse activity). Despite this, model 5e achieves a time series which appears similar to 5a. The 5f model implements fIPSP synapses with a fast rise time. The 5f model achieves a sustained oscillatory pattern of activity. Thus the neuron population appears to be sensitive to the relative time courses of

fIPSP and fEPSP model synapses. The 24mS oscillatory period of the 5f model is the same as the mean of all the models period for the RS autocorrelation first maximum.

5.4 Discussion

5.4.1 RS neuron population synchronisation

The synchronisation of RS population activity appears to be a robust phenomenon, appearing in the activity of all the networks. (Network 5d is a partial exception as the pattern of RS activity is less clear in the latter half of the activity time series.)

The network models are sparsely connected and individual synapse weightings are set randomly (within a band), so the innervation of each model neuron is different, yet RS activity is largely confined to narrow peaks of activity. Although connectivity is sparse, 'fan out' ensures that each model neuron is indirectly connected to the rest of the network population via another model neuron. In addition, although individual synapse weights vary, the individual neuron 'sees' innervation from a number of synapses, smoothing out the variation. Despite the randomisation of certain parameters, the numbers of synapses and neurons enforces some homogeneity on the network.

The narrowest peaks of RS collective impulse activity precludes the direct recruitment of many RS neurons by other RS neurons as the duration of the peak is too short (<5mS). (RS chain model cross-correlation indicates a lag of 4 or 5mS for RS to RS recruitment, chapter 4, section 4.3.1, table 4.4 .) Certain RS activity peaks occur with a greater duration (for example 8mS in the time series of model network 5c) thus allowing direct RS recruitment. However, RS autocorrelations show a chance level of firing probability at 4mS lag and below chance at greater lags towards the first minimum, indicating that fast RS to RS impulse recruitment is not a major feature of network behaviour.

The regularity and synchronisation of RS impulses is likely to be driven by the sub-threshold cycle and recovery of firing probability related to the model neuron adaptation current. The RS model neurons are implemented with a range of adaptation

time constants (section 5.1.1), so it is notable that the RS population is capable of relatively 'tight' synchronisation. It seems likely that RS model neurons receive a 'resetting' input, and the inhibitory synapses from FS neurons are a likely candidate for this role.

5.4.2 FS neurons and RS population activity

FS neuron activity contributes to the regularity of network behaviour. In model 5d, the mean rate of FS activity is much less than the RS rate (RS $42S^{-1}$ and FS $34S^{-1}$) and RS population activity in model 5d is less regular than other models.

The timing of FS activity, or strictly the time course of model fIPSPs, contributes to the regularity of network behaviour. Network 5f, where a faster fIPSP is implemented, exhibits distinctly oscillatory RS population activity. A model RS impulse recruits the FS impulse at a delay of 9ms (Chapter 4, section 4.3.1, table 4.4), and the RS - FS cross-correlations (example figure 5.3f) indicate a similar delay of 8mS. FS action results in a depression of RS activity at about 4mS in the 5f model network. Considering the chain of action RS - FS - RS, there is a maximum inhibition of network activity at 12mS following the initiating peak of RS population activity. The intrinsic period of action of the 5f model network is about 24mS, the effect of FS action, out of phase at 12mS, may contributing to RS phase cycle and help preserve the regular network activity.

As a corollary the slower fIPSP rise time, implemented in the other models, results in less regular network activity. In models 5a to 5e the fIPSP supports an extended depression of RS activity in the range 4mS to 12mS following FS activity. In this case the chain of action RS - FS - RS results in fIPSP action that will tend to depress network RS activity as late as 20mS following an initial RS activity peak. The 'intrinsic' cycle of the RS model neuron, culminating in the generation of an impulse, is likely to be delayed or disrupted (where that intrinsic period is around 24mS).

Model network 5f intrinsic population oscillation tends to resist the disturbance of phase caused by the independent noise input. In contrast, the population activity of

model 5a (and others) is less stable, although an intrinsic period of action is evident.

5.4.3 Model limitations

The simulation results must be qualified. The model networks incorporate many assumptions and compromises. The scale of the models is limited to ensure tractability. The number of neurons being included in each network is limited. The 'upper layer model' presented here is limited to a homogenous assembly of FS and RS model neurons, whereas a variety of neuron types are distributed through the neocortical upper layers (layers 1 to 4).

Model synapse conductances are based on estimates from neurophysiology studies, however the balance of conductivities has been significantly adjusted to achieve a functioning network. A number of model parameters are estimated using minimal empirical information. Network parameters were adjusted so that FS and RS mean impulse rates achieved a similar level, but the relative in-vivo rates of activity are not well known. The adjustment of model parameters to achieve an approximate balance of activity in RS and FS model neurons was adopted as a modelling expedient. Ideally this heuristic method would be replaced by parameter setting that conforms to physiological principle.

Identified GABAergic neurons include different morphological types. However differences in physiology corresponding to the variety of morphological types are not well known. The model implements just one FS neuron type and makes no systematic distinction between sIPSP and fIPSP connectivity (within the upper layer model). In addition the balance of synaptic conductances on smooth neuron types (ie inhibitory neurons) is not well known.

Risetimes of individual synaptic conductances are known to be very variable for an individual synapse type. The model PSC risetimes are chosen from population studies with the assumption that the collective PSP 'averages out' to an empirical mass value. This 'average' value may ignore distinctive fast or slow local circuits. The model implements a randomisation of synapse weights, but within a narrow band. This is

partly justified by the view that a functional model synapse represents a population of real synapses, therefore variability is likely to be reduced by averaging. This again may ignore a systematic feature of a real local circuit.

5.4.4 Alternative neocortical models

Bush and Sejnowski (1996) present a model of synchronisation in an assembly of neocortical neurons. Their model is similar to the models presented above in a number of respects:

excitable membrane models are implemented;
model neurons are sparsely connected by alpha function synapses;
network parameters for individual components are set within a range;

Model parameters such as individual PSC risetimes and individual synaptic conductances are set within a range of approximately 1:2 in their model (using a Gaussian distribution). The upper layer model, uses the somewhat narrower ranges of 1:1.5 (risetime 0.8 to 1.2 and conductance 0.8 to 1.2 uniform interval random multipliers, section 5.1.1 above).

The Bush and Sejnowski model is significantly different to the upper layer model 5a in other areas:

neurons are implemented as simplified compartment neurons;
pyramidal neurons are intrinsically bursting (IB) ;
pyramidal adaptation rate time constant varies by 1:5 ;
fIPSC rise time is set to a fast value;
sIPSP synapses are omitted;
synaptic latency is separated from synapse risetime;
synapses act on different neuron model compartments;
the total fEPSC : fIPSC ratio per neuron is 1:1 ;

Bush and Sejnowski present this as a model of a neocortical column, ie including upper and lower layers. This approach substantially differs from this thesis where two layers are implemented with contrasting inhibition levels and connectivity (a two layer

model is presented in the next chapter). The inclusion of IB neurons and omission of sIPSPs would be appropriate for a lower layer model, however the relatively high level of fIPSP inhibition suggests that the Bush and Sejnowski model resembles the upper layer.

Model 5f may be compared to the Bush and Sejnowski column model. In model 5f sIPSPs are omitted and the fIPSC time constant is set to the same value as that of the fEPSC. Despite the different model implementation a similar synchronised behaviour is obtained. The peaks of population activity in 5f are formed from the combination of single impulses of RS model neurons, not by the burst firing of IB neurons. The individual pyramid neuron time course is more variable in the Bush and Sejnowski model, but this is consistent with the setting of network parameters to a wider range and the duration of impulse bursts. Both network models achieve a periodic population activity of around 40 Hz from the combination of inhibitory connections and pyramidal intrinsic frequency.

Model 5e examines the effect of setting a slower fIPSC rise time than in model 5f. Network model 5f achieves a synchronised population behaviour similar to that of model 5a. As model 5e omits sIPSP, it can be concluded that sIPSP action is not a strong determinant of its oscillatory behaviour. The population activity of model 5e is markedly less regular than the 5f time series. Model 5f demonstrates that the slower fIPSC rise time reduces the stability of the population activity cycle, making the timing of network activity more sensitive to disturbance by 'external' inputs.

As reported synaptic timings are very variable, it remains open as to which fIPSC rise time value is the more plausible (also note that in this thesis model synapses, latency and rise times are lumped together). Although there is a great variety of observed fIPSP rise times, it would seem reasonable to implement a model that achieves PSP timings that represent the bulk of a population. The fIPSC rise time values used here (except model 5f) are based on recordings of collective synaptic action (discussed in chapter 2, section 2.3.3). This 'slower' fIPSC rise time is used in the two layer model in the next chapter.

Despite these differences there is a broad agreement between the results from models 5a to 5d and the Bush and Sejnowski single column model. Synchronisation of a network is sensitive to aspects of inhibition: in model 5b, where synapses are strengthened, oscillation is weakened; in model 5d, where inhibitory FS activity is proportionately less than RS activity, collective oscillation is weakened.

Other biologically detailed models include pyramidal and inhibitory neuron types and fE, fI and sI synapse types but do not examine oscillatory activity. These are mentioned here to provide a comparison of some approaches to physiologically based modelling.

Bush and Priebe (1998) examine a layer 4 model including GABAb inhibition (sIPSP). GABAa conductances are set to a fast rise time (1.1ms). The implementation includes IPSCs that are set to a lower value when the postsynaptic cell type is inhibitory, although the values used differ from the IPSC weights implemented on FS neurons in the layer models presented in this thesis. The Bush and Priebe model examines the response to a thalamic input, oscillation is not examined. They suggest that a role for GABAb inhibition is to subtract a DC component from thalamic input, controlling the sustained response.

Douglas and Martin (1992) present a 'canonical microcircuit' of the local cortex in a series of papers, closely based on empirical measurement. This includes model elements representing separate superficial, deep layer and inhibitory subpopulations. Their intention is to simulate the neocortical response to thalamocortical stimulation, and model orientation preference. They do not specifically examine oscillatory activity.

Douglas and Martin do not state a specific fIPSC risetime, however they do observe GABAa mediated fIPSPs persisting for 50mS (which is not consistent with a 1ms rise time alpha function - see above). They observe that lower layer inhibitory conductance ratios differ from the upper layer, in the lower layers GABAa are proportionately

stronger than GABAb conductances. To preserve this ratio they implement the same GABAb conductance in upper and lower layers, and set a 2 times stronger GABAa conductance in the lower layer compared to the upper layer. This method implements a stronger general inhibition in the lower layer. The relative amplitudes of fast and slow IPSPs in the deep layer could have been achieved by setting a weaker sIPSP input. This would bring their model closer to the generally observed condition. The Douglas and Martin model is in contrast to the weakly inhibited lower layer model presented in this thesis, and contradicts the observation of weaker lower layer inhibition by a number of workers (lower layer IPSPs are discussed in chapter 2, section 2.2.1.b). Their model also contrasts in that they implement a common inhibitory population that directly acts on both upper and lower layers.

5.5 Conclusion

An upper layer model, based on a sparsely connected network of RS and FS neurons, is examined. The population of RS neurons have a tendency to synchronise their impulse activity under different conditions. This synchronisation is a result of the timing of fIPSP inhibition and the intrinsic frequency of the model RS neurons. sIPSP inhibition does not strongly affect the synchronisation of RS activity, but provides a slowly varying level of inhibition. Synchronisation and oscillation of RS population activity is sensitive to fIPSC rise time. Collective oscillations are relatively weak using a slower fIPSC rise time (model 5a). Collective oscillations are made more robust by setting the fIPSC rise time to a faster value similar to the fEPSC rise time.

Inhibitory action plays an important role influencing the pattern of collective activity. It is less clear how fEPSPs contribute to the synchronised regular network activity. Local RS to RS connectivity might appear redundant in an oscillatory local assembly as direct RS to RS impulse recruitment generates EPSPs which coincide with a depression in RS firing probability (section 5.3.3 and autocorrelograms 5.2a to 5.2f). The isolated homogeneous 'upper layer model' may be misleading. An extension of the model to include distinct RS subpopulations (layers) opens the possibility of phase

differences so that RS to RS innervation may contribute to the cycle of network activity. The next chapter examines a two layer column model.

6 A model of the neocortical column

Introduction: the Layer Difference Column Model

The purpose of this chapter is to examine a model of an assembly of neurons that includes a representation of the neocortical layer differences. The model presented in this chapter represents the local connectivity within a functional neocortical column including local connections within a layer of the column and interlaminar connections ('vertical' connections between the layers). A distinctive feaure of the model implementation is the contrast between the upper and lower layers and is referred to as a 'layer difference column model' (LDCM). The LDCM includes 200 neurons distributed in two distinct layers. The upper layer includes RS and FS model neurons and associated synapse types. The lower layer includes RS, IB and FS model neurons. The lower layer FS neurons do not support sIPSPs on their targets. Inhibition of the lower layer is weaker than the upper layer. A noise input acts strongly on the upper layer (representing 'ascending' afferents).

The LDCM is based on empirical studies of neuron distribution (Hendry et al 1987; McCormick et al 1985), relative synaptic strengths (Connors et al 1988; van Brederode and Spain 1995) and local and interlaminar connectivity (Nicoll et al 1996; Thomson and Deuchars 1994; van Brederode and Spain 1995) (discussed in chapter 2). The LDCM implements a stronger level of inhibition in the upper layer, representing the stronger inhibition found in the neocortical layers 2 to 4 compared to the model lower layer representing the layers 5 and 6. It is intended to examine how the interlaminar vertical circuit contributes to synchronisation and oscillation in the local neocortex. An independent noise input represents uncorrelated inputs, the noise input acts to disturb the timing of the model's activity as the collective oscillations become established.

The behaviour of the network under different conditions is examined. The strongest noise input, representing non-local afferents, targets the model upper layer. This may

be considered to represent modulated inputs from 'external' sources such as the LGN (in vivo LGN afferents are dense in layer 4, which is part of the model's upper layer neural population).

Impulse time series are recorded under three conditions:

6a, the upper layer receives a strong noise input and parameters are set to balance the rate of activity in neuron subpopulations;

6b, the strength of the noise input to the upper layer is reduced;

6c, an additional, independent noise input acts on upper and lower layers.

In condition 6a the upper layer RS neurons receive a strong noise input and much weaker noise inputs act on the other model neurons. In 6b the strength of the upper layer noise input is reduced. Both of these arrangements represent the feedforward case ie where LGN input or 'lower' cortical area is feeding forward to a 'higher' cortical area, preferentially contacting layer 4 and layer 2/3 neurons. In 6c an additional independent noise input acts on both upper and lower layers, representing the case where feedback from 'higher' cortical areas innervates layers 2/3 and 5 (via layer 1). (This laminar difference between feedforward and feedback laminar targets is suggested by a number of workers, for example Sanes and Yamagata 1999; Thomson and Bannister 2003; Zeki and Shipp 1988).

The main results indicate that the neuron population of the whole column exhibits synchronised oscillatory activity, but the synchronisation of the neurons within each layer is different. The neurons in the upper layer are more sharply synchronised; the timing of impulse firing is more variable in the lower layer. This behaviour is seen most clearly in condition 6a, the synchronisation of the neurons in 6b and 6c is weaker. The significance of this layer difference in behaviour is discussed in chapter 7.

6.1 Method

Network implementation is similar to that above (chapter 5, section 5.1). The model is extended by defining two layers. The FS model neuron is redefined as two sub-types supporting either fIPSPs or sIPSPs on their targets, indicated as FSf and FSs respectively (to facilitate the implementation of layer differences). The assigned layer of a model neuron is indicated by a suffix (lower l, upper u). As in the models in chapter 5, the relative numbers of RSu and FSfu neurons are chosen to reflect the reported frequency of GABAergic neurons (chapter 2, section 2.1.2b, Hendry et al 1987). The numbers of other neuron types are chosen as a modelling expedient (partly guided by the weaker inhibitory PSPs reported for the lower layers, for example van Brederode and Spain 1995).

The column model network comprises two layers:

an upper layer of 80 RSu, 20 FSfu and 10FSsu ;

a lower layer of 70 RSl 10 IBl 10FSfl.

The upper layer parameters are similar to model 5a. The layer model 5e omits sIPSP synapses and may be compared to the lower layer of the column model which receives weak sIPSP synapses. However, the lower layer implements a weaker fIPSC, in line with the observation of weaker inhibition in the lower layers (reviewed in chapter 2, section 2.3.4).

Connections between neuron subpopulations are randomised, directly reciprocal connections and self connections are not allowed. Upper layer FS neurons directly contact neurons in the lower layer, but the lower layer FS neurons do not project to the upper layer. Individual synapse conductance weights and time constants are set using a random multiplier to give a uniform range of 0.8 to 1.2 times the mean value. The adaptation rate parameter for individual RS and IB model neurons is set using a random multiplier to give a uniform range of 0.7 to 1.3 times the typical adaptation rate for the neuron type.

Figure 6.1 is a sketch of the connectivity between neuron subpopulations in the column model. Table 6.1 lists the number of connections made on each neuron type according to the layer position.

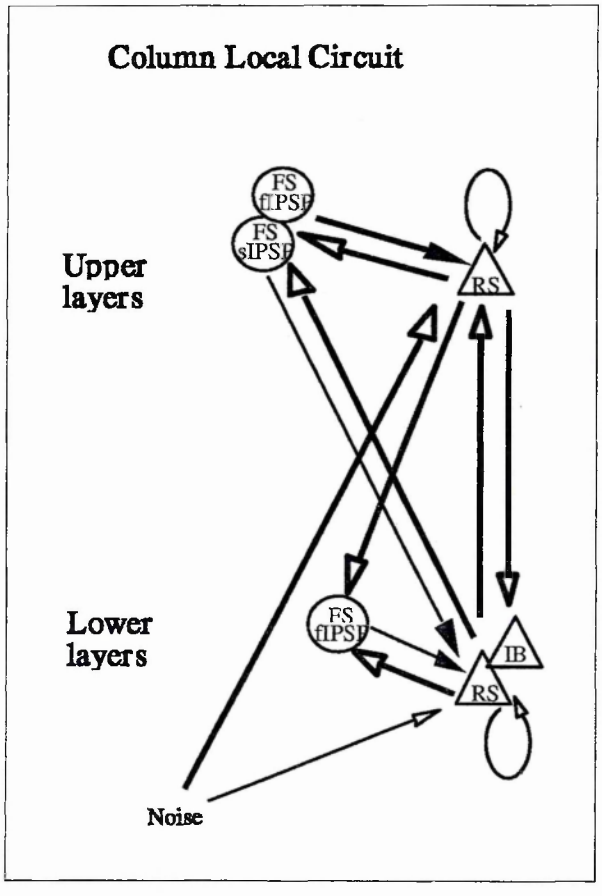

Figure 6.1 Sketch of two layer column model. Triangles represent RS or IB model neuron populations (Cf chapter 2, figure 2.5). Circles represent FS neuron populations. Weight of arrows represents relative synaptic weight. Open arrowhead indicates fEPSP, solid arrowhead indicates IPSP on respective targets. The lower layer receives weak IPSPs and does not directly inhibit upper layer neurons. The lower layer does not possess a FS-sIPSP subpopulation.

Post synaptic neurons	Presynaptic neurons and synapse type					
	RSu	FSfu	FSsu	RSl	IBl	FSfl
	fE	fI	sI	fE	fE	fI
RSu	15	6	6	8	2	0
FSfu	15	6	1	8	2	0
FSsu	15	6	1	8	2	0
RSl	10	2	1	12	3	3
IBl	10	2	0	12	3	3
FSfl	10	2	0	12	3	2

Table 6.1 Connection densities and layer position. Upper layer suffix u, lower layer suffix l.. Numbers of functional synapses made by the presynaptic neuron type on the postsynaptic neuron types. Within layer innervation is denser than between layer innervation. The upper layer has more inhibitory synapses. Lower layer FS neurons do not contact the upper layer neurons.

This scheme of connectivity is partly compromised by low numbers of FS connections, especially between FS neuron subpopulations. These low numbers result from the restricted scale of the model (for reasons of tractability) and the division of the neuron types into layer subpopulations.

Post synaptic neurons	Synapse total weight per postsynaptic neuron					
	upper layer origin			lower layer origin		noise
	fE	fI	sI	fE	fI	fE
RSu	.195	.180	.072	.130	-	0.2
FSfu	.150	.090	.009	.100	-	0.02
FSsu	.150	.090	.009	.100	-	0.02
RSl	.130	.020	.001	.195	.030	0.02
IBl	.130	.020	0	.195	.030	0.02
FSfl	.100	.030	0	.150	.030	0.02

Table 6.2 Model 6a synapse conductance weight totals, by presynaptic origin and postsynaptic target. Individual model synapse weights are found by dividing the conductance total by the number of functional synapses on the postsynaptic target neuron. For example, one RS upper layer neuron receives 15 fE synapses from the upper layer, hence individual fE synapse weight is 0.013 (=0.195/15).

The ratio of synaptic conductances for the upper layer is based on the revised conductance ratios found in chapter 5 (section 5.1.5). Lower layer fI conductances are set to be substantially weaker. Between layer conductances are set so that their

contribution is less than within layer innervation. This arrangement roughly approximates the results reported by van Brederode and Spain (1995) (layer differences are discussed in chapter 2 section 2.3.4).

A preliminary examination of network activity and parameter levels was made with the intention of achieving a similar rate of activity in the neuron subpopulations. Tonic inputs *I* were set: RSu 2.9, all FS 0.155, RSl 1.8, IB 0.8. The noise input was set to a level approximately equal to the upper layer fE afferents in model 6a (noise process implementation described in chapter 3 section 5.1.4).

The column models differ in the configuration of the noise input:
6a one noise source,

RSu noise synapse input weighted at 0.2, other neurons 0.02;

6b one noise source,

RSu noise synapse input weighted at 0.1, other neurons 0.01;

6c two noise sources n_1 and n_2,

RSu n_1 weight 0.1, RSu n_2 weight 0.1, RSl n_2 weight 0.1, others n_1 0.01.

The upper layer noise input represents uncorrelated 'feedforward' inputs. The upper layer noise input in model 6b is half that in 6a. Model 6c implements a common noise input to both the lower and upper layers and a concurrent independent noise input to the upper layer only, representing a combination of feedforward input to the upper layer and feedback to both layers (with feedforward and feedback in terms of the hierarchy of cortical areas, for example Zeki and Shipp 1988). This difference in the targeting of different layers according to feedforward or feedback direction of cortical innervation is also suggested by others (Sanes and Yamagata 1999; Thomson and Bannister 2003). The implementation of two independent noise sources in condition 6c is intended to portray a 'worst case' for synchronisation within the model column (where feedforward and feedback inputs are uncorrelated), where the independent noise inputs will tend to disrupt the synchronisation of the upper and lower layers.

6.2 Results

The main results indicate a synchronisation of impulse firing by the neuron population of the whole column. The synchronisation of the neurons within each layer is different. The neurons in the upper layer exhibit more strongly synchronised impulse firing; the timing of impulse firing is more variable in the lower layer.

a

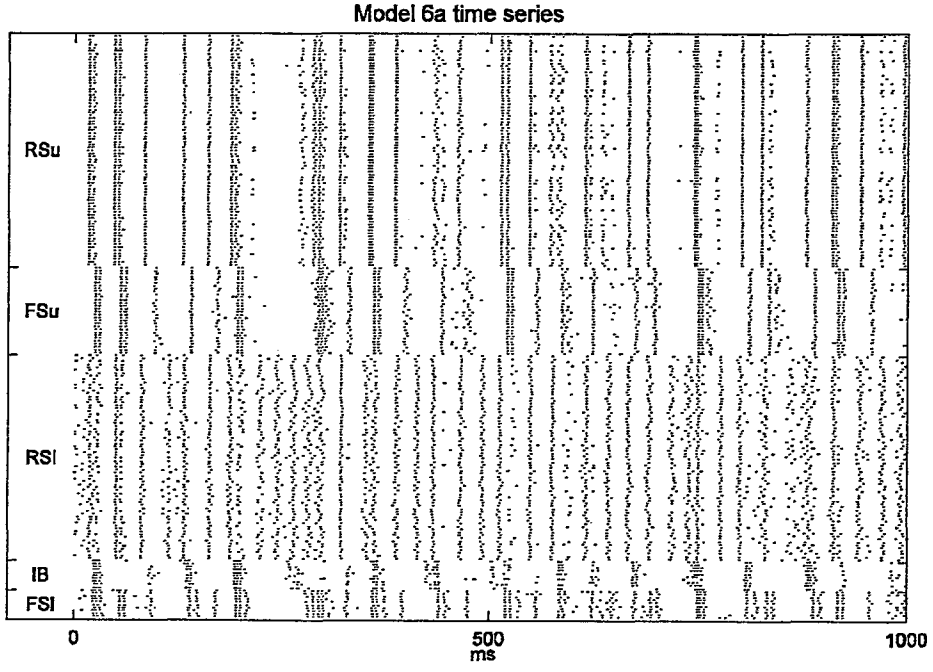

Figure 6.2a

b

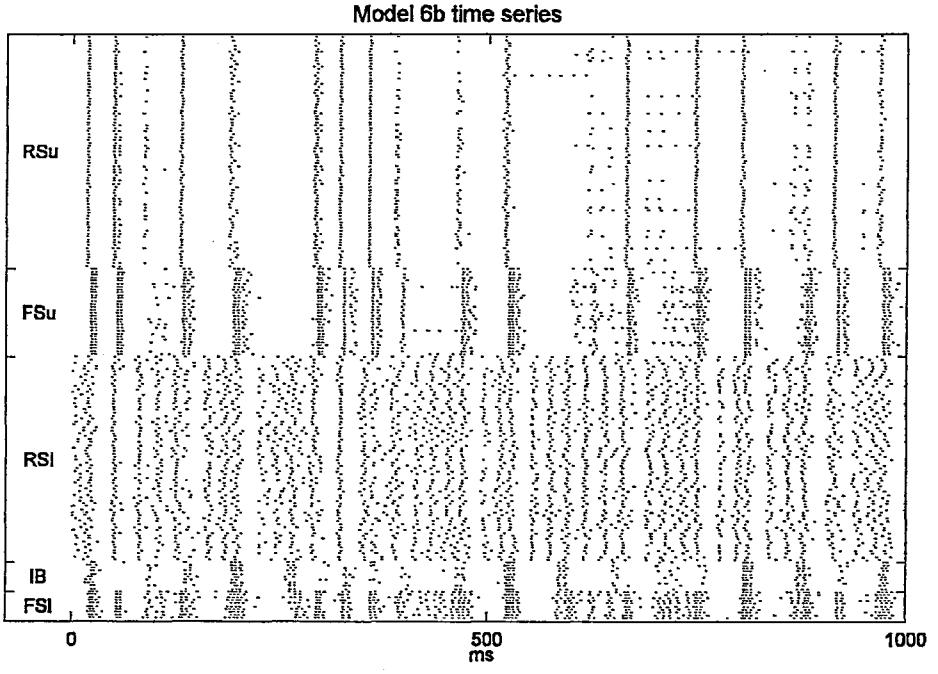

Figure 6.2b

c

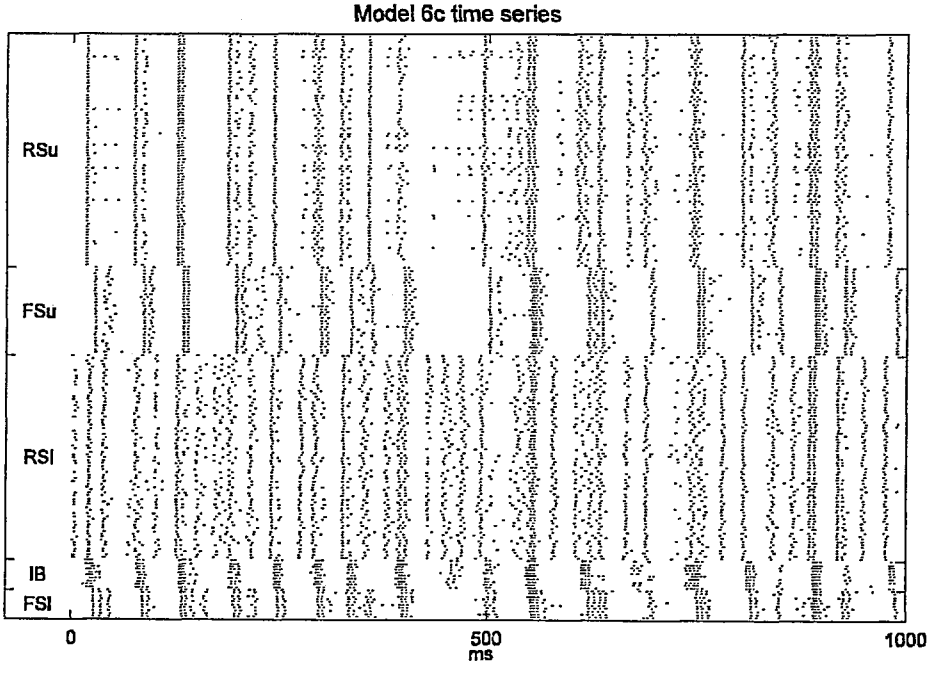

Figure 6.2c

Figures 6.2 a - 6.2 c Column model impulse time series.

Time of individual impulse marked by single dot

Inspection of the raw time series shows the synchronisation of population activity over the whole column (figures 6.2a-6.2c above). Peaks of population activity involve the majority of RS and IB model neurons. The onset of bursts of IB neuron activity coincides with the peaks of RS activity. FS activity closely follows these peaks.

Model	Impulse rate mean per neuron S^{-1}	
	RSu	RSl and IBl
6a	39	42
6b	17	41
6c	33	43

Table 6.3 Pyramidal neuron rates of activity.

The synchronisation of RS neurons, especially in the upper layer, is distinctive. In model 6a, activity in the whole column is strongly synchronised and oscillatory. The upper layer is more sharply synchronised than the lower layer. Model 6b is less synchronised as a whole column, however most upper layer neurons are involved in (a reduced number of) population activity peaks. The whole column activity of model 6c is less well synchronised and the upper layer is less sharply synchronised than in model 6a. In model 6b it is notable that although the rate of RSu activity is substantially less than the lower layer, the pattern of activity remains relatively tightly synchronised.

The coherence of whole column activity can be compared in the autocorrelograms in figure 6.3 below. Model 6a exhibits a stronger oscillatory pattern than 6b or 6c.

a

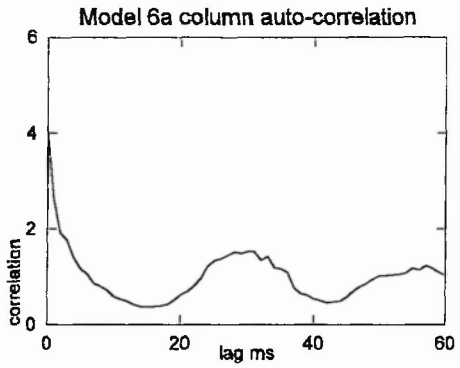

Figure 6.3a

b

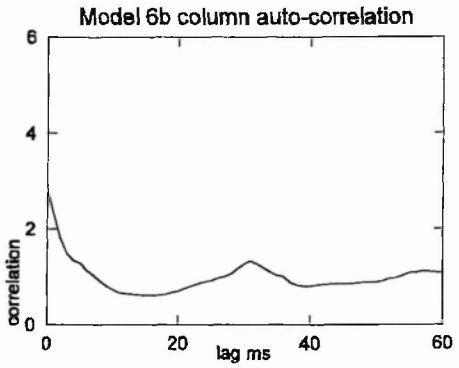

Figure 6.3b

c

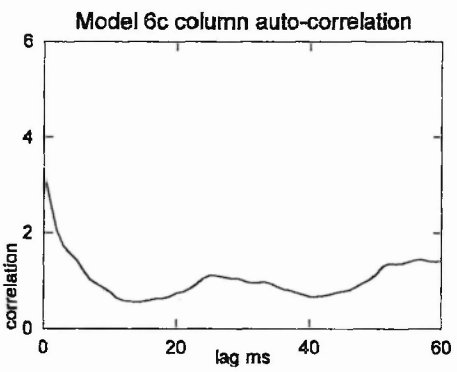

Figure 6.3c

Figures 6.3a-c Column autocorrelation of impulse time series, RS and IB model neurons.

6.2.1 Model 6a

The relationship of the different model neuron subpopulations is seen in Figures 6.4 - 6.15. The RSu population shows a strong depression of firing probability following an initial impulse, recovering to twice the chance level at 32mS lag (figure 6.4a), consistent with the strong synchronisation of upper layer activity.

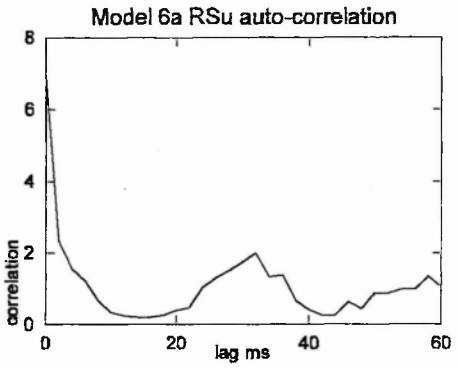

Figure 6.4 a

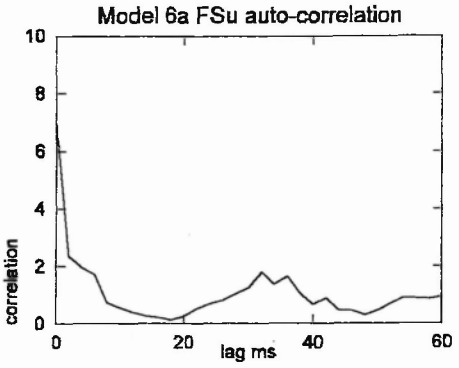

Figure 6.5 a

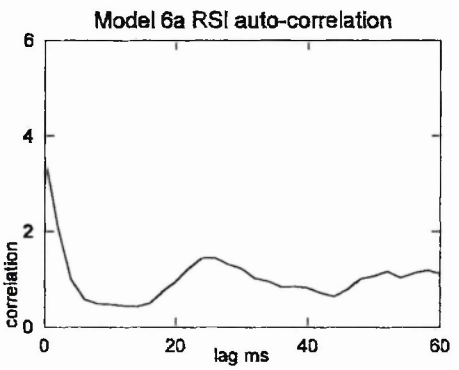

Figure 6.6 a

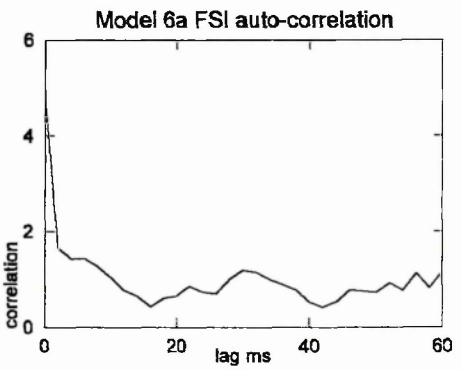

Figure 6.7 a

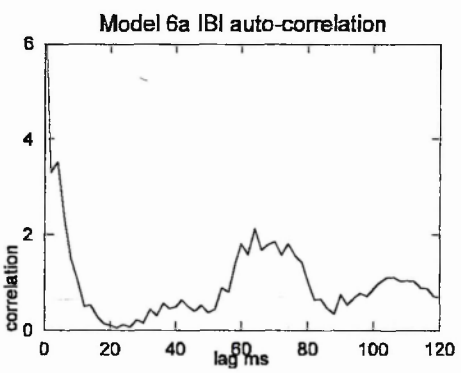

Figure 6.8 a

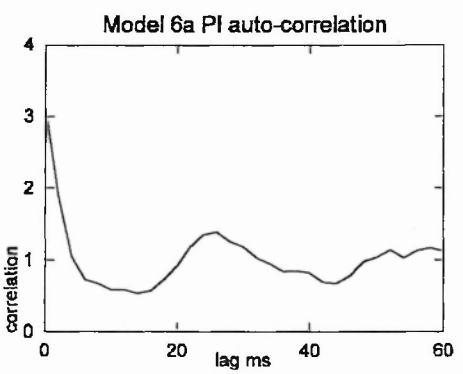

Figure 6.9 a

Figures 6.4a to 6.9a Autocorrelations of column model subpopulations

The modulation of FSu activity echoes this pattern (figure 6.5a). In the lower layers, RSl and FSl activity is less strongly modulated (figures 6.6a and 6.7a). Notably the IB neuron population shows a distinctive period of action. IB activity recovers to a strong maximum at 64mS (figure 6.8a). However the IB neurons are only a fraction of the lower layer pyramidal neuron population and the Pl autocorrelation (figure 6.9a) of the

combined population of RSl and IBl closely resembles the autocorrelation of RSl alone (figure 6.6a).

The FSl autocorrelogram appears to incorporate something of the shape of both the IB and RS autocorrelograms (figure 6.7a). FSl activity remains above chance until a lag of around 10mS, reflecting the persistence of IB activity at short lags. Following a lag of 20ms, FSl activity recovers towards a maximum at a lag of 32mS, reflecting RS activity.

Cross-correlations of column model subpopulations are shown in figures 6.10a to 6.15a, below. The RSu FSu cross-correlation exhibits a maximum at a lag of 8mS (Figure 6.10 a). This lag is consistent with earlier results for RS to FS impulse timing (chapter 4 section 4.3.1, chapter 5 section 5.4.2). The cross-correlation of RSu and lower layer pyramid (Pl) activity exhibits a strong central peak.

The central maximum, symmetry and modulation of the RSu Pl cross-correlogram indicates the synchronisation and periodic pattern of the model column activity (Figure 6.11 a).

Figure 6.12a indicates that FSl activity lags RSl by 8mS. The symmetry of modulation about this time echoes the general oscillatory pattern of column activity. Figure 6.14a, the RSl IBl cross-correlogram, follows a remarkably similar pattern of modulation.

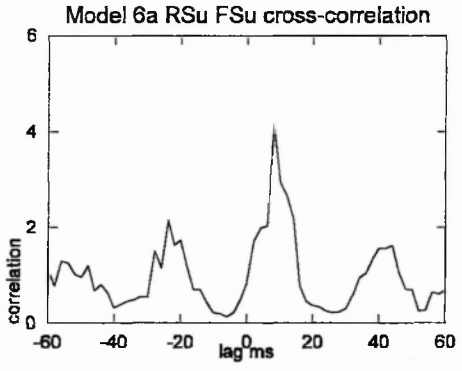

Figure 6.10 a

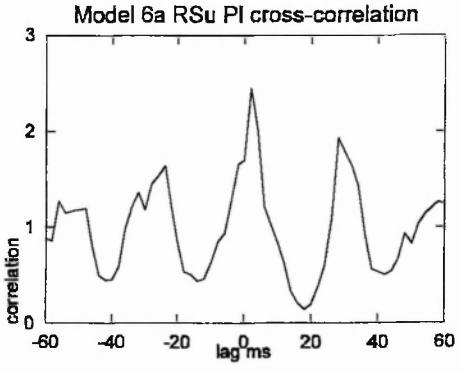

Figure 6.11 a

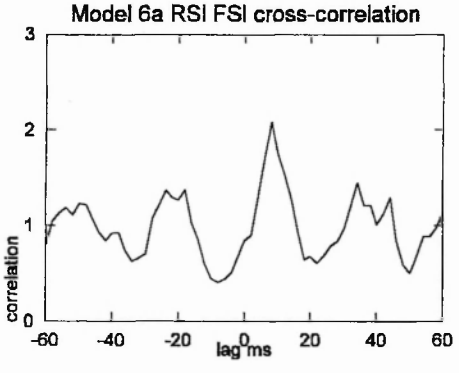

Figure 6.12 a

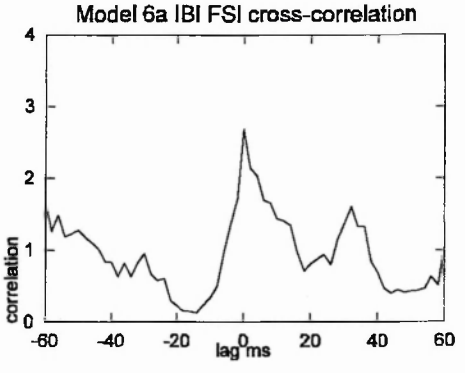

Figure 6.13 a

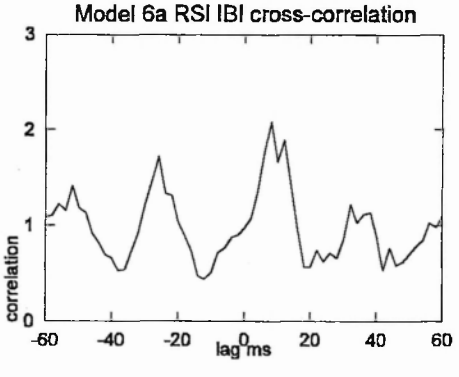

Figure 6.14 a

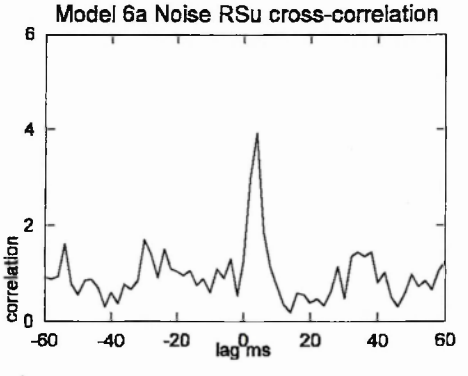

Figure 6.15 a

Figures 6.10a to 6.15a Cross-correlations of column model subpopulations

The central maximum of the IBI FSI cross-correlogram confirms the coincidence of FSI and IBI activity (figure 6.13a). The effect of noise input is indicated in the last

correlogram of this series. Noise input quickly evokes RSu activity around a lag of 4mS (figure 6.15a).

6.2.2 Model 6b

The RSu autocorrelation indicates a periodic action similar to RSu activity in the 6a model. Following initial activity firing probability is strongly depressed, recovering to a maximum at 32mS of more than twice the chance level (figure 6.4b). Although this modulation is strong, the absolute rate of RSu action is low, and its influence on other neurons is weakened. The FSu autocorrelation barely echoes the periodicity of the RSu population (figure 6.5b). The FSu autocorrelogram also shows some influence of the lower layer, since a 'shoulder' of enhanced impulse activity persists after the initial FS action (to a lag of approximately 8mS, figure 6.5b).

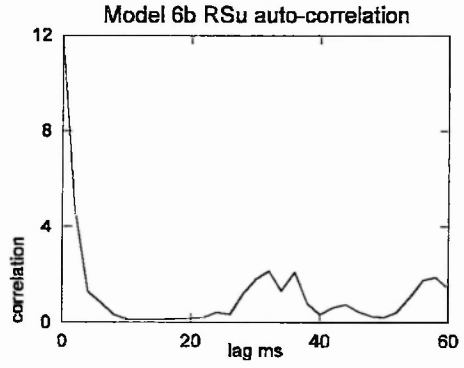

Figure 6.4 b

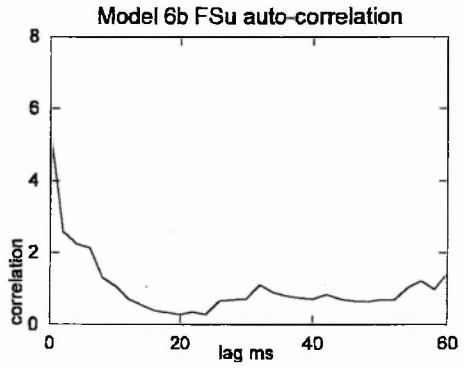

Figure 6.5 b

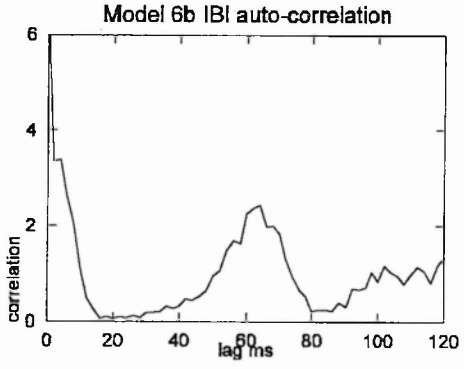

Figure 6.8 b

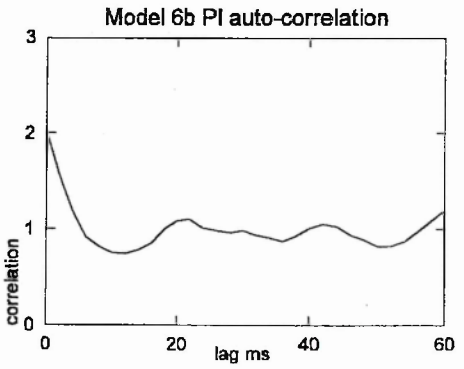

Figure 6.9 b

The collective activity of the lower layer pyramidal population is weakly modulated (figure 6.9a), but the activity of the IBI neurons is strongly modulated with a period of

about 64mS (figure 6.8b). (Figures 6.6b and 6.7b omitted.)

Cross-correlations of the neuronal subpopulations of model 6b follow similar patterns to those of 6a, but with lower amplitudes and less symmetry.

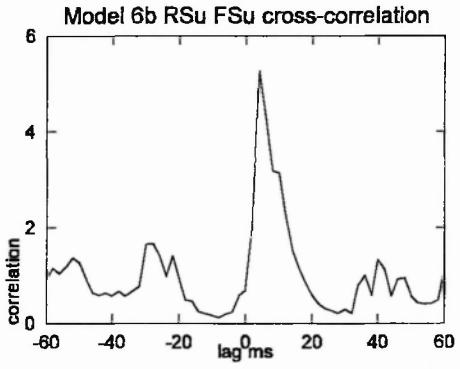

Figure 6.10 b

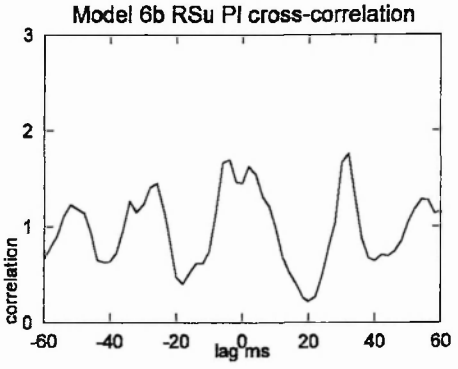

Figure 6.11 b

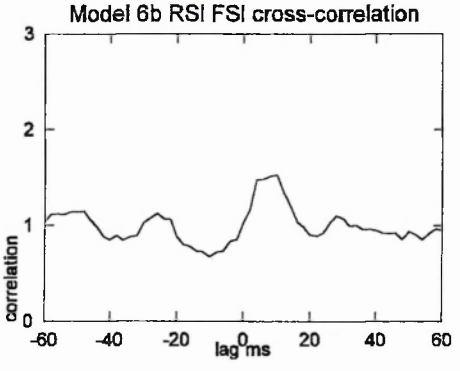

Figure 6.12 b

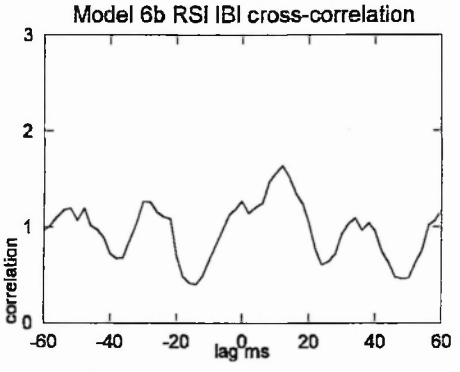

Figure 6.14 b

Figures 6.10b to 6.12b and 6.14b (figures 6.13b and 6.15b omitted)

6.2.3 Model 6c

The column autocorrelogram (figure 6.3c) does not show a strong periodic modulation of activity. Similarly the individual cross-correlograms of the RSu and PI subpopulations (figures 6.4c and 6.7c) do not show strong modulation of activity. However an increase of impulse activity towards a lag of 60mS is evident. The IBI cross-correlogram does show strong modulation, indicating a characteristic period of 60mS (figure 6.8c).

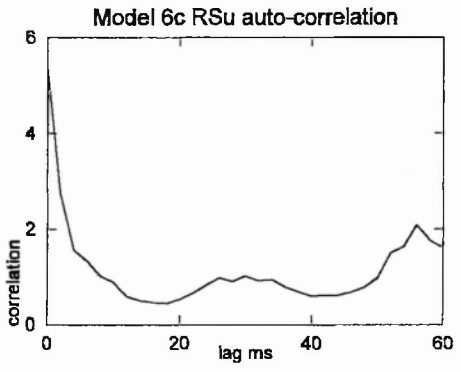

Figure 6.4 c

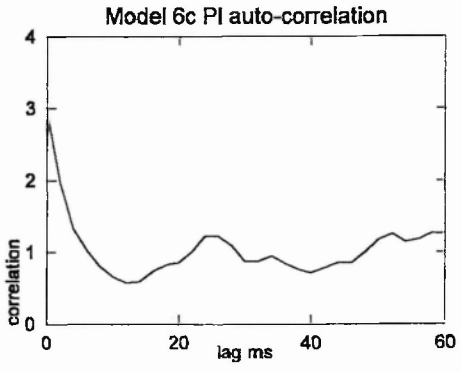

Figure 6.7 c

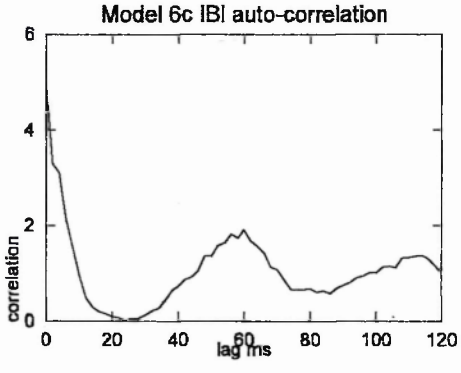

Figure 6.8 c

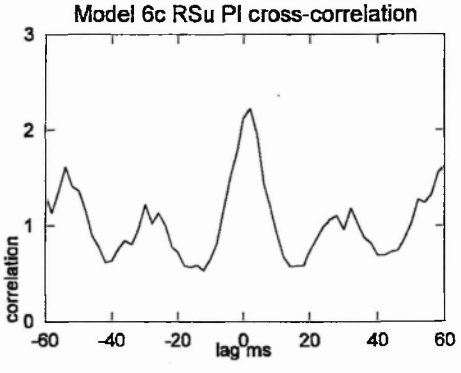

Figure 6.11 c

Figures 6.4c 6.7c 6.8c 6.11c

The cross-correlation of RSu and PI activity is nearly symmetrical and correlation of activity is well above chance at a lag of 60mS. At 30mS lag, activity recovers to about the chance level (figure 6.11c). The 6c column model exhibits a significant component of activity at a period of 60mS. The 60mS period forms a significant component of the activity exhibited by the 6c column model.

6.2.4 Summary of results

Model 6a: The model is configured to achieve a similar rate of activity in upper and lower layers. The upper layer is innervated by a noise signal. The column achieves strongly synchronised and oscillatory activity. The upper layer is more sharply synchronised than the lower layer.

Model 6b: The upper layer noise input weight is reduced. Synchronisation of the RSu subpopulation remains strong. Column activity is less synchronised, oscillations are weaker.

Model 6c: A common noise input acts on upper and lower layers in addition to the noise input to the upper layer. Column activity is less synchronised, a long period oscillation is more evident in the activity of the whole column. This slower period (60mS) is associated with the lower layer IB model neurons.

In each model condition the upper layer is more strongly synchronised than the lower layer. FS population activity lags peaks in RS action by about 8mS in all the models. The bursts of IB neuron subpopulation activity tends to synchronise with population activity in all the models.

6.3 Discussion

The RSu neurons in model 6a have a 32mS period of action, this is similar to the period of RS activity identified in the 5a model. It is suggested that the mechanism of strong synchrony and oscillation of RS neurons arises from combination of the intrinsic period of RS action and inhibitory fIPSP timing. As the upper layer FSu neurons receive a proportion of inputs from the lower layer, this upper layer synchronisation may be modified by differences in the timing of lower layer activity. The sharply synchronised impulse activity of RSu model neurons in 6a results in large compound fEPSPs acting on neurons throughout the LDCM.

It is notable that strong synchronisation of RS model neurons occurs despite the setting of individual neuron adaptation rate variables to a range of values. The variation of input weights is to some extent averaged out over a number of synapses. The fan-out of connectivity keeps neuron models closely coupled despite 'sparse' connectivity. Individual RS neurons are likely to 'see' similar conditions. RSu neurons are more strongly synchronised than lower layer RSl neurons. The main layer

difference is the stronger level of inhibition applied to RSu neurons. The timing of fIPSPs can reduce the variability population action by inhibiting 'early' or 'late' RSu impulses.

It is notable that 6b model RSu neurons retain strong synchronisation with whole column activity despite a lower rate of activity. This is achieved by phase slipping of whole periods as the RSu population remains quiet for a column cycle. This suggests that the RSu population is following a subthreshold cycle as it receives fEPSPs originating in the lower layer and fIPSPs due to the recruitment of upper layer FSu neurons by lower layer activity.

The lower layer IB population has an interburst period of action that is approximately twice the period of column activity in 6a. The IB model neurons are silent during certain column impulse activity peaks, but when they do occur IB bursts tend to synchronise to the cycle of column activity. The IB population is a small fraction of the population of pyramidal model neurons in the lower layer. The effect of each episode of IB population activity is enhanced by the synchronisation of impulse bursts and the number of impulses per burst. In the lower layer, compound fEPSPs arising from synchronised IB innervation may approach the amplitude of fEPSPs arising from highly synchronised RSu activity (assuming 3 impulses per IB burst in 10mS, impulses x synapse number x weight: IB fEPSC total 3x3x0.195=1.755 in approximately 10ms; RSu to RSl fEPSC 1x10x1.95 = 1.95 in approximately 4mS).

The initiation of impulse bursts by IB model neurons tend to coincide with the RS population synchronised action. However the IB impulse bursts persist for a number of mS and this activity overlaps that of the FS neurons. The effect of this timing is ambiguous, as resulting fEPSPs and fIPSPs may be acting against each other according to their relative timings. The effect of this may differ between the layers. The lower layers are weakly inhibited and so IB fEPSPs may dominate and contribute to the timing of RSl impulses. In the upper layer, IB action may recruit FSu neurons resulting in some fIPSPs occurring relatively late stage in a population cycle (allowing approximately 8+8+8mS for IB burst, FS recruitment and fIPSP effective rise time

respectively), relatively suppressing the ~30mS upper layer recovery of activity. Action of this kind may account for the pattern of activity seen in RSu neurons in model 6c. However seeking a causal explanation at this level of detail is perhaps stretching a fair interpretation of the model. Model elements and parameters include a large margin of working assumptions and approximation and so any interpretation should be suitably coarse grained.

6.3.1 LDCM limitations

It is appropriate to consider model limitations when interpreting the behaviour of the LDCM.

The fIPSC rise time implemented in this thesis is based on a particular set of empirical studies (chapter 2, section 2.3.3). However other empirical studies have reported a range of faster values. The upper layer model 5f implements a fIPSC with a fast rise time and finds greater network synchronisation.

Neurophysiological studies describe a wide variation in the neocortical pyramid population. It is not clear that pyramid subpopulations are separable. IB neurons may represent one extreme of a continuous distribution of pyramid morphology. The LDCM implements RS and IB neurons as distinct populations. For example minimum possible individual RS neuron adaptation rate is more than twice the maximum IB adaptation rate. (Adaptation rate parameter r defined in Chapter 3 section 3.2.1, means: IB $r = 0.02$; RS $r = 0.08$. Randomised range 1.3:0.7: IB maximum r =0.026, minimum RS $r = 0.056$.) In addition the bursting parameter k is set so that IB model neurons support burst firing and RS model fire single impulses (see chapter3 section 3.2.1d).

The LDCM RSu neurons do not support bursting, however there is some evidence that bursting pyramidal neurons do occur in the upper layers. Fast bursting neurons with an interburst frequency up to 75Hz are observed in the upper layers (Gray and McCormick 1996). The intraburst frequency of these neurons is very high, so that a 3 or 4 impulse burst might occur within 4mS. The inclusion of bursting neurons in the

upper layer is likely to enhance the action of the synchronised upper layer on the whole column. The inclusion of faster cycle neurons in the upper layer of the LDCM would enable the LDCM to synchronise to higher frequencies. The basic mechanisms of synchronisation by inhibition and phase slipping are not ruled out by the addition of biological detail of this kind. Faster pyramids in the upper layer raises the possibility of the upper layer contributing to a finer temporal resolution compared to the lower layer (if the response of an individual pyramidal neuron is sensitive to relative phase timing of inputs then an upper layer pyramid, posessing a faster cycle of action, will 'see' a larger phase change for a certain input time series than the phase change 'seen' by the slower lower layer pyramids).

The LDCM is partly compromised by low numbers of synapses between FS neurons. Low numbers of connections are to be avoided because of the increased possibility of certain connection paths dominating neuron interaction. The relatively weaker FS to FS synaptic weights partly mitigates this, and each FS model receives 25 fEPSP synapses, which are likely to dominate FS activity. A single model sIPSP synapse occurs on each upper layer FS neuron. This extreme is mitigated by the long time period of sIPSP action, effectively smoothing out short term changes in presynaptic impulse rates (sIPSC rise time is in the order of 100mS, the half width of the synapse model alpha function is around 250mS).

The LDCM implementation of FS distribution only distinguishes an upper and lower layer. The LDCM does not consider a 'feedforward' or 'feedback' topology of projection (beyond different levels of noise input). Any extension of modelling to include subcortical connections and other cortical columns should consider the anisotropic pattern of inhibitory connections suggested by empirical observations. Differences in the directivity of GABAa-ergic and GABAb-ergic synapses are implemented in a model of layer 4 orientation selectivity (Bush and Priebe 1998). Bush and Priebe propose that sIPSP action removes a DC component from a thalamic input signal. In the LDCM sIPSP action powerfully inhibits upper layer activity and a tonic input is used to offset this. The slow negative feedback provided by sIPSPs moderates upper layer RS mean activity, but does not block short term variability.

6.3.2 Mechanisms of synchronisation and oscillation

The conclusion of chapter 5 raised the possibility of a phase difference between pyramidal neuron activity in upper and lower layers (section 5.4). However, the LDCM simulations demonstrate the tendency towards synchronisation of impulse activity in the whole column. There is no systematic phase difference between RSu and RSl activity. The emergence of synchronised activity may be accounted for by the two factors: a population oscillation produced by the coupling together of excitatory and inhibitory populations (i-e oscillator); phase coupling of the pyramidal neurons' intrinsic periodicity. The i-e oscillator takes the form: $\dot{i}=e\,;\ \dot{e}=-i\,;$ and is used in many abstract network models (for example von der Malsburg and Buhmann 1992).

The property of adaptation is capable of synchronising a network of pyramidal neurons (Crook et al 1998b). The adaptation rate of the pyramid neuron is determined by a set of adaptation currents, and affects the regular spiking period (or inter burst period for bursting cells). The adaptation cycle provides a mechanism to shift the timing of impulse generation as the adaptation process is sensitive to depolarisation (z adaptation variable, chapter 3 section 3.2.1b). The phase response function of coupled adapting pyramid model neurons is continuous (Crook p844 figure 2), suggesting that a pyramid network is a single phase system and is not likely to support multiple phase representations (Cairns et al 1993).

The higher level of inhibition in the upper layer reinforces the synchronisation of upper layer RS neurons. The lower layer RS neurons are more weakly inhibited, and their synchronisation is weaker. Correspondingly: reduced input to the upper layer, reducing activity in the upper layer, reduces synchronisation in the whole column; increased input to the lower layer, evoking more activity in the lower layer, reduces the synchronisation of the whole column. In addition the lack of direct connections from lower layer inhibitory neurons (FS) synapsing on the upper layers may indicate a differentiation of temporal function between the layers. The possibility that the observed differences in the behaviour of the layers of the LDCM are functionally

significant is explored in the next chapter.

I am not aware of published models that are directly comparable with the LDCM examined in this chapter. Local neocortex models incorporating models of different neuron types include the local circuit model of Douglas and Martin (1992) and the column model of Bush and Sejnowski (1996). The Douglas and Martin model identifies layer differences and include GABAa and GABAb model synapses (fIPSP and sIPSP synapses), but implements a two layer model where a common inhibitory population acts on both upper and lower layers. Douglas and Martin use this model is used to examine the local response to thalamocortical afferents, they do not examine the synchronisation of oscillations. Bush and Sejnowski implement a column model that includes different neuron types but does not implement layer differences (and so is closer to the single layer model of chapter 5). The Bush and Sejnowski model demonstrates synchronised oscillations, but synapse parameters differ from the networks implemented in this thesis (except model 5f). (Differences between the Douglas Martin and Bush Sejnowski models and this thesis are discussed in chapter 5, section 5.4.4 .) Traub et al (1997b) implement a model including different neuron types that exhibits oscillations. This model does not include layer differences and uses a specific mechanism to generate oscillatory activity (a mutually inhibitory circuit based on hippocampal physiology) and is not directly comparable with the model presented here. This model is discussed further in chapter 7 (section 7.5.4). These studies illustrate different approaches to modelling local neocortical activity, but they do not examine the contribution of layer differences to synchronisation and oscillation of neocortical activity.

6.4 Summary

A neocortical functional column model (LDCM) is implemented. The LDCM incorporates RS, FS and IB neurons distributed in two layers. The upper layer is more strongly inhibited.

Synchronisation and oscillation of the whole column is demonstrated. The upper layer is more tightly synchronised than the lower layer. When the balance of column activity favours the upper layer, the whole column is more synchronised and oscillatory.

Synchronisation of population impulse activity is facilitated by fIPSP inhibition. RS and IB model neurons possess a characteristic period of action associated with the respective adaptation rates. When the RS or IB rate of activity is less than the column oscillation rate, synchronisation occurs by phase slips, with silent periods.

It is proposed that the upper layer is concerned with a finer temporal resolution, and the lower layer supports a broader temporal tuning. The consequences of this layer difference are considered in the next chapter. Approaches to extending the model to include lateral and more distant connectivity are also discussed.

7 Discussion, a New Model and Future Work

In previous chapters this thesis has developed a simplified model of local neocortex that portrays the dynamic relationship of upper and lower layers. Here the results of chapter 6 are reviewed in relation to existing theory and models concerning local cortical function. A new synthesis of theoretical and empirical results is suggested, a new model of local cortical circuit functioning and areas of further investigation are proposed.

7.1 Consequences of results

The simple column of chapter 6 demonstrates the synchronisation of oscillatory activity in a two layer column model (the 'layer difference column model' : LDCM). The greater level of inhibition in the upper layer contributes to the tighter synchronisation of that layer. How do these results inform an understanding of different theoretical approaches to oscillating activity in the local neocortex? The existence of oscillation and synchrony is consistent with many theoretical models and empirical studies, and is not a novel contribution. The finding of a laminar differences in the quality of synchronisation in the LDCM leads to a new proposal of a functional circuit for the integration of laminar activity, inputs from distant cortical areas and the role of collective oscillatory activity.

Chapter 1 briefly introduced some empirically based proposals regarding cortical synchronised gamma oscillations. These are revisited in the light of the results from chapter 6.

7.1.1 Multiple synchronised assemblies

Engel and Singer find stimulus dependant synchronisations of cortical activity (review Engel and Singer 2001). They propose that the responses evoked by a single stimulus

object are bound together by the temporal correlations of spatially separated neuronal responses, forming a synchronised neural assembly. Because of the temporal precision of synchronisation, the assembly supports a more effective interaction with other assemblies and contributes to 'bottom up' activity. Because of the persistence of the active assembly, interaction with 'top down' processing is also supported. They further suggest that multiple assemblies can be active in the network at the same time, and these multiple representations can participate in larger scale coherence, binding into higher order arrangements. Mechanisms which support such higher levels of integration are not described. As Engel and Singer's account does not portray specific mechanisms, the 'laminar difference' results of chapter 6 do not contradict their general account, however this hardly takes us any further forward.

7.1.2 Synchronisation over distance

Traub et al propose a model where interneuron inhibition (disinhibition) develops an oscillation that modulates the action of pyramidal neurons (Traub et al 1997b). The model is based on the physiology of the hippocampus where excitatory to excitatory connectivity is sparse. It is proposed that the phase timing of an excitatory impulse relative to the inhibitory clock is a functional 'code'. In addition interneuron 'spike doublet' firing supports synchronisation despite conduction delay of the order of several milliseconds (eg 5mS delay over 1.5mm (Traub et al 1996). A motivation for this model is the possibility of the phase timing of an individual impulse supporting a radial basis function code (RBF) (Hopfield 1995; Sejnowski 1995).

Local inhibitory oscillation may be supported by the denser interneuron to interneuron connections that appear in the upper layers (layers 2/3: Gonchar and Burkhalter 1999). But it is certainly the case that the majority of neocortical synapses are excitatory, reducing the probability that 'inhibitory oscillation' can be a sole modulatory influence. In addition it is not clear if sufficient long range inhibitory connections exist to support this mechanism of inhibitory oscillation across more distant cortices.

Recordings of PSP activity during oscillatory synchronous activity in neocortex found a contribution from both IPSPs and EPSPs to sub-threshold membrane potential

oscillations (Fetz et al 2000). Indeed, recordings on the same postsynaptic cells measured a larger collective EPSP component during oscillatory activity than recordings made during periods of unsynchronised activity (oscillation indicated by the local field potential). The view that inhibitory action plays a separate role in synchronisation is not supported by these observations. However, a mechanism of relative phase coding of impulses is still possible, but less tractable as the oscillatory 'clock' is inseparable from the local collective activity.

The oscillation of the LDCM is not exclusively driven by an inhibitory field. On balance, the inhibitory clock mechanism of Traub et al (1997b) must be rejected for neocortical oscillations. However the possibility of a 'timing code', where the timing of individual impulses carries significant information, remains open. The more variable timing of individual RS impulses in the lower layer of the LDCM is consistent with the possibility of a 'timing code', with the tightly synchronised upper layer population providing a clock.

7.1.3 Stimulus locked and stimulus induced oscillatory responses

The proposals of Eckhorn et al are based on visual cortex empirical results and the modelling of activity in single layer multiple area networks (Eckhorn 1999). In common with the results of Engel and Gray (Engel et al 1990; Gray and Singer 1989), Eckhorn et al finds that the response to a common stimulus involves a synchronisation of the oscillatory local field potential across a populations of neurons (Eckhorn et al 1988). Following stimulus onset a 'stimulus locked' response is observed. A local area of cortical neurons is active, but a collective oscillation is not evident in the LFP (local field potential). If the stimulus is maintained, a collective oscillation is observed by around 100ms following the stimulus onset. This response is typical for smoothly moving stimuli (gratings). Eckhorn et al observe that the frequency of the single unit activity (SUA) is more variable than the oscillatory LFP (Eckhorn et al 1993).

Eckhorn et al suggest a variation of the 'binding by synchronisation' hypothesis (Eckhorn et al 2001). They observe that the lateral cortical range of gamma synchronisation is only a few millimetres (which is not large enough to accommodate

the responses from a single large stimulus object). They demonstrate the existence of a larger oscillatory response field using a different analysis of the empirical results. They find a gamma wave, with continuous phase shifts over the responding cortical area and suggest that object continuity is coded by phase continuity of the wave. Eckhorn et al suggest that distant cortico-cortical cooperation is not by gamma wave phase locking, but by the amplitude envelope of the local gamma wave. If it is allowed that this 'amplitude envelope' may represent modulation by a lower frequency wave then Eckhorn et al's proposal is consistent with the proposals of von Stein and Sarnthein (2000).

The in-vivo local cortical response contains different frequency components (Frien and Eckhorn 2000). Using two recording sites it was found that high and low frequency components of coherent oscillations depended on the orientation preference of the two sites and the orientation of the stimulus. The coherence of the low frequency component showed a dependence on the co-axiality of the two receptive fields and the gamma frequency component did not. This result introduces the possibility of parallel coding streams in the activity time series of the local cortex neurons at different frequencies.

7.1.4 Scales of EEG frequencies and spatial scale of cortical integration

Based on EEG recordings, it is suggested that different temporal scales correspond to the integration of activity across different cortical spatial scales (von Stein and Sarnthein 2000). Gamma frequency EEG is associated with local area visual processing. Synchronisation between neighbouring cortices occurs in the beta1 range (12-18Hz). Long range interactions (fronto-parietal) involved the alpha and theta frequencies (8-12Hz and 4-8Hz). It is suggested that the lower frequencies are involved in top-down or feedback processing.

The results and proposals of Eckhorn, Frien and von Stein introduce the idea of different scales of responses, that may impinge on the local cortical circuit. This is relevant to an extension of the LDCM. The problem of the incorporation of distant cortico-cortical inputs is discussed below.

7.1.5 Antithesis: gamma oscillations as epiphenomena

The view that oscillation and synchronisation is important in the generation of a cortical response is questioned (Lamme and Spekreijse 1998). Lamme and Spekrijse did not find that gamma oscillations were ubiquitous. They obtained good RF responses without noticeable oscillations. They consider that gamma oscillations are epiphenomena of lateral connectivity. Similar views have been expressed by others (Tovee and Rolls 1992).

Eckhorn et al reply that differences in results may be because Lamme and Spekrijse measured multi unit activity (MUA) which is a less reliable indicator of local population oscillation than the LFP (Eckhorn et al 2001). In addition Eckhorn (1999) observes an initial 'stimulus locked' response that corresponds to the stimulus onset (section 7.1.3 above), that may account for a fast non-oscillatory RF response.

Engel et al make a similar reply to Tovee and Rolls, defending their observations of synchronised oscillations, pointing to difficulties in methodology. Engel et al point out that as correlograms may be compiled over a number of trials and where the oscillation frequency varies, the correlogram may fail to exhibit characteristic oscillatory peaks and troughs (Engel et al 1992).

7.1.6 Layer differences in synchronisation

The LDCM, presented in chapter 6, demonstrates a difference in temporal behaviour between the upper and lower layers. What is the functional significance of this?

The layer difference does not seem useful for a 'vanilla' theory of binding by synchronisation. Why is the lower layer less synchronised than the upper layer?

A neural oscillator time delay coding network has been modelled (Traub et al 1997b), but the clock was formed from mutual inhibitory action, and not driven by the local excitatory action. From the results of chapter 6, collective oscillations occur as a result of the interlaminar circuit. This includes both inhibitory and excitatory components, if

the upper layer is used to provide a clock, the clock cycle is simply a characteristic of the whole circuit. The 'clock' mechanism of the Traub model may not be correct in the neocortex, however the possibility of a 'time code' still exists. The variability of impulse timing in the lower layer might allow a response characteristic that could support a temporal code.

Eckhorn reports that the correlations of SUA are variable and are weaker than correlations of the collective population oscillations (as seen in the LFP: Eckhorn et al 2001; Eckhorn et al 1992). This variation in the timing of the individual neuron impulse response, within a population supporting synchronised oscillatory activity, allows the possibility of a time coding mechanism.

Before strong claims of the existence in cortex of a particular temporal coding mechanism can be supported, a further consideration of neurophysiology is necessary.

7.2 Local cortical physiology

7.2.1 Neuron types

Nowak et al provide a classification of neuron types based on morphology and electrophysiology that extends earlier work (Nowak et al 2003). Four main classes of neurons are distinguished:
RS regular spiking are pyramidal in layers 2,3,5,6 and spiny stellate in layer 4;
FS fast spiking are sparsely spiny or aspiny nonpyramidal cells;
IB intrinsically bursting are pyramidal in all layers, but concentrated in layer 5; CH chattering neurons are in layers 2 to 4, concentrated in layer 3, they are pyramidal or spiny stellate cells and produce high frequency bursts of action potentials.
These layer differences will contribute to the behaviour of the local 'vertical' columnar circuit. Modelling of local activity has included representation of IB neurons (for example LDCM in chapter 6 or Bush and Sejnowski 1996). The LDCM includes IB model neurons in the lower layer. The existence of CH neurons (higher frequency

bursting neurons concentrated in layer 3) suggests a differentiation of the layers 2/3 and 4 that may repeat the lower/upper differentiation implemented in the LDCM.

7.2.2 Cortical connections and the local circuit

7.2.2a Local circuit afferents

An extensive and historic literature addresses the complex pattern of connectivity in the local neocortex (Gilbert and Wiesel 1979; Lorente de No 1922) and later reviews (Callaway 1998; Gilbert and Wiesel 1983). Callaway (pp64-68) reviews local connectivity and identifies feedforward connections: thalamic (LGN) input to layer 4c, layer 4c to 2-4b and then to 'higher' areas. And feedback connections: layer 4c to 6 to 4c; layers 2-4b to 5 to 2-4b. Layers 2-4b provide the source of cortico-cortical feedforward flow to 'higher' areas. Local horizontal projections allow intralaminar reciprocal connections (with patchy lateral arbourisation). At a greater scale, cortico-cortical feedback occurs from a 'higher' area layer 5 to a 'lower' cortical area layer 5 and upper layers (via layer 1) (Felleman and Van Essen 1991; Tanaka 1997). The general pattern of feedforward and feedback innervation involves a different targeting of the layers, hence one might expect that behavioural layer differences are likely to be important for larger scale cortico-cortical integration.

7.2.2b Interlaminar connections

Thomson and Bannister make an extensive review of interlaminar connections in the neocortex (Thomson and Bannister 2003). They note a general pattern of connections: 'forward' projections from layer 4 to 3 and 3 to 5 target pyramid cells and interneurons; 'back' projections from 5 to 3 and 3 to 4 primarily target interneurons. They find very specific interlaminar selectivity. For example layer 3b pyramids target layer 5a IB pyramids, and do not contact layer 5 smaller pyramids (RS neurons). Intriguingly, both the layer 3b pyramids and 5a large pyramids (assumed to be IB) have apical dendrites that enters layer 1. The apical dendrites of layer 5 smaller neurons (RS) do not reach layer 1. The layer 5 RS pyramids have extensive lateral axonal arbours in layer 5 and they innervate the IB neurons, but return IB to RS connections appear to be infrequent (at a ratio of 1:10). These differences suggest a

convergence of processing streams. Interneuron classes show highly selective connectivity patterns, contacting specific regions of the target cells.

Thomson and Bannister present a generalised classification of interneurons into proximally targeting and dendrite targeting cells. In addition to the anisotropy of 'vertical' inhibitory connections, they note a difference in horizontal connectivity. The horizontally projecting axons of pyramidal neurons are fine and largely unmyelinated with a conduction velocity in the order of 0.3 metres S^{-1}. Interneuron axons are thicker and strongly myelinated, and for a diameter in the order of 10μm the conduction velocity is approximately 4m S^{-1} (p137 Nicholls et al 1992). The difference in conduction velocity is in the order of 3ms per millimetre. Thomson and Bannister note that this may form the basis of a time delay network and contribute to temporal signal processing.

These observations (7.2.2a and 7.2.2b) provide a more general context for the consideration of the results from the LDCM considered in chapter 6. This and earlier chapters made a number of simplifying assumptions and have excluded a consideration of some typical physiological features of local neocortex as being beyond the scope of the local circuit model. The results from the LDCM are qualified by these simplifying assumptions. An extension of the model must reconsider features which will allow the extension of the model vertically, for example to include additional interlaminar connections, and extension of the model horizontally to allow interaction with adjacent column circuits.

7.3 Modelling more local physiology

The development of the LDCM omitted a number of features of local cortical physiology and organisation that may be relevant to a more extensive model concerned with temporal activity and the integration of inputs from lateral and distant areas. For example the active apical dendrite is not portrayed. The apical dendrite of a pyramidal neuron provides a vertical pathway through the laminae. The LDCM does

not address the possibility of active processes on the apical dendrite, however there is good evidence that the apical dendrite supports active conductances (Connors et al 1994). Lateral locally projecting axons differ in their myelination and the different conduction velocities may support a local delay line network (Thomson and Bannister 2003). The inclusion of additional layers would modify the chapter 6 LDCM, the implementation of layers 4 and 1 would allow an investigation of the influence of 'distant' feedforward and feedback inputs.

7.3.1 Apical dendrite function

Passive transmission of PSPs on the apical dendrite is inconsistent with empirical results. The pyramidal neuron's apical dendrite may act as a sharp coincidence detector, correlating distal inputs with local layer inputs (Larkum et al 1999).

Passive integration of synaptic activity acts as a weaker coincidence detector, as PSPs arriving at the same time will sum to a greater amplitude than PSPs that are separated in time. The integration of PSPs on the proximal or basal dendritic arbour may be predominantly passive.

7.3.2 Local lateral axon conduction velocity

Local lateral pyramidal isocortex axons are unmyelinated or sparsely myelinated and propagation velocity is around 0.3m S^{-1}. Interneuron axons are myelinated and achieve a propagation velocity in the order of 4m S^{-1}. For a cortical lateral distance of 10mm the EPSP IPSP timing difference is in the order of 30mS. The local lateral axonal connections may provide a time delay network. The faster inhibitory pathway may serve as a reference timing signal (so partially reintroducing a theme from the models of Traub et al 1997a and 1997b).

7.3.3 Subcortical and intercortical inputs: Layers 4 and 1

A more detailed local circuit may be implemented by the separation of layer 4 as a distinct input layer, contributing to an upper layer reciprocal circuit. Inputs from distant neurons arriving at layer 1 innervate the apical dendrites of larger pyramidal cells.

7.3.4 The functioning local circuit

The implementation of active apical dendrites, providing coincidence detection and a lateral axonal 'delay' network may introduce a new signal processing capability to an extended model of the local cortical circuit. A time delay network and coincidence detection are necessary elements for a time based implementation of a Radial Basis Function Network (RBF) (Hopfield 1995; Sejnowski 1995). RBF is a powerful pattern recognition algorithm. The interactions of cortical column circuits with lateral connections may achieve this role.

7.4 A new synthesis for local cortical action

This proposal is based on an extension of the simple LDCM of chapter 6, including further features of local cortical physiology. Thomson and Bannister (2003, section 7.2.2b above) observe that layer 3 pyramids innervate large layer 5 pyramidal cells (IB neurons) and these IB neurons preferentially contact layer 3 interneurons achieving a vertical circuit similar to the LDCM.

The neocortical layer 1 is not represented in the LDCM, the upper layer of the LDCM represents layers 2 to 4 and the lower layer represents layers 5 and 6.
However, it is known that the apical dendrite of IB neurons ascends to layer 1. The LDCM may be extended vertically to connect to another input layer by the implementation of the apical dendrite extending from lower layer IB neurons to a superficial input layer (representing layer 1, above the upper layer of the LDCM). The action of the active apical dendrite introduces a coincidence detection function to the local circuit. The response of the IB neuron depends on the relative timing of superficial inputs and local activity.

The LDCM does not implement lateral connectivity to 'horizontally' adjacent columns. The horizontal extension of the model network's circuit involves the local

lateral axonal projections. Differences in inhibitory and excitatory axonal conduction velocities (section 7.3.2) may provide the basis for a local time delay network.

The combination of the local circuit oscillation (providing a time frame), coincidence detection and a delay network may provide the elements necessary for the time coding network proposed by Hopfield and Sejnowski (1995, and section 7.4.1).

The above description of this arrangement uses the example of the interlaminar connectivity of layers 3 and 5. It may be noted that layers 4 and 2/3 appear to have many aspects in common with the interlaminar relationship of layers 3 and 5. Layer 4 possesses a high density of interneurons, implying a higher level of local inhibition. Layers 2/3 receive excitatory and inhibitory inputs from layer 4, but layer pyramid 3 neurons preferentially target the interneurons in layer 4. In addition, layer 3 pyramid neurons possess apical dendrites that ascend to the superficial layer 1. It is a short step to propose that the CH neurons that are concentrated in layer 3b are the neurons that preferentially project to layer 4 interneurons and to propose that these CH neurons possess apical dendrites that arbourise in layer 1. This proposal suggests that the fast bursting CH neurons of layer 3b play a role in the 4 to 2/3 circuit that is similar to the role of IB neurons in the 3 to 5 vertical circuit. The proposal of a generalised functional 'local columnar circuit' is elaborated below (section 7.4.2).

7.4.1 The components supporting local cortical action:

The vertical circuit and layer differences achieve a synchronised oscillation (in the LDCM), providing a timing reference.

The pyramidal active apical dendrite provides a coincidence detection function vertically across layers. Horizontal local axonal projections provide a time delay network. The less strongly synchronised layer (less inhibited, lower layer in the LDCM) contains the soma of the pyramid neuron, and the impulse timing of the individual pyramidal neuron is a function of the coincidence detected between the 'home' layer and the distal input layer. The combination of these components may support the time coding function proposed by Hopfield and Sejnowski (1995).

7.4.2 Proposal for a prototype 'time coding' local columnar circuit

The minimum arrangement comprises:

a cortical 'input' layer A;

a local cortical feedback layer B;

a cortico-cortical 'distant input' layer C.

Layer A includes RS, FS, and may include bursting neurons.
Layer B includes RS, FS, and bursting neurons (CH or IB).
Local lateral connections in layers A and B form time delay networks. The vertical connection from A to B innervates both pyramidal and interneurons.
The bursting pyramidal neurons in layer B preferentially innervate layer A interneurons, and the reciprocal A to B circuit is oscillatory. This collective oscillation provides a reference time frame for a time code.

The distal apical tufts, of the apical dendrites of bursting pyramids in layer B, receive inputs from layer C. The apical dendrite can provide a 'coincidence detection' function between the distal inputs and the local inputs in layer B. According to the timing of distal inputs, relative to the local (oscillatory) activity, the layer B pyramidal neuron will produce an impulse that is delayed or advanced relative to the collective activity. This 'time code' impulse in conjunction with the lateral time delay network may achieve Hopfield's proposal of "action potential timing for stimulus representation"(1995).

Layer B sends intercortical projections to distant layer C areas. (The 'distant' circuit is reciprocal between local area layer B projecting to distant area layer C, and the return projection from distant B to the local area layer C.) This circuit is sketched in figure 7.1 below.

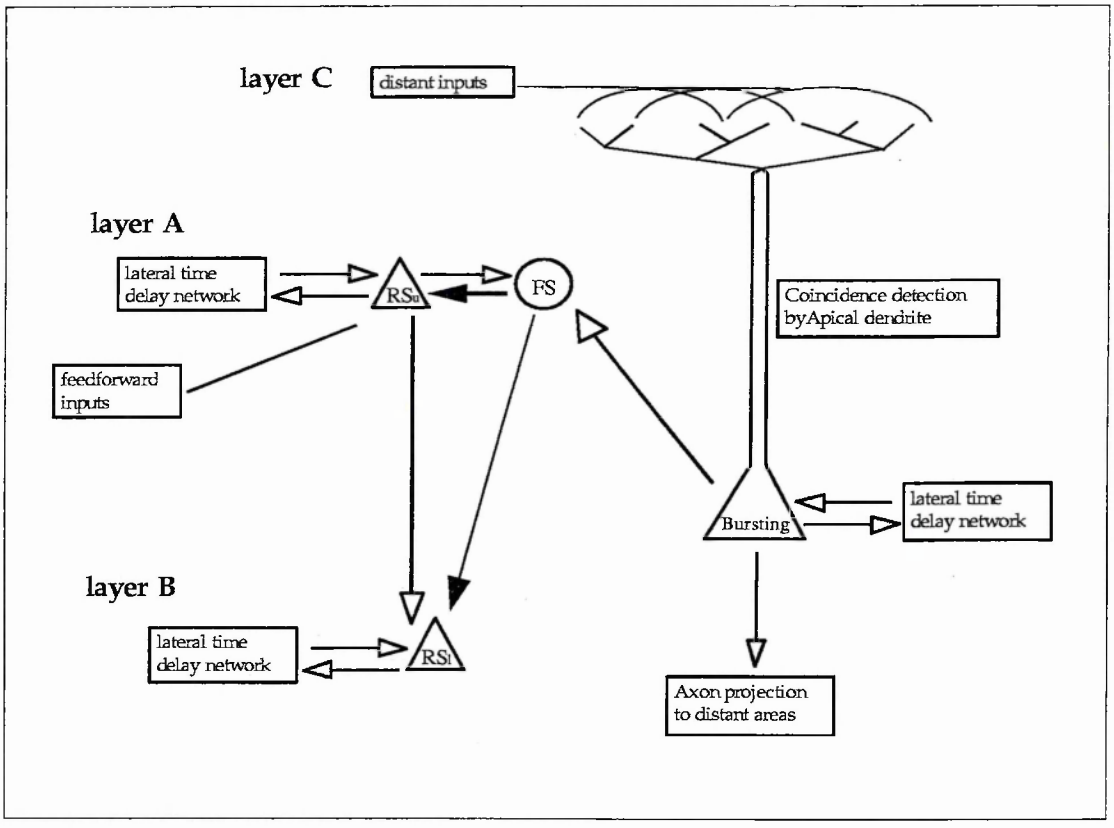

Figure 7.1 Sketch of local columnar circuit. Three layers are distinguished: a cortical 'input' layer A; a local cortical feedback layer B; a cortico-cortical 'distant input' layer C. Triangles represent populations of RS neurons, circles represent populations of inhibitory FS neurons (a small population of FS neurons in layer B is not shown). The shape labelled 'Bursting' represents a population of bursting pyramidal neurons (CH or IB cells). Open arrowheads represent excitatory synapses, solid arrowheads represent inhibitory synapses. Arrow weight represents the relative strength of a connection.

A local vertical recurrent circuit is formed between the layers A and B. The feedback from layer B to inhibitory FS cells in layer A contributes to the oscillatory activity of the local neuron population. The bursting cells in layer B mediate the feedback to layer A, and so play an important role in the local oscillatory circuit. The bursting neuron also receives inputs to the distal apical tuft in layer C. These inputs are modified by the action of the active apical dendrite, which acts as a coincidence detector. When the timing of the inputs to the apical tuft is correlated to the local activity (inputs to the pyramids basal dendritic arbour) burst firing is enhanced. This 'coincidence detection' then affects the local activity as the bursting neuron innervates: the layer A interneurons, potentially shifting the phase of the local oscillatory cycle; and the lateral 'time delay' network of layer B.

This proposal is novel because the oscillation 'clock' is closely coupled to the activity of the bursting neurons. As the bursting neuron population provides coincidence

detection between distant layer C inputs and local activity, the 'clock' oscillations are sensitive to the interaction of 'distant' inputs and local activity.

This scheme is extended to described relations between the cortical layers 1 to 5. (For simplicity I will ignore layer 6 for the moment.)

7.4.3 A scheme of neocortical local circuit function

It is proposed that the column vertical circuit consists of two main component circuits: the reciprocal layer 4 to 2/3 circuit; the reciprocal layer 2/3 to 5 circuit. Both circuits interact with layer 1. Figure 7.2 sketches the arrangement for the circuit 4-2/3 (layers 4, 2/3 and 1 are comparable with layers A, B and C respectively in figure 7.1).

7.4.3a A local circuit for layers 4, 2/3 and 1

A mechanistic account of the circuit 4 to 2/3 follows:

i. layer 4 activity receives LGN thalamic inputs;
ii. activity spreads laterally within layer 4 (but is restricted), layer 4 relays activity to layer 2/3;
iii. activity spreads laterally within layer 2/3;
iv. layer 2/3 RS cells innervate layer 3b CH cells but CH cells do not (mostly) contact other layer 2/3 RS neurons (prediction 1);
v. CH cells have apical dendrites that arbourise in layer 1 (prediction 2);
vi. the CH cells serve as coincidence detectors, integrating layer 1 inputs with the temporal responses of layer 3;
vii. the predominant layer 4 targets of CH cells are interneurons (prediction 3), completing the vertical circuit.

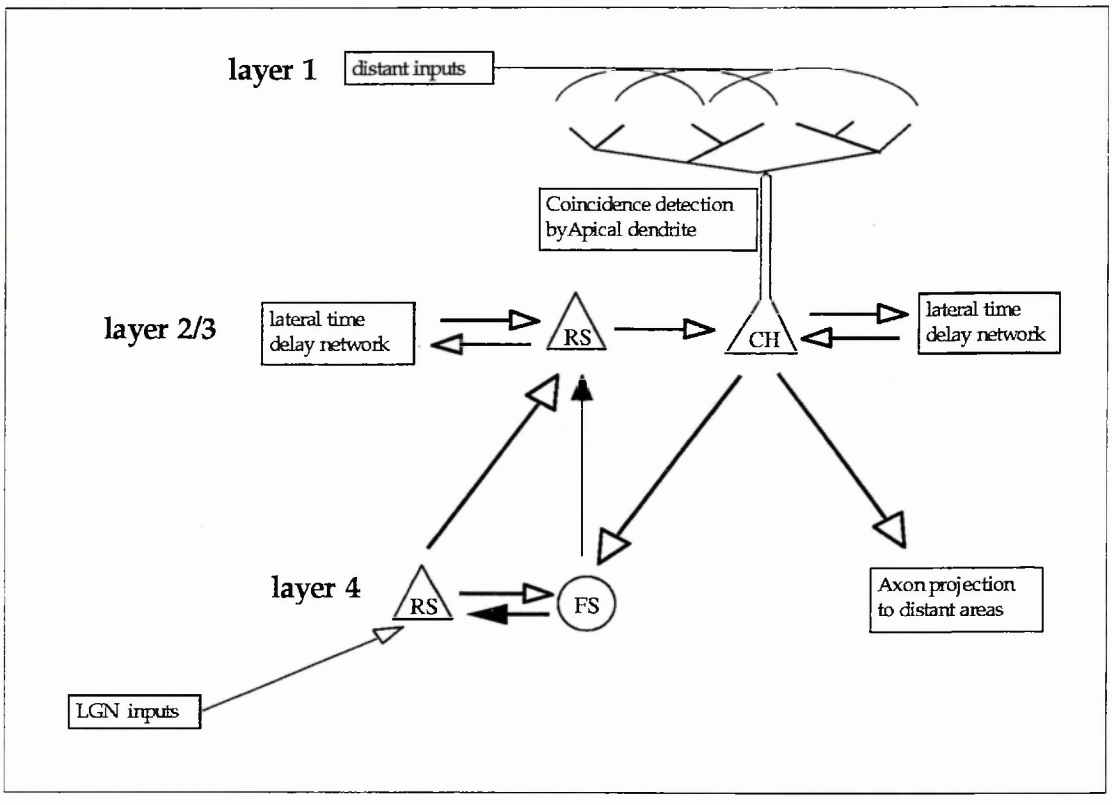

Figure 7.2 Sketch of layer 4 to 2/3 circuit. Layer 2/3 inhibitory interneurons not shown. Lateral projection from layer 4 neurons is restricted to the 'home' column. Lateral projections in layer 2/3 extend to several millimetres.

The feedback innervation of inhibitory interneurons in layer 4 enhances the oscillatory action of the circuit. During an oscillatory episode, the phase timing of impulse firing by layer 2/3 RS neurons and CH cells will be more variable than layer 4 spiny cells (prediction 4; predictions are listed in table 7.1 below). Crudely, it may be thought that layer 4 is providing a clock, and the timing of layer 2/3 RS and CH impulses are varying 'coincidence detection' changes the timing of impulse production. The 'clocking' mechanism is subtle as it will be influenced by the functioning of the CH population, ie: the coincidence of layer 1 activity and layer 2/3 activity.

7.4.3b A local circuit for layers 2/3, 5 and 1

This circuit schema is similar for the layer 4 to 2/3 reciprocal circuit, with some additions (figure 7.3 below). Layer 2/3 neurons project to layer 5, preferentially contacting IB neurons. Layer 2/3 interneurons are innervated by layer 5 IB neurons.

Layer 5 IB neurons receive inputs from layer 5 RS neurons, but return connections are infrequent. The vertical circuit differs from the 4-2/3 scheme, because it integrates at a larger scale. Layer 5 RS neurons have apical dendrites that arbourise in layers 4. It seems then that layer 5 RS neurons can integrate the local responses of layer 4 with layer 5, and the resulting activity is relayed to the IB neurons. As the IB neuron apical dendrite arbourises in layer 1, the response of the IB neurons can code for coincidence between layer 5 and layer 1. IB neurons contact the interneurons in layers 2/3, enhancing the oscillation of the circuit and linking the inhibitory activity to the coincidence between distal inputs and local activity. (Patterns of interlaminar connectivity reviewed by Thomson and Bannister 2003).

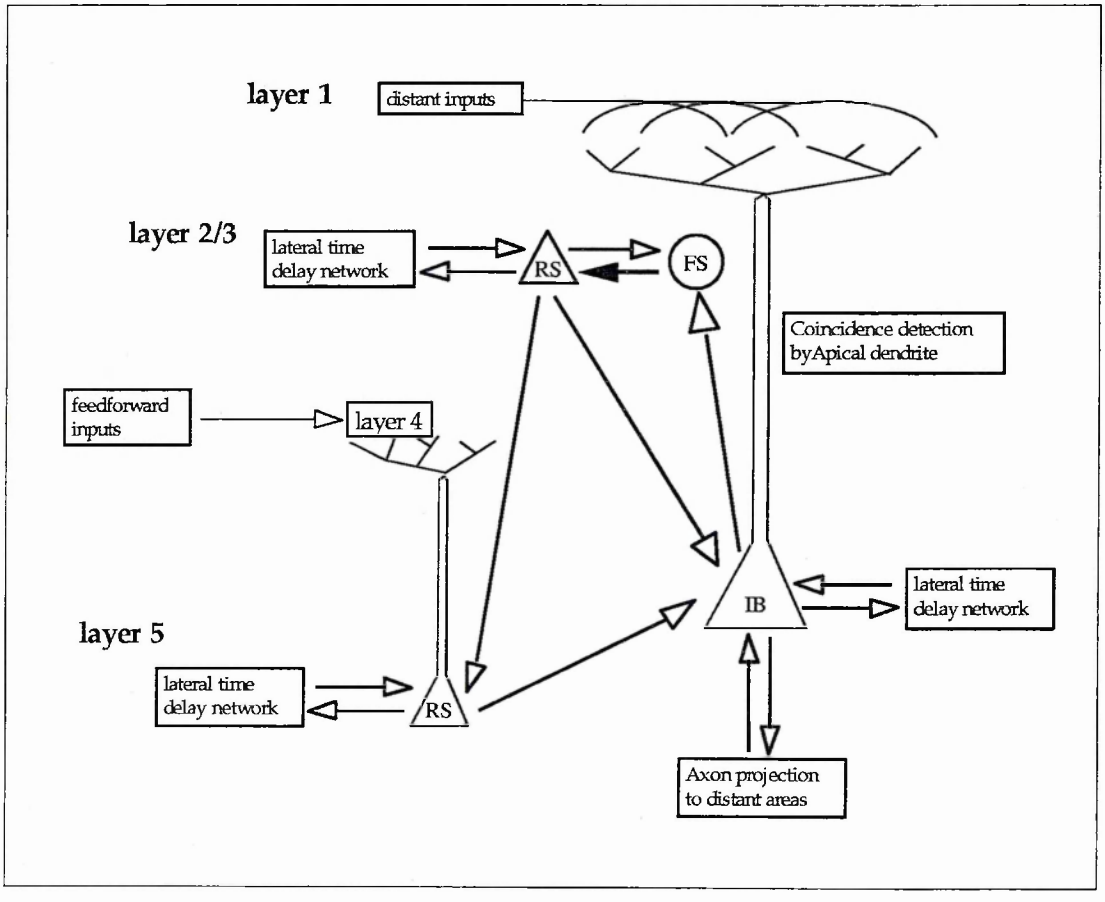

Figure 7.3 Sketch of layer 2/3 to 5 vertical circuit.
Connections between layer 4 and 2/3, and apical dendrite from layer 3 pyramid to layer 1 not shown (see figure 7.2). Inhibitory interneurons in layer 5 not shown.

The common features of these proposed circuits include inhibition of an 'input' layer being driven by bursting neurons in a different layer. The bursting neurons are

involved with the integration of local activity and distant (layer 1 inputs) activity. Axon fibres innervating layer 1 have dispersed terminations over a several mm^2 so individual inputs to apical dendrites are likely to achieve a small amplitude and relatively subtle interactions are likely.

The circuits (4 to 2/3 and 2/3 to 5) are closely linked as layer 2/3 is common to both and the apical dendrite of layer 5 RS pyramids arbourise in layer 4c; so local collective oscillations will be strongly coupled.

The layer 4 to 6 reciprocal circuit has some features common to the above: a sublamina of layer 4 innervates layer 6 and layer 6 large pyramids (Mynert cells) selectively target interneurons in layer 4. However the apical dendrite of the layer 6 pyramids does not reach layer 1, so it may be thought that this circuit is more concerned with the coordination of local activity and not directly concerned with integrating a response with distant cortical areas. As layer 6 large pyramids project subcortically this circuit may be more concerned with the coordination of sub-cortical activity. (The 4 to 6 circuit is coupled to the other vertical circuits as in addition to the common layer 4, layer 6 receives inputs from layer 5.)

7.4.3c Testable predictions

The application of the prototype circuit (7.4.2) to the 4-2/3 circuit and 2/3-5 circuit cast the CH neurons in a similar role to IB neurons. Flowing from this, some predictions are made concerning the morphology and connectivity of CH neurons (in section 7.4.3), which may be tested by an investigation of neurophysiology. Specific predictions are listed in table 7.1, below.

Prediction 2, 'CH cells have apical dendrites that arbourise in layer 1', is the most likely to be confirmed by empirical results. It is already known that, of pyramids in layers 4 to 2, a subpopulation concentrated in layer 3b have apical dendrites that arbourise in layer 1, also CH cells are concentrated in layer 3b.

	Predictions of CH neuron morphology, connectivity and functioning
1	Intralaminar asymmetry of connectivity: layer 2/3 RS cells innervate layer 3b CH cells but CH cells do not (mostly) contact other layer 2/3 RS neurons.
2	Morphology: CH cells have apical dendrites that arbourise in layer 1.
3	Interlaminar asymmetry of connectivity: layer 4 innervates both neurons and interneurons in layer 3; the predominant layer 4 targets of CH cells are interneurons.
4	During an oscillatory episode, the phase timing of impulse firing by layer 2/3 RS neurons and CH cells will be more variable than layer 4 spiny cells.

Table 7.1 Predictions regarding CH neurons

The other predictions are less likely to be tested quickly as they would require the identification of morphology and functioning of pairs of connected neurons (1 and 3) or identification and detailed analysis of activity (4).

7.4.4 Summary of the proposal

This 'working hypothesis' of local circuit functioning combines the ideas of a time coding network and interlaminar 'coincidence detector' afforded by the action of the apical dendrite. A strong feature of the proposal is the action of the bursting neurons. It is proposed that the bursting neurons provide coincidence detection between local lateral activity and distant inputs via layer1. In addition to this the bursting neurons drive the local oscillatory 'clock' by their innervation of local interneurons, so the local oscillation is inseparable from the action of the bursting neurons. (For further reference this model will be referred to as IOTCN: the Intrinsic Oscillating Time Coding Network.)

The IOTCN proposal is a powerful one because:

i. different theoretical approaches to local brain function and empirical physiology, morphology and function are unified;

ii. specific mechanisms are falsifiable, for example the range of axonal time delay differences must be consistent with the coincidence function achieved by the pyramidal neurons;

iii. the proposal may be extended to include interaction with sub-cortical centres and other circuits, for example the reciprocal layer 4c to layer 6 circuit;

iv. the proposal may be extended to include interaction with distant cortices. The local 'clock' may interact with distant clocks. Modelling possibilities for a phase shifting local oscillation are discussed in the section 7.6.4 below.

Before considering a programme of future work I will briefly review a range of published modelling studies:

7.5 Cortical neuron and network models

7.5.1 Neuron compartment models: one or a few cells

The interaction of the cell body and active conductances on the dendritic arbour produces a distinctive firing pattern in a detailed compartment model of a pyramidal neuron (Mainen and Sejnowski 1996). This study is relevant to investigating the response function of pyramidal neurons.

Other studies implementing a small network of biophysically based neuron models (compartment models or reduced compartment models) consider oscillation and synchronisation (Bush and Douglas 1991; Lytton and Sejnowski 1991) and find that synchronisation is a consequence of local inhibition. These studies are relevant to the issue of the stability of the local 'clock' oscillator.

Crook et al find that a network of adapting neurons (including networks of biophysically based reduced compartment pyramid models) are capable of synchronisation by adaptation alone in the absence of inhibition (Crook et al 1998b). This is also relevant to the nature of local oscillations.

Douglas and Martin (1991) examine the response of a small model network that represents the cortical response to a thalamic pulse input. They include compartment models of pyramidal cells and inhibitory interneurons. This model is of interest because they represent an upper and lower neocortical layer. They identify three subpopulations of neurons in the 'microcircuit'. The model upper layer represents the layers 2 to 4, the lower layer represents the cortical layers 5 and 6. An inhibitory subpopulation is not divided between the layers and acts on both upper and lower layers, a stronger level of inhibition acts on the lower layer (assumptions leading to this implementation are discussed in chapter 5, section 5.4.4). Douglas and Martin do not implement action potential generation with each subpopulation, and each subpopulation is represented by a single 'population average' model neuron (p764 1991); the network model contains three non-spiking neurons. The sustained response is not examined and the emergence of circuit oscillation is not considered.

7.5.2 Networks of many cells with reduced morphology

Bush and Sejnowski investigate the behaviour of a sparsely connected network of adapting pyramidal neurons and interneurons (reduced compartment models) (Bush and Sejnowski 1996). Oscillation and synchronisation within and between columns is demonstrated. They find that synchronisation is sensitive to inhibitory strength. Their column model does not differentiate layers or implement a vertical circuit. In terms of the representation of adapting pyramids and interneurons, this model is nearest to the single layer model presented in chapter 5 (especially 5f).

Another biologically motivated model is studied by Series and Tarroux. Networks of sparsely connected spiking neurons and interneurons are implemented. Synchronisation of columns is demonstrated (Series and Tarroux 1999). This model is harder to compare to the results of chapter 5 as the neuron models are bistable (latching on to produce a spike train; this may be considered to be an extreme form of the Hindmarsh and Rose 'triggered firing' property: see chapter 2) and adaptation is not implemented. Layers are not implemented.

Sommer and Wennekers study a biologically inspired Hebbian learning network (Sommer and Wennekers 2000). The oscillatory network is formed from an over connected array of bursting neurons, with global feedback inhibition. Layers are not implemented. This study does not implement axonal delay, but it has some relevance to a consideration of local lateral interactions.

7.5.3 Simplified 'neuron' model networks

Simplified neuron models are often used to make the implementation of extensive networks with large populations tractable. A very large literature exists. As most of these models do not implement, even in a reduced form, properties such as adaptation or bursting I will not review them here. Multiple layer models have been implemented (Ross et al 2000; von der Malsburg and Buhmann 1992). The Malsburg model uses an abstract oscillator to represent the variation of neural activity (this may be considered to represent the 'mean field' of a local oscillation) and does not implement layer differences. Ross et al implement differences in layer connectivity in a hierarchical model of columns and areas. However the Ross model uses a non-spiking leaky integrator model to represent the individual models. Neuron types are not differentiated hence layer differences in neuron behaviour are not well represented. These models are not particularly useful in the task of developing a local circuit model that portrays details of layer differences.

Korner et al (Korner et al 1999) implement a detailed large scale model that includes five layers, multiple columns and thalamic nuclei. A hierarchy of processing levels is implemented. Populations of columns forming a single cortical level, project forward to a higher cortical level representing V1, V2 to V4 and the inferotemporal cortex, and reciprocal projections feedback. Much of the structure of this model resembles the proposal by Gilbert (2001) regarding cortical function.

Gilbert (2001) proposes "an outline of brain function" that includes cortico-thalamic units, hippocampal input and sub-cortical areas. Of interest here is the view of the 'column circuit'. Upper layers 4,3 and 1 receive inputs from the subcortical areas,

hippocampus and other cortical areas. Layers 2,3 innervate the lower layer 5. The lower layers form an output layer to subcortical areas (especially the thalamus).

Fundamental to the Korner et al model is the implementation of a 'latency firing code'. At each level of a hierarchy a feature detector signals a perfect match by the timing of its activity in relation to a clocking mechanism. Korner et al implement a global network clock, representing the activity of the thalamic intralaminar nuclei (they do acknowledge that the origin of real cortical oscillations is more complex).

Korner do not examine the question of the contribution of laminar difference to synchronisation or oscillatory activity. Their network neurons are implemented as integrate and fire models (Rodemann and Korner 2001), and so their column models do not include the dynamics of RS or IB neurons or the active apical dendrite.

However, Korner et al do suggest the columnar modules provide parallel modes of processing, a feed-forward categorisation route, and a top-down feedback refinement or prediction. Feedforward categorisation is placed in layers 4 and 3c, refinement occurs by feed back provided by layers 5 and 6, activating partial matches in the refinement system in layers 2,3a and 3b (which subsequently feedforward).

Although this architecture does not capture the dynamics of local reciprocal circuits that contribute to columnar synchronisation and oscillation, it is a reminder of interlaminar functional differences and goes some way to developing a time coding model of cortical functioning.

7.5.4 Multilayer network with biophysically based neurons -

The LDCM presented in chapter 6 is unique. There are no published cortical models that include layer differences with spiking, adapting neurons (ie FS, RS and IB or CH). In addition there are no models that implement the proposed IOTCN, with active apical dendrites acting across layers, layer differences and adapting neurons. Table 7.2 compares a selection of neuron assembly models.

Model implementation		Layers Number	Difference	Neuron Model field equation	integrate & fire	biophysically based	Intrinsic population oscillation
Colenso	2003	**2**	**Y**	-	-	**Y**	**Y**
Bush	1996	1	-	-	-	Y	Y
Traub	1997b	1	-	-	-	Y	*Y
Sommer	2000	1	-	-	-	Y	Y
Malsburg	1992	8	N	Y	-	-	Y
Ross	2000	3	Y	Y	-	-	N
Korner	1999	5	Y	-	Y	-	*N

Table 7.2 Comparison of neuron assembly model features.

*Y Traub et al (1997b) implement a cortical inhibitory oscillator that omits excitatory to excitatory connectivity Traub et al (1997a) include excitatory to excitatory synapses but find that these tend to disrupt oscillatory activity. *N Korner et al (1999) implement an 'external' thalamic oscillator that drives the cortical population activity.

A number of models share some of the features included in the LDCM presented in chapter 6. A few models implement neocortical layer differences but they do not implement different neuron types.

The Bush and Sejnowski model (1996) is closest to the LDCM and single layer model in chapter 5. Collective oscillations occur through the interaction of the neuron population. The Bush and Sejnowski column model is implemented as a sparsely connected network, and does not differentiate the features that are distinguished between two layers in the LDCM. Bush and Sejnowski include bursting neurons and omit sIPSP synapses, features which are appropriate for the lower layer. The strength of fIPSP synapses in the Bush and Sejnowski model are set at a level which is comparable to the fIPSP weight in the upper layer of the models in chapters 5 and 6.

Traub et al (1997a,b) implement models which achieve synchronised oscillations and include biophysically based model neurons. These single layer models are based on findings from the hippocampus. A specific oscillatory mechanism is proposed which emphasises the role of an inhibitory circuit, and a phase coding response is described. Traub et al find that excitatory to excitatory recurrent activity tends to disrupt the phase coding response (Traub et al 1997a). The emphasis on an inhibitory interneuron circuit as the basis of local oscillations is hard to reconcile to the typical pyramid to

pyramid connectivity that is found in the local neocortex (although this may be an appropriate model for the hippocampus). The Traub et al approach is of interest because a 'phase delay code' response is demonstrated.

Sommer and Wennekers (2000) implement a single layer model with all to all pyramid connectivity and global inhibition. This is hard to reconcile with known local connection probabilities. However, the model demonstrates Hebbian learning in an oscillating network. This may be relevant to a consideration of very local lateral functioning (for example in layer 4 lateral projection is very limited and high cell density may indicate a high connection probability). Layers are not differentiated so this model is not informative about the local vertical circuit.

The large model of Korner et al differentiate cortical layers but neuron dynamics are not differentiated (beyond inhibitory or excitatory). The multilayer model of Korner is interesting because layer connectivity differences are implemented. But model neurons are based on integrate and fire units so dynamics of the local circuit are not captured. Oscillation is driven by a centre that is external to the local neocortex (thalamic ILN). The character of locally generated 'intrinsic' oscillations is not examined and again, it is hard to compare to the LDCM presented in this thesis.

Korner et al do implement a time delay coding, so, like the Traub et al model, they provide an example of Hopfield's impulse timing proposal (1995). To a degree both the Traub and Korner models isolate the generation of oscillations from local excitatory activity (stabilising the oscillation and simplifying any temporal code). However the results of chapter 6 indicate that the neocortical interlaminar circuit is capable of supporting a local population oscillation involving both pyramidal and inhibitory neurons. The model proposal of this chapter portrays the oscillatory population 'clock' as an intrinsic behaviour of the local cortical circuit, with the neurons engaged in a 'time code' response directly contributing to the 'clock' oscillator.

7.6 Further modelling studies

The proposal for an Intrinsically Oscillating Time Coding Network (IOTCN) of local neocortex function is incomplete. Many aspects require a more precise definition before a model may be implemented.

A number of preliminary studies must be conducted to define the functional limits for different model components. A primary task is an exploration of the 'coincidence function' that each neuron type can support. The 'coincidence' results of Larkum (1999) need to be generalised for the different pyramid types. Single cell compartment model simulations are suited to this task and some published single neuron studies are relevant (for example Bush and Sejnowski 1994; Rhodes and Gray 1994). Differences in the response function of RS, CH and IB pyramids, and the contrast between distal apical and proximal dendritic inputs will be highly significant in a time coding model implementation. Differences between RS and bursting response functions may indicate the functional difference of integrating layer 1 to local activity compared to local vertical interlaminar integration.

The action of interneurons must be considered. Modelling may allow the classification of interneuron type according to the modification of the response function: modulatory action supporting a clock (providing a sub-threshold oscillation together with EPSPs); gating acting on the shaft of apical and axon initial segment; firing rate stabilisation by the action of sIPSP negative feedback. (Gating action may be associated with a lateral 'logical' network, supporting a feedforward response.)

The effect of variable synaptic activity on the response function may be investigated by modelling (see variable oscillation frequency below). In addition, longer term synaptic modification as a function of the coincidence of the action potential impulse (AP) and EPSPs and IPSPs have been reported (Holmgren and Zilberter 2001; Magee and Johnston 1997; Markram et al 1997). Other findings regarding synaptic LTP, LTD and the coincidence of the AP and synaptic PSP are reviewed by Paulsen and Sejnowski (2000). These process of synapse plasticity appears to arise from a coincidence timing mechanism that is related to the enhanced impulse firing

coincidence timing mechanism and therefore may provide a learning rule that is entirely consistent with the short term 'time coding' behaviour. A model incorporating different learning rules according to the apical or basal synaptic site difference has been implemented (Kording and Konig 2001).

7.6.1 Challenges for the implementation of the IOTCN model

However some immediate problems exist. If the oscillations are providing a coding clock, why in-vivo are the oscillations variable between different presentations of the same stimulus, and within the same response episode?

If the clock is required to 'code' and decode a response, how can a fast RF response be achieved in-vivo before the local oscillations are established (Tovee and Rolls 1992)? The former objection is considered in the sections 7.6.3 and 7.6.4 below. I will consider the latter objection first.

7.6.2 Reconciling fast responses and oscillatory activity

One constraint on the functional model is that it should support the 'fast feedforward' receptive field response that can be established before widespread oscillations can emerge. The IOTCN proposal does not prevent fast 'feedforward' responses. It is likely that the stronger synapses mediate the early response to thalamocortical inputs. Coincidence detection and axonal time delays are available as activity propagates laterally between the most strongly interconnected neurons. In this case the time code is in relation to the onset of a stimulus. In Eckhorn's terms this is a 'stimulus locked' response, that occurs before collective oscillations are observed. However the pattern of temporal activity which is evoked by a different stimulus, with a different onset time, is displaced in time and so cannot integrate with the temporal pattern of the first stimulus (in the absence of collective oscillations and so without the emergence of a common time frame).

Further, in the case where the only timing reference is the time of the stimulus onset (again, in the absence of collective oscillations), as a stimulus persists the precision of the timing of collective activity will be lost (the timing of successive impulses will

accumulate small timing differences that will tend to disrupt a precise timing 'code'). The response of a neural assembly will initially achieve the precision of a time delay network, where the timing of each neuron impulse is significant, but in the absence of another timing mechanism the response will degrade to an average firing rate encoding.

A model that can support both a 'fast feedforward' response (with no collective synchronising oscillations) and an oscillatory response will go some way to meeting the objections of Lamme (Lamme and Spekreijse 1998) (see section 7.1.5 above).

7.6.3 Variable oscillation frequency

A problem for a IOTCN in a real cortex is that the local oscillation frequency (or coding reference 'clock') is not fixed. It varies between successive presentations of the same stimulus. So if a time coding is generated is it coded by relative phase with respect to the clock, or an absolute time difference? Axon conduction is likely to remain the same for different response epochs, but the collective oscillation 'clock' frequency varies somewhat.

This problem may be investigated by modelling and different mechanisms may contribute to 'time code stability'. One possible solution arises from typical synapse function. Common EPSPs exhibit 'depressing' firing. At a single synapse site the amplitude of a train of EPSPs diminishes. Repeated activations of the same synapse results in reduced EPSP amplitude (asymptotic to a limit that is frequency dependant). Now, if the clock is faster, then EPSPs will be more frequent, but smaller. A smaller EPSP will not evoke postsynaptic cell impulse as quickly as a larger EPSP, hence the pyramid may time the coincidence at a later time (a phase delayed). Axon conduction times are relatively fixed, so for a high frequency clock the delay line signal will arrive at a relatively late phase. Such effects stabilises the coding over a range of frequencies and may maintain the efficacy of the IOTCN. Modelling could test this mechanism and compare the action of different synapse interactions on the temporal coding.

7.6.4 Phase continuity and phase shifts

Why does local oscillation frequency vary? If IOTCN is the main mechanism of local cortical integration, then why didn't evolution implement a stable clock? For example the inhibitory oscillation of the Traub model (Traub et al 1997b) or the external thalamic clock as modelled by Korner(Korner et al 1999).

The tentative explanation (which goes beyond the local cortical area) is that phase shifts or phase modulation would be expected if there is interaction with other cortices at a lower frequency. Now this raises the possibility of two interacting timing schemes running concurrently. It may be suggested that layer5 IB neurons are 'tuned' to a lower frequency and so will be more sensitive to a slower modulation. It may be recalled that different stimulus related frequency components have been found in the local LFP (Frien and Eckhorn 2000). Such a mechanism might correspond to the 'amplitude envelope' interaction proposals (Eckhorn et al 2001) or the 'scales of synchronisation' proposal (von Stein and Sarnthein 2000). In the IOTCN model this distant feedback is interesting because as the IB neuron activity changes, the local population 'clock' will be modified.

7.6.5 Local clock location

In an above section it is indicated that the coding 'clock' is in the more inhibited and synchronised layer (upper layer of model 6a)(layer 4 in 4-2/3 circuit; section 7.4.3). This is somewhat misleading as model 5a (upper layer only) has similar parameters and relatively poor oscillation compared to the upper layer of model 6a. A better interpretation is that the lower layer of model 6a contributes to upper layer synchronisation and oscillation, therefore the 'clock' is a collective property of that circuit. In network 6c inputs to the lower layer are increased and it appears that the whole column oscillation is exhibiting some characteristics of the IB neurons in the lower layer. The collective 'clock' is then more associated with characteristics of the lower layer, because the lower layer is more active. The balance of activity between the layers is important in determining the nature of the collective oscillatory activity. The simple assumption that the 'upper' layer provides timing information may be

wrong. In vivo there are mechanisms that can balance activity (negative feedback) and so large changes in the balance of layer activity may not arise.

The specific pattern of interlaminar connections appears to highlight the importance of the bursting neurons (for IB neurons, the specificity of CH to layer 4 interneurons is a proposal of this thesis). Layer 5 IB neurons will have a strong effect on the modulation of column activity as they preferentially target layer 3 interneurons. In addition the IB neurons are (it is proposed that) achieving a coincidence detection function comparing distal layer 1 inputs and local inputs. The local circuit 'clock' is a product of this resolved population activity.

7.6.6 Temporal binding hypothesis

The temporal binding hypothesis proposes that responses corresponding to a common stimulus will be bound together by a synchronised oscillatory activity (sections 7.1.1 and 7.1.3). The IOTCN proposal requires a common time frame for 'time code' responses to be effective across different areas. The exchange of precisely timed impulses will be confused if two local areas use two different unsynchronised clocks. IOTCN does not rule out a 'temporal binding hypothesis' that correlated oscillations provide a mechanism for perceptual grouping. However a different functional explanation is given. For IOTCN the oscillations do not encode stimuli details, the population oscillations provide the time frame calibration against which detailed response impulse timings can be measured.

7.7 Summary

LDCM results are discussed in relation to theories of cortical oscillations and synchronisation. The consequences of the LDCM property of differences in laminar temporal behaviour is considered in conjunction with additional physiological features of the local neocortex. The possibility of a neural timing code is examined.

A novel prototype circuit is proposed, the "Intrinsically Oscillating Time Coding Network", as a functional model for local neocortex. The model includes: layer differences of neuron types and connectivity; active apical dendrite supporting interlaminar coincidence detection; axonal delay providing a lateral time delay network.

Future modelling tasks are proposed. Central to these is an exploration of the coincidence response function, mediated by the apical dendrite, of RS CH and IB neurons.

8 Conclusion

This thesis develops a simplified model of the local neocortex column that portrays the dynamic relationship of upper and lower layers. The model includes a sub-set of typical local physiology, with particular emphasis on layer differences (layer difference column model: LDCM). Modelling results indicate that the layer differences give rise to differences in the temporal behaviour of the layers. Using this result together with a consideration of further typical local physiology and theoretical proposals of neural coincidence detection a new model of local cortical functioning is proposed.

8.1 Review of chapters

8.1.1 Introduction and thesis motivation

Chapter 1 introduces the background to this thesis. Empirical findings of stimulus related cortical oscillations and theories of oscillation synchronisation and theories of binding of the neural response are briefly introduced.(The discussion of chapter 7 returns to consider these theoretical approaches in the light of the thesis results.) The question of which local cortical properties might contribute to this behaviour is raised. A modelling approach that considers simplifications of 'typical' local neurophysiology is proposed. Thesis contributions are listed in this chapter.

8.1.2 Physiological bases for modelling

Chapter 2 includes a review of neurophysiology and proposes the development of neuron and synapse models. The distribution of neurons through the layers, connection patterns and layer differences are considered. A simplified modelling scheme is proposed that includes a representation of common features of the local neocortex: three neuron types RS, FS and IB; three synapse types supporting fEPSP, fIPSP and sIPSP; upper and lower layers with stronger inhibition in the upper layer

and IB neurons restricted to the lower layer; connection asymmetry between upper and lower layers.

The scale of the proposed modelling is restricted. It is intended to investigate a model at the level of a small local population of neurons. Empirical results involving the actions of populations of synapses are considered, and strengths of connectivity are estimated from compound PSPs.

8.1.3 Model elements

Models of the excitable membrane and a simplified synapse are examined in chapter 3. The excitable membrane model is based on a modification of the Hindmarsh and Rose system. The modification allows control of the triggered firing property. Three parameter sets implement the characteristic firing behaviours of the FS , RS and IB neuron types. The model synapse is implemented using an alpha function to give a characteristic time course. The strength of the synapse is implemented using a weight multiplier.

Correlations and power spectra of time series are examined. The FS model is found to have a flat frequency response and passes all frequencies in range of interest. RS and IB model exhibit a band pass characteristic and are resonant at their preferred frequencies. The synapse model alpha function acts as a low pass filter.

8.1.4 Simple model circuits

Illustrative simple circuits are examined in chapter 4. General findings include:
inhibitory feedback by FS neurons reduces average circuit rates of activity (unsurprisingly) but transient response of RS model neurons is not impaired;
RS to RS impulse recruitment time is similar under different conditions;
RS to IB impulse recruitment delay is more variable.

The consistency of timing of RS to RS impulse recruitment is noted. This is consistent with a time delay model (but does not rule out many other models).

The interpretation of the behaviour of these small circuits must include the caveat that the circuits are somewhat pathological as they include low numbers and large connection weights which is not typical of the majority of connections in the local neocortex.

8.1.5 The single layer model

Chapter 5 implements a model network including 100 neurons of RS and FS model neurons. The network model is configured to represent the upper layers of a neocortical column. Parameters are chosen to balance the average rate of impulse activity in RS and FS neurons. The network's response to a noise input is examined under different conditions.

The model exhibits a tendency for RS neuron impulse synchronisation. A collective oscillation occurs, but is not very robust. Variation of the conditions reduces the strength of the oscillation: an imbalance in the rates of RS and FS activity reduced the oscillation, reducing the rate of inhibitory activity reduces synchronisation (result 5d). The inhibitory effect of sIPSP stabilises the network response rate and opposes tonic input.

The model configuration is adjusted (models 5e and 5f) to allow comparison with the Bush and Sejnowski column model (Bush and Sejnowski 1996). The 5f model achieves a relatively strong synchronised oscillation (compared to 5a) and broadly reproduces the single column results of Bush and Sejnowski.

Contrasts between the Bush and Sejnowski column model and the modelling approach in this thesis are made. Bush and Sejnowski do not implement layer differences in their column model. The Bush and Sejnowski model uses a fast fIPSP rise time (based on empirical results examining single synapse IPSPs). Models in this thesis (except 5f) implement a slower fIPSP based on the empirical recording of the time course of compound IPSPs involving multiple simultaneously active inhibitory synapses.

8.1.6 The layer difference column model

The LDCM implemented in chapter 6 includes biophysically based neuron models and layer differences of neuron distribution and connectivity (the neuron models are simplified, but preserve properties of impulse firing, adaptation of firing rate and burst firing). No other published models incorporate these features.

Bush and Sejnowski implement a column model that includes bursting neurons, but they do not implement layer differences (Bush and Sejnowski 1996). Traub et al also implement a single layer model of cortical oscillation, however the oscillation is driven by a mutually inhibitory population of interneurons (Traub et al 1997b).

Multiple layer models are published, and they do implement some interlaminar connection differences. However the layered distribution of different neuron types is not included. The model neurons are implemented as integrate and fire, or mean field oscillators, and do not include adaptation of firing rate or bursting behaviours. The multilayer model of Ross et al does not implement spiking neurons (Ross et al 2000), similarly Malsburg's coupled neural oscillator layers are based on a non-spiking phase plane model that does not capture bursting, adaptation or refractoriness (von der Malsburg and Buhmann 1992). The extensive multiple layer model of Korner et al implements layers, columns and cortical areas, however these networks are built with integrate and fire neuron models, so the adaptation and bursting behaviour of typical pyramidal neurons is not included (Korner et al 1999; Rodemann and Korner 2001). In addition the Korner model includes oscillation that is driven by a source external to the cortical layers (thalamic oscillator).

(Note that the terminology of cortical structure and neural network modelling sometimes requires translation: some neural network models that are described as 'multiple layer' networks are, in cortical terminology, implementing the connection of single layers in multiple areas, for example in a model portraying the hierarchy of different cortices.)

The LDCM introduced in chapter 6 comprises RS and FS neurons distributed over two layers. IB neurons are restricted to the lower layer. The upper layer is more strongly inhibited than the lower layer. The upper layer neurons projects to all neurons in the lower layer. Interlaminar inhibitory connections are asymmetric. The lower layer FS neurons do not directly project to the upper layer. The lower layer pyramidal neurons (RS and IB) project to the upper layer.

Strong synchronisation and oscillation of the whole column is demonstrated. The upper layer is more tightly synchronised than lower layer. It is proposed that the collective action of the upper layer supports a finer temporal resolution than the lower layer, complementing this the variability of individual neuron impulse timing in the lower layer may support a time code mechanism (discussed in chapter 7).

8.1.7 Discussion and proposal for a new model of local cortical integration

The results from the LDCM are discussed in relation to different theories of neural integration and further features of local neocortex neurophysiology are considered.

A new model of cortical function is proposed. The key features of this model include: the generation of local oscillations in a vertical interlaminar reciprocal circuit; the apical dendrite providing a sharp coincidence detection function between the layers; slow axonal lateral propagation providing a time delay network; apical dendrites of bursting cells (CH and IB) providing coincidence detection between inputs from distant areas (layer 1 inputs) and local activity; bursting cell innervation of interneurons, linking the local oscillation cycle to coincidence detection. This model has been termed an intrinsically oscillating time coding network (IOTCN). Specific predictions are made concerning the functioning of the local circuit in neocortex, and the connectivity of CH neurons.

The IOTCN proposal differs from other time coding proposals which distance the generation of oscillations from the local excitatory neuron population (Korner et al 1999; Traub et al 1997b). In the IOTCN model local population activity oscillations

arise from the local interlaminar circuit, and the 'time coding' pyramidal neurons are a key component of this circuit.

Further modelling work is suggested to test the proposal of the IOTCN. Initial studies should concentrate on defining the coincidence function that pyramidal neurons support, and how this varies with different pyramidal types. It is suggested that interneuron types might be classified according to their effect on the coincidence function achieved by a pyramidal cell.

8.2 Conclusion

The LDCM of chapter 6 is based on some simplifying assumptions and details could be refined, however the basic result is likely to remain the same. The upper layer achieves a more tightly synchronised pattern of activity than the lower layer. This result opens the question: what is the functional role of differences in layer behaviour?

Extending the LDCM raises further questions of how other 'typical' features of local neocortex will contribute to circuit activity. The IOTCN proposal arises from the consideration of these common features. Extending the LDCM to connect laterally to adjacent columns invites consideration of why lateral excitatory and inhibitory axons should have different conduction velocities (answer: delay network). Extending the LDCM to include intercortical connections via layer 1, raises the question of what is the functional role of the apical dendrite (answer: coincidence timing detector).

The proposal of IOTCN opens up many further questions, which may be studied by modelling or addressed by results from physiological studies:
For example, I have not given a strong account for the role of interneurons in IOTCN. This is an area which should be investigated by modelling. As a starting point it would seem likely that inhibitory synapses, providing a graded modulation, may contribute to an oscillatory modulation, providing a phase reference for the timed response of a pyramidal neuron. 'Vetoing' inhibition may be more appropriate for implementing the

logical structure of the local lateral circuit.

Also, it seems that the bursting neurons IB and CH are strongly associated with the integration of inputs from layer 1 into local activity. Perhaps the bursting dynamic provides a particular response function suitable for this. Again this is a suitable area for investigation by modelling.

Bibliography

Bonhoeffer T. and Grinvald A. "Iso-orientation domains in cat visual cortex are arranged in pinwheel-like patterns." Nature 353 (6343 1991): 429-431.

Bush P. and Priebe N. "GABAergic Inhibitory Control of the Transient and Sustained Components of Orientation Selectivity in a Model Microcolumn in Layer 4 of Cat Visual Cortex." Neural Computation 10 (4 1998): 855-867.

Bush P. and Sejnowski T. "Inhibition Synchronizes Sparsely Connected Cortical Neurons Within and Between Columns in Realistic Network Models." Journal of Computational Neuroscience 3 (1996): 91-110.

Bush P.C. and Douglas R.J. "Synchronization of Bursting Action Potential Discharge in a Model Network of Neocortical Neurons." Neural Computation 3 (1991): 19-30.

Bush P.C. and Sejnowski T.J. "Effects of Inhibition and Dendritic Saturation in Simulated Neocortical Pyramidal Cells." Journal of Neurophysiology 71 (6 1994): 2183-2193.

Cairns D.E., Baddeley R.L. and Smith L.S. "Constraints on Synchronising Oscillator Networks." Neural Computation 5 (1993): 260-266.

Callaway E.M. "Local circuits in primary visual cortex of the macaque monkey." Annual Review of Neuroscience 21 (1998): 47-74.

Chagnac-Amitai Y., Luhmann H.J. and Prince D.A. "Burst Generating and Regular Spiking Layer 5 Pyramidal Neurons of Rat Neocortex Have Different Morphological Features." The Journal of Comparative Neurology 296 (4 1990): 598-613.

Chay T.R. "Chaos in a three-variable model of an excitable cell." Physica D 16D (1985): 233-242.

Connors B.W., Cauller L.J., Kim H.G. and Bulthoff I. "Layer I and the Excitable Apical Dendrite: Substrates for Intracortical Communication." In Structural and Functional Organisation of the Neocortex, ed. Albus K. Albowitz B., Kuhnt U., Nothdurft H.-Ch., Wahle P. Berlin: Springer Verlag, 1994.

Connors B.W. and Gutnick M.J. "Intrinsic firing patterns of diverse neocortical neurons." Trends in Neurosciences 13 (3 1990): 99-104.

Connors B.W., Gutnick M.J. and Prince D.A. "Electrophysiological properties of neocortical neurons in vitro." Journal of Neurophysiology 48 (1982): 1302-1320.

Connors B.W., Malenka R.C. and Silva L.R. "Two inhibitory postsynaptic potentials, and GABAa and GABAb receptor-mediated responses in neocortex of rat and cat." Journal of Physiology 406 (1988): 443-468.

Conti F., Rustioni A., Petrusz P. and Towle A.C. "Glutamate-positive neurons in the somatic sensory cortex of rats and monkeys." The Journal of Neuroscience 7 (6 1987): 1887-1901.

Crick F. and Asanuma C. "Certain Aspects of the Anatomy and Physiology of the Cerebral Cortex." In Parallel Distributed Processing Explorations in the Microstructure of Cognition, ed. Rumelhart D.E. McClelland J.L., PDP Research group. 333-371. 2. Cambridge, Mass., London: MIT Press, 1986.

Crook J.M., Kisvarday Z.F. and Eysel U.T. "Evidence for a contribution of lateral inhibition to orientation tuning and direction selectivity in cat visual cortex: reversible inactivation of functionally characterized sites combined with neuroanatomical tracing techniques." European Journal of Neuroscience 10 (6 1998a): 2056-2075.

Crook S.M., Ermentrout G.B. and Bower J.M. "Spike Frequency Adaptation Affects the Synchronisation Properties of Networks of Cortical Oscillators." Neural Computation 10 (4 1998b): 837-854.

Destexhe A., Mainen Z.F. and Sejnowski T.J. "Synthesis of Models for Excitable Membranes, Synaptic Transmission and Neuromodulation Using a Common Kinetic Formalism." Journal of Computational Neuroscience 1 (1994): 195-231.

Destexhe A. and Pare D. "Impact of network activity on the integrative properties of neocortical pyramid neurons in vivo." Journal of Neurophysiology 81 (1999): 1531-1547.

Deuchars J., West D.C. and Thomson A.M. "Relationships between morphology and physiology of pyramid-pyramid single axon connections in rat neocortex in vitro." Journal of Physiology 478 (3 1994): 423-435.

Douglas R.J. and Martin K.A.C. "A Functional Microcircuit for Cat Visual Cortex." Journal of Physiology 440 (1991): 735-769.

Douglas R.J. and Martin K.A.C. "Exploring Cortical Microcircuits." In Single Neuron Computation, ed. Davis J. McKenna T., Zornetzer S.F. 381-412. San Diego: Academic Press Inc, 1992.

Douglas R.J. and Martin K.A.C. "The Canonical Microcircuit: A Co-operative Neuronal Network for Neocortex." In Structural and Functional Organisation of the Neocortex, ed. et al. Albowitz B. 131-141. Berlin: Springer Verlag, 1994.

Eckhorn R. "Neural Mechanisms of Visual Feature Binding Investigated with Microelectrodes and Models." Visual Cognition 6 (3 1999): 231-265.

Eckhorn R., Bauer R., Jordan W., Brosch M., Kruse M., Munk M. and Reitboeck H.J. "Coherent Oscillations: A Mechanism of Feature Linking in the Visual Cortex?" Biological Cybernetics 60 (1988): 121-130.

Eckhorn R., Bruns A., Saam M., Gail A., Gabriel A. and Brinksmeyer H.J. "Flexible cortical gamma-band correlations suggest neural principles of visual processing." Visual Cognition 8 (4 2001): 519-530.

Eckhorn R., Dicke P., Arndt M. and Reitboeck H. "Flexible Linking of Visual Features by Stimulus-Related Synchronisations of Model Neurons." In Induced Rhythms in the Brain, ed. Bullock T.H. Basar E. 397-416. Boston: Birkhauser, 1992.

Eckhorn R., Frien A., Bauer R., Woelbern T. and Kehr H. "High frequency (60-90 Hz) oscillations in primary visual cortex of awake monkey." Neuroreport 4 (3 1993): 243-246.

Engel A.K., Konig P., Gray C.M. and Singer W. "Stimulus-Dependent Neuronal Oscillations in Cat Visual Cortex: Inter-Columnar Interaction as Determined by Cross-Correlation Analysis." European Journal of Neuroscience 2 (7 1990): 588-606.

Engel A.K., Konig P. and Singer W. "The functional nature of neuronal oscillations (reply)." Trends in Neurosciences 15 (1992): 387-388.

Engel A.K. and Singer W. "Temporal binding and the neural correlates of sensory awareness." Trends in Cognitive Sciences 5 (1 2001): 16-26.

Felleman D.J. and Van Essen D.C. "Distributed hierarchical processing in the primate cerebral cortex." Cerebral Cortex 1 (1991): 1-47.

Ferster D. and Jagadeesh B. "EPSP-IPSP Interactions in Cat Visual Cortex Studied with in vivo Whole-Cell Patch Recording." Journal of Neuroscience 12 (4 1992): 1262-1274.

Fetz E.E., Chen D., Murthy V.N. and Matsumura M. "Synaptic interactions mediating synchrony and oscillations in primate sensorimotor cortex." Journal of Physiology (Paris) 94 (2000): 323-331.

FitzHugh R. "Mathematical model of excitation and propogation in nerve." In Biological Engineering, ed. Schwann H.P. McGraw-Hill, 1967.

Freund T.F., Martin K.A.C., Soltez I., Somogyi P. and Whitteridge D. "Arbourization pattern and postsynaptic targets of physiologically identified thalamocortical afferents in striate cortex of the macaque monkey." Journal of Comparitive Neurology 289 (1989): 315-336.

Frien A. and Eckhorn R. "Functional coupling shows stronger stimulus dependency for fast oscillations than for low-frequency components in striate cortex of awake monkey." European Journal of Neuroscience 12 (2000): 1466-1478.

Gilbert C.D. and Wiesel T.N. "Morphology and Intracortical projections of functionally characterized neurons in the cat visual cortex." Nature 280 (1979): 120-125.

Gilbert C.D. and Wiesel T.N. "Laminar Specialization and Intracortical Connections in Cat Primary Visual Cortex." In The Organisation of the Cerebral Cortex, ed. Worden F.G. Schmitt F.O., Adelman U., Dennis S.G. 163-191. Cambridge Mass.: MIT Press, 1981.

Gilbert C.D. and Wiesel T.N. "Functional organisation of the visual cortex." Progress in Brain Research 58 (1983): 209-218.

Gilbert C.D. and Wiesel T.N. "Intrinsic connectivity and receptive field properties in visual cortex." Vision Research 25 (3 1985): 365-374.

Gilbert P.F.C. "An outline of brain function." Cognitive Brain Research 12 (1 2001): 61-74.

Gonchar Y. and Burkhalter A. "Connectivity of GABAergic calretinin-immunoreactive neuorns in rat primary visual cortex." Cerebral Cortex 9 (7 1999): 683-696.

Gray C.M., Konig P., Engel A.K. and Singer W. "Oscillatory responses in cat visual cortex exhibit inter-columnar synchronisation which reflects gobal stimulus properties." Nature 338 (1989): 334-337.

Gray C.M. and McCormick D.A. "Chattering cells: superficial pyramidal neurons contributing to the generation of synchronous oscillations in the visual cortex." Science 274 (1996): 109-113.

Gray C.M. and Singer W. "Stimulus-specific neuronal oscillations in orientation columns of cat visual cortex." Proceedings of the National Academy of Sciences of the USA 86 (1989): 1698-1702.

Hendry S.H.C., Schwark E.G., Jones E.G. and Yan J. "Numbers and properties of GABA-Immunoreactive Neurons in Different Areas of Monkey Cerebral Cortex." Journal of Neuroscience 7 (5 1987): 1503-1519.

Hindmarsh J.L. and Rose R.M. "A model of the nerve impulse using two first-order diferential equations." Nature 296 (1982): 162-164.

Hindmarsh J.L. and Rose R.M. "A model of neuronal bursting using three coupled first order differential equations." Proceedings of the Royal Society of London Series B 221 (1984): 87-210.

Hirsch J.A. and Gilbert C.D. "Synaptic Physiology of Horizontal Connections in the Cat's Visual Cortex." Journal of Neuroscience 11 (6 1991): 1800-1809.

Hodgkin A.L. and Huxley A.F. "A Quantitative Description of Membrane Current and its Application to Conduction and Excitation in Nerve." Journal of Physiology 117 (1952): 500-544.

Holden A.V., Hyde J., Muhamad M.A. and Zhang H.G. "Bifurcating Neurones." In Coupled Oscillating Neurons, ed. Mannion C.L.T. Taylor J.G. 41-80. London: Springer Verlag, 1992.

Holmgren C.D. and Zilberter Y. "Coincident spiking activity induces long-term changes in inhibition of neocortical pyramidal cells." Journal of Neuroscience 21 (20 2001): 8270-8277.

Hopfield J.J. "Pattern recognition computation using action potential timing for stimulus representation." Nature 376 (1995): 33-36.

Hubel D.H. and Wiesel T.N. "Receptive fields, binocular interaction and functional architecture in the cat's visual cortex." Journal of Physiology 160 (1962): 106-154.

Hubel D.H. and Wiesel T.N. "Shape and arrangement of columns in cat's striate cortex." Journal of Physiology 165 (1963): 559-568.

Kasper E.M., Larkman A.U., Lubke J. and Blakemore C. "Pyramidal neurons in layer 5 or the rat visual cortex. I. Correlation among cell morphology, intrinsic electrophysiological properties and axon targets." The Journal of Comparative Neurology 339 (4 1994): 459-474.

Keeling A., Freeman R. and Nicoll A. "Synaptic connections of layer 2/3 pyramidal neurons in rat visual cortex *in vitro*." Journal of Neurophysiology 495.P (1996): 61-62.

Kistler W.M., Gerstner W. and van Hemmen J.L. "Reduction of the Hodgkin-Huxley Equations to a Single Variable Threshold Model." Neural Computation 9 (1997): 1015-1045.

Kisvarday Z.F., Martin K.A.C., Friedlander M.J. and Somogyi P. "Evidence for interlaminar inhibitory circuits in the striate cortex of the cat." Journal of Comparitive Neurology 260 (1 1987): 1-19.

Kisvarday Z.F., Martin K.A.C., Whitteridge D. and Somogyi P. "Synaptic connections of intracellularly filled clutch cells: a type of small basket cell in the visual cortex of the cat." Journal of Comparitive Neurology 241 (1985): 111-137.

Komatsu Y., Nakajima S., Toyama K. and Fetz E.E. "Intracortical connecticity revealed by spike-triggered averaging in slice preperations of cat visual cortex." Brain Research 442 (1988): 359-362.

Kording K.P. and Konig P. "Neurons with two sites of synaptic integration learn invariant representations." Neural Computation 13 (12 2001): 2823-2849.

Korner E., Gwaltig M.O., Korner U., Richter A. and Rodemann T. "A model of computation in neocortical architecture." Neural Networks 12 (1999): 989-1005.

Lamme V.A.F. and Spekreijse H. "Neural synchrony does not represent texture segregation." Nature 396 (1998): 362-366.

Larkum M.E., Zhu J.J. and Sakmann B. "A new cellular mechanism for coupling inputs arriving at different cortical layers." Nature 398 (1999): 338-341.

Lorente de No R. "La corteza cerebral del raton." Trab Lab Invest Biol (Madrid) 20 (1922): 41-78.

Lund J.S. "Anatomical organisation of Macaque monkey striate visual cortex." Annual Review of Neuroscience 11 (1988): 253-288.

Lytton W.W. and Sejnowski T.J. "Simulations of cortical pyramidal neurons synchronised by inhibitory interneurons." Journal of Neurophysiology 66 (3 1991): 1059-1079.

Magee J.C. and Johnston D. "A Synaptically Controlled, Associative Signal for Hebbian Plasticity in Hippocampal Neurons." Science 275 (5297 1997): 209-213.

Mainen Z.F. and Sejnowski T.J. "Influence of dendritic structure on firing pattern in model neocortical neurons." Nature 382 (1996): 363-366.

Markram H., Lubke J., Frotscher M. and Sakmann B. "Regulation of Synaptic Efficacy by Coincidence of Postsynaptic APs and EPSPs." Science 275 (5297 1997): 213-215.

Martin K.A.C. "Microcircuits in Visual Cortex." Current Opinion in Neurobiology 12 (2002): 418-425.

Mason A. and Larkman A. "Correlations between morphology and electrophysiology of pyramidal neurons in slices of rat visual cortex. II. Electrophysiology." Journal of Neuroscience 10 (5 1990): 1415-1428.

Mason A., Nicoll A. and Stratford K. "Synaptic Transmission between Individual Pyramidal Neurons of the Rat Visual Cortex in vitro." Journal of Neuroscience 11 (1 1991): 72-84.

McCormick D.A., Connors B.W., Lighthall J.W. and Prince D.A. "Comparative Electrophysiology of Pyramidal and Sparsely Spiny Stellate Neurons of the Neocortex." Journal of Neurophysiology 54 (4 1985): 782-806.

Nicholls J.G., Martin A.R. and Wallace B.G. From Neuron to Brain. 3 ed., Sinauer Associates Inc., 1992.

Nicoll A. and Blakemore C. "Patterns of Local Connectivity in the Neocortex." Neural Computation 5 (5 1993): 665-680.

Nicoll A., Kim H.G. and Connors B.W. "Laminar origins of inhibitory synaptic inputs to pyramidal neurons of the rat neocortex." Journal of Physiology 497 (1 1996): 109-117.

Nowak L.G., Azouz R., Sanchez-Vives M.V., Gray C.M. and McCormick D.A. "Electrophysiological classes of cat primary visual cortical neuons in vivo as revealed by quantitative analyses." Journal of Neurophysiology 89 (3 2003): 1541-1566.

O'Kusky J. and Colonnier M. "A laminar analysis of the number of neurons, glia and synapses in the visual cortex (area 17) of adult macaque monkeys." Journal of Comparative Neurology 210 (3 1982): 278-290.

Paulsen O. and Sejnowski T.J. "Natural patterns of activity and long-tern synaptic plasticity." Current Opinion in Neurobiology 10 (2 2000): 172-179.

Press W.H., Teukolsky S.A., Vetterling W.T. and Flannery B.P. Numerical recipies in C : the art of scientific computing. Second ed., Cambridge, New York: Cambridge University Press, 1992.

Rall W., Burke R.E., Holmes W.R., Jack J.J.B., Redman S.J. and Segev I. "Matching dendritic neuron models to experimental data." Physiology Review 72 (4(S) 1992): 159-186.

Rhodes P.A. and Gray C.M. "Simulations of Intrinsically Bursting Neocortical Pyramidal Neurons." Neural Computation 6 (1994): 1086-1110.

Rockel A.J., Hiorns R.W. and Powell T.P.S. "The basic uniformity in the structure of the neocortex." Brain 103 (1980): 221-244.

Rodemann T. and Korner E. "Two separate processing streams in a cortical-type architecture." Neurocomputing 38-40 (2001): 1541-1547.

Ross W.D., Grossberg S. and Mingolla E. "Visual cortical mechanisms of perceptual grouping: interacting layers, networks, columns and maps." Neural Networks 13 (6 2000): 571-588.

Sanes J.R. and Yamagata M. "Formation of lamina-specific synaptic connections." Current Opinion in Neurobiology 9 (1999): 79-87.

Segev I. "Single neurone models: oversimple, complex and reduced." Trends in Neurosciences 15 (11 1992): 414-421.

Sejnowski T.J. "Time for a new neural code?" Nature 376 (1995): 21-22.

Series P. and Tarroux P. "Synchrony and delay activity in cortical column models." Neurocomputing 26-27 (1999): 505-510.

Sommer F.T. and Wennekers T. "Modelling studies on the computational function of fast temporal structure in cortical circuit activity." Journal of Physiology (Paris) 94 (5 2000): 473-488.

Sompolinsky H. and Shapley R. "New perspectives on the mechanisms for orientation selectivity." Current Opinion in Neurobiology 7 (1997): 514-522.

Stewart M. "Columnar activity supports propagation of population bursts in slices of rat entorhinal cortex." Brain Research 830 (1999): 274-284.

Stratford K.J., Tarczy-Hornoch K., Martin K.A.C. and Bannister N.J. "Excitatory synaptic inputs to spiny stellate cells in cat visual cortex." Nature 382 (1996): 258-261.

Tanaka K. "Columnar Organisation in the inferotemporal cortex." In Cerebral Cortex, ed. Peters A. Jones G.E. 469-498. New York: Plenum Press, 1997.

Thomson A.M. and Bannister A.P. "Interlaminar Connections in the Neocortex." Cerebral Cortex 13 (1 2003): 5-14.

Thomson A.M. and Deuchars J. "Temporal and spatial properties of local circuits in neocortex." Trends in Neurosciences 17 (3 1994): 119-126.

Thomson A.M., Deuchars J. and West D.C. "Large, Deep Layer Pyramid-Pyramid Single Axon EPSPs in Slices of Rat Motor Cortex Display Paired Pulse and Frequency-Dependent Depression, Mediated Presynaptically and Self-Facilitation, Mediated Postsynaptically." Journal of Neurophysiology 70 (6 1993): 2354-2369.

Thomson A.M. and West D.C. "Fluctuations in Pyramid-pyramid excitatory postsynaptic potantials modified by presynaptic firing pattern and postsynaptic membrane potential using paired intracellular recordings in rat neocortex." Neuroscience 54 (2 1993): 329-346.

Tovee M.J. and Rolls E.T. "The functional nature of neuronal oscillations." Trends in Neurosciences 15 (1992): 387.

Traub R.D., Jefferys J.G.R. and Whittington M.A. "Simulation of Gamma Rhythms in Networks of Interneurons and Pyramidal Cells." Journal of Computational Neuroscience 4 (2 1997a): 141-150.

Traub R.D., Whittington M.A. and Jefferys J.G.R. "Gamma Oscillation Model Predicts Intensity Coding by Phase Rather than Frequency." Neural Computation 9 (6 1997b): 1251-1264.

Traub R.D., Whittington M.A., Stanford I.M. and Jefferys J.G.R. "A mechanism for generation of long-range synchronous fast oscillations in the cortex." Nature 383 (1996): 621-624.

van Brederode J.F.M. and Spain W.J. "Differences in Inhibitory Synaptic Input Between Layer II-III and Layer V Neurons of the Cat Neocortex." Journal of Neurophysiology 74 (3 1995): 1149-1166.

von der Malsburg C. and Buhmann J. "Sensory segmentation with coupled neural oscillators." Biological Cybernetics 67 (3 1992): 233-242.

von Stein A. and Sarnthein J. "Different frequencies for different scales of cortical integration: from local gamma to long range alpha/theta synchronization." International Journal of Psychophysiology 38 (3 2000): 301-313.

Zeki S. and Shipp S. "The functional logic of cortical connections." Nature 335 (1988): 311-317.